

UNCLASSIFIED

AD NUMBER

AD423718

LIMITATION CHANGES

TO:

Approved for public release; distribution is unlimited. Document partially illegible.

FROM:

Distribution authorized to U.S. Gov't. agencies and their contractors;
Administrative/Operational Use; NOV 1963. Other requests shall be referred to Office of Naval Research Laboratory, Washington, DC 20350.
Document partially illegible.

AUTHORITY

onr ltr, 4 may 1977

THIS PAGE IS UNCLASSIFIED

THIS REPORT HAS BEEN DELIMITED
AND CLEARED FOR PUBLIC RELEASE
UNDER DOD DIRECTIVE 5200.20 AND
NO RESTRICTIONS ARE IMPOSED UPON
ITS USE AND DISCLOSURE.

DISTRIBUTION STATEMENT A

APPROVED FOR PUBLIC RELEASE;
DISTRIBUTION UNLIMITED.

UNCLASSIFIED

AD 4 2 3 7 1 8

DEFENSE DOCUMENTATION CENTER

FOR

SCIENTIFIC AND TECHNICAL INFORMATION

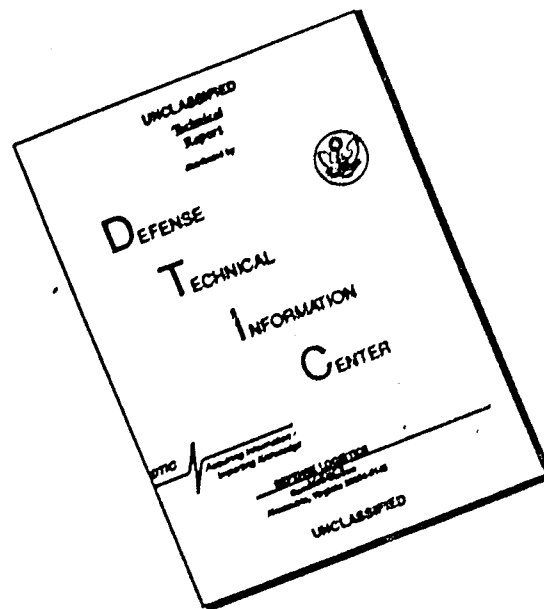
CAMERON STATION, ALEXANDRIA, VIRGINIA



UNCLASSIFIED

NOTICE: When government or other drawings, specifications or other data are used for any purpose other than in connection with a definitely related government procurement operation, the U. S. Government thereby incurs no responsibility, nor any obligation whatsoever; and the fact that the Government may have formulated, furnished, or in any way supplied the said drawings, specifications, or other data is not to be regarded by implication or otherwise as in any manner licensing the holder or any other person or corporation, or conveying any rights or permission to manufacture, use or sell any patented invention that may in any way be related thereto.

DISCLAIMER NOTICE



THIS DOCUMENT IS BEST QUALITY AVAILABLE. THE COPY FURNISHED TO DTIC CONTAINED A SIGNIFICANT NUMBER OF PAGES WHICH DO NOT REPRODUCE LEGIBLY.

423718



MHD research, inc.

POST OFFICE BOX 1815, NEWPORT BEACH, CALIFORNIA

FINAL REPORT

HIGH POWER LASER PHYSICS

PART A. ON THE PHYSICAL THEORY OF LIQUID LASERS

PART B. NUCLEAR PUMPING OF SEMICONDUCTOR LASERS

prepared for

OFFICE OF NAVAL RESEARCH

by

Francis H. Webb, Jr., Principal Investigator

Paul Thiene

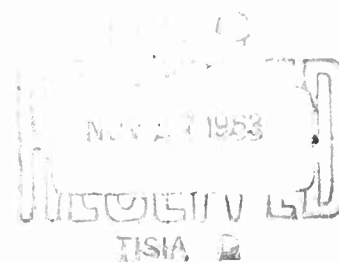
Paul Levine (Consultant)

M H D Research, Inc.

and

Joseph Eerkens

Terra Nova, Inc.



Contract No. NONR-4124(00)

November, 1963

MHD Report No. 645

HIGH POWER LASER PHYSICS

PART A. ON THE PHYSICAL THEORY OF LIQUID LASERS

PART B. NUCLEAR PUMPING OF SEMICONDUCTOR LASERS

prepared for
OFFICE OF NAVAL RESEARCH

FINAL REPORT

by

Francis H. Webb, Jr., Principal Investigator

Paul Thiene

Paul Levine (Consultant)

M H D Research, Inc.

and

Joseph Eerkens

Terra Nova, Inc.

Contract No. NONR-4124(00)

November, 1963

MHD Report No. 645

This research is part of Project DEFENDER under
the joint sponsorship of the Advance Research
Projects Agency, The Office of Naval Research
and the Department of Defense

Reproduction in whole or in part is permitted for any
purpose of the United States Government

ABSTRACT

A theoretical investigation of two possible high power laser concepts has been made; one, an investigation of liquid lasers and the other, an investigation of the nuclear pumping of semiconductors.

Liquid lasers are attractive for high power purposes since a large number of active centers per unit volume may be obtainable. Furthermore, the cooling requirements and the damage inflicted by pump radiation should be greatly reduced compared to solids. Nuclear pumping appears attractive as a high power pump source due to the high specific power levels which are obtainable.

The physics of liquid lasers is investigated. Both gain and loss processes are considered including stimulated emission and losses due to diffraction, absorption, scattering, and refraction. Two rare-earth doped halide systems are investigated in detail. One system considered employs AsCl_3 (UCl_3); here an optimum threshold power of $Q = 3.77 \text{ w/cm}^3$ was computed whereas for an AsCl_3 (NdCl_3) system an optimum threshold power of $Q = 1280 \text{ watts/cm}^3$ was determined. The output wavelength should be $\lambda = 2.46$ micron using uranium and $\lambda = 1.06$ micron for neodymium.

A detailed study of possible laser action in nuclear pumped semiconductors has been made.

It is known that laser action can be achieved by free carrier injection into the junction region of a forward biased direct gap semiconductor. Also free carrier generation by the passage of nuclear radiation in matter is well known.

On the basis of our analysis it appears possible to achieve laser action by nuclear pumping in bulk direct gap semiconductors. Bulk free carrier threshold levels are calculated for intrinsic GaAs. The effects on the threshold due to donor and acceptor levels are also included. High conversion efficiencies appear possible. The degradation of performance due to radiation damage appears to be the major uncertainty.

On the basis of our studies it is felt that experimental work should be initiated. Consequently we have suggested a demonstration experiment.

TABLE OF CONTENTS

ABSTRACT	i
TABLE OF CONTENTS	iii
LIST OF ILLUSTRATIONS	vii
GENERAL INTRODUCTION	ix
PART A <u>THE PHYSICAL THEORY OF LUMINESCENT</u> <u>LIQUID LASERS</u>	1
1. INTRODUCTION	1
2. MACROSCOPIC THEORY OF LASERS	3
2.1 Basic Photon Processes and Conditions for Laser Action	3
2.2 Geometric Considerations	8
3. DIFFRACTION LOSSES	12
3.1 Plane Reflectors	12
3.2 Confocal Reflectors	13
4. ABSORPTION	13
4.1 General Discussion	13
4.2 Dielectric Absorption	16
4.3 Conduction-band Absorption	18
5. SCATTERING	23
5.1 Discussion	23
5.2 Rayleigh Scattering	25
6. REFRACTIVE LOSSES	26
6.1 General Discussion	26
6.2 Refractive Losses Due to Laser Heating	27
7. PHOTON MULTIPLICATION BY STIMULATED EMISSION	33
7.1 General Considerations	33
7.2 Spectroscopic Data of the Rare Earth Ions	36

Table of Contents (cont'd)

7.3	The Laser Multiplication Coefficient	39
7.4	Nuclear Chemogenics	45
7.5	The critical Laser Ratio	47
7.6	Threshold Conditions	51
8.	THE AsCl_3 (NaCl_3) AND AsCl_3 (UCl_3) LASER SYSTEMS	53
8.1	Conditions for Lasing	53
9.	REFERENCES	57
	APPENDIX I	65
PART B	<u>NUCLEAR PUMPING OF SEMICONDUCTOR LASERS</u>	77
1.	INTRODUCTION	79
1.1	General Preface	79
1.2	Background	80
1.3	Outline of Study	83
2.	THRESHOLD CRITERIA FOR SEMICONDUCTOR LASERS	86
2.1	Photon Detailed Balance	86
2.2	Interband and Intraband Transitions	89
2.3	Transitions Involving Impurity Levels	95
2.4	The Threshold Condition	99
2.5	Threshold Excess Carrier Densities - Intrinsic Semiconductor	103
2.6	Threshold Excess Carrier Densities - Effects of Impurities	107

Table of Contents (cont'd)

2.7	Frequency Dependence of Stimulated Emission	112
3.	FURTHER CHARACTERISTICS OF LASER ACTION	116
3.1	Laser Action	116
3.2	Magnitudes of Rate Coefficients	120
3.3	Density Variation of Rate Coefficients	123
3.4	Mode Structure	129
3.5	Line Width	130
3.6	Approach to Threshold-Effect of Carrier Lifetimes	133
4.	NUCLEAR PUMPING	135
4.1	Physical Processes	135
4.3	Fission Pumping	146
5.	RADIATION DAMAGE IN SEMICONDUCTORS	147
6.	LIQUID SEMICONDUCTORS	149
7.	DEMONSTRATION EXPERIMENT	150
8.	CONCLUSIONS	154
	APPENDIX II	157
PART C	RECOMMENDATIONS	159
	ACKNOWLEDGEMENT	161
	DISTRIBUTION LIST	

LIST OF ILLUSTRATIONS

	Page No.
Figure 2.2.1: Basic Laser Geometry	9
Figure 2.2.2: Comparison of Geometrical and Physical Modes for Geometry-Controlled Lasing	11
Figure 2.2.3: Comparison of Geometrical and Physical Modes for Geometry-Controlled Lasing	11
Figure 3.1.1: Diffraction loss per transit versus $N = a^2/L\lambda$ for circular plane mirrors	14
Figure 4.2.1: Structure and Aggregation of Liquid AsCl_3	19
Figure 4.3.1: Absorption Coefficient of InSb	22
Figure 5.1.1: Scattering Cross-Section for Spherical Particle of Radius a ; λ = Photon Wavelength	24
Figure 6.2.1: Geometry of Scattering by Thin Layer	29
Figure 7.1.1: Low Temperature Halide Liquids	35
Figure 1: Semiconductor Level Scheme	87
Figure 1a: Influence of Unequal Electron and Hole Effective Masses on Threshold Carrier Density	102
Figure 2: Possible Transitions When Impurities are Present	107
Figure 3: Effect of Uncompensated Donors (Te) and Acceptors (Zn) on Threshold Excess Carrier Concentration for GaAs Laser	110
Figure 4: Photon Gain for Conduction Band - Acceptor Level Laser Transition in p-type GaAs	115
Figure 5a: Energy Level diagram for laser action	118
Figure 5: Free-Carrier Generation by Nuclear Radiation	124

Figure 6:	Total number of electrons in conduction band n_e vs energy level ($\Delta E = E - E_c$)	125
Figure 7:	Estimated Negative Absorption Coefficient (GaAs) as Function of $\Delta E = (h\nu - E_g)$	127
Figure 8:	Free Carrier Absorption Coefficient	128
Figure 9:	Excitation of electrons in a semiconductor due to passage of an energetic charged particle.	136
Figure 10:	Residual hole-electron excitation after a time $\approx 10^{-11} - 10^{-12}$ sec.	137
Figure 11:	Range energy curve of protons and alphas in Gallium Arsenide	139
Figure 15:	Experimental Setup	151
Figure 16:	Liquid Nitrogen Setup	153

GENERAL INTRODUCTION

This report presents work conducted under a study Contract No. NONR-4124(00) with the Office of Naval Research. MHD Research, Inc. was the prime contractor and Terra Nova, Inc. was the principal subcontractor.

The contract consisted of a study of two aspects of laser physics.

Part A is concerned with the investigation of physics of liquid lasers, and possible ways of making such a laser including a study of various pumping techniques with emphasis on photonic and nuclear pumping.

Part B is concerned with a detailed study of the nuclear pumping of semiconductors.

Finally, a third part (Part C) is presented which contains recommendations for further work in these areas.

Mention should be made of the contributions made by the several physicists associated with this effort.

Dr. Jozef Eerkens originated the concept of nuclear pumping, and the present contract was a direct result of a proposal submitted to the Office of Naval Research prepared by Dr. Jozef Eerkens and Dr. Francis H. Webb. Dr. Francis H. Webb of MHD Research, Inc. was the principal investigator on this contract. Dr. Webb and Dr. Paul Levine (consultant to MHD Research, Inc.) jointly prepared the section concerned with the nuclear pumping of semiconductors (Part B). Dr. Eerkens of Terra Nova, Inc. prepared the Part A on liquid lasers. Dr. Paul Thiene of MHD Research, Inc. carried out more detailed calculations on the scattering losses which may be encountered in liquid lasers: this material is attached as Appendix I to Part A.

PART A

THE PHYSICAL THEORY OF LUMINESCENT LIQUID LASERS

BY:

Joseph W. Eerkins

1. INTRODUCTION

In this section an investigation of the lasability of certain liquids is carried out. In the first section a discussion of the macroscopic theory of lasers is presented. This section is followed by a detailed examination of the losses which may be encountered including such processes as diffraction losses, absorption losses in the medium, scattering losses, and refractive losses. The discussion on losses is followed by an examination of the conditions which must be present in order to achieve photon multiplication by stimulated emission. Finally, a discussion of two promising laser liquid systems employing AsCl_3 (UCl_3) and AsCl_3 (NdCl_3) is presented.

Appendix I is included which presents a more detailed discussion of the scattering losses which may be encountered in liquid lasers.

2. MACROSCOPIC THEORY OF LASERS

2.1 Basic Photon Processes and Conditions for Laser Action

Rather than following a rigid wave mechanical or quantum point of view for photon interactions, we shall treat these processes such that they can be easily visualized but still maintain all features of rigorous theory.

A photon possesses four (4) basic properties which completely identify it in a laser, namely,

1. Energy (or frequency, or wavelength)
2. Direction of travel
3. Phase
4. Polarization

In passing through a laser medium, a photon may interact with the medium in a number of ways such that one or more of the above properties are changed. In fact, we shall define an interaction as an event which alters the magnitude of one or more of the basic photon properties listed above.

In lasers, one is interested in generating a beam of photons whose four basic properties are as closely identical in magnitude as possible. The closer these magnitudes, the more coherent the beam is. The following interactions or processes may be experienced by photons traveling through a laser resulting in the enhancement or decrease of coherence:

Gainful Processes:

- (1) Multiplication by stimulated emission.

For each photon striking an excited luminescent center in a pumped lasing state, a second photon with identical four basic properties is created.

- (2) Multiple Reflection through 360° .
Photon energy remains the same. Phase direction and polarization are changed in steps (through two or more reflections) until the total change is 360° and the multiply reflected photon possesses the same direction, phase and polarization as before.

Loss Processes:

- (1) Transmission:
Photons are lost from the system by passing through the laser reflector or other boundaries.
- (2) Removal Reflection:
Photons may be reflected at interfaces or boundaries at such an angle that they can never return to the original direction of travel or regain their original phase and polarization. Photons are lost.
- (3) Refractive Losses:
Due to inhomogeneities in the laser medium, photons change their direction of travel and are eventually lost.
- (4) Absorption:
Photons are annihilated (resulting in heat) due to absorption by atoms or molecules of the liquid medium.
- (5) Scattering:
Due to the presence of scattering centers in the medium, photons change their direction of travel and/or energy resulting in a loss of the photon from the lasing beam.

(6) Diffraction:

Due to the wave nature of photons, a loss in coherence occurs between photons traveling over some distance. Changes in energy, direction, phase, and polarization all take place.

Let a photon beam of Φ photons/cm² sec travel along the axis of a cylindrical laser (geometry will be discussed in more detail in Section 2.2). The the net gain or loss of photons after traveling a distance dx in the laser medium is given by:

$$\frac{d\Phi}{dx} = K_l \Phi - K_a \Phi - K_r \Phi - K_s \Phi - K_d \Phi \quad (2.1.1)$$

where

K_l = Multiplication Factor (by stimulated emission)

K_a = Absorption Factor

K_r = Refractive Loss Factor

K_s = Scattering Factor

K_d = Diffraction Factor

Integrating, we find that the loss or gain of photons in the laser medium is given by:

$$\Phi(x) = \Phi_o e^{\alpha x} \quad (\text{photons/cm}^2 \cdot \text{sec}) \quad (2.1.2)$$

where

$$\alpha = K_l - K_a - K_r - K_s - K_d, \text{ cm}^{-1} \quad (2.1.3)$$

We shall be primarily concerned with cylindrical lasers of length L with spherical end reflectors (see Section 2.2) and axial laser beams. For this geometry, a steady build-up and oscillation of laser photons will result if after one pass through the laser medium, enough photons have been added through stimulated emission to make up for absorptive, dispersive, etc. losses and for the transmission and loss of photons upon reflection from the reflectors. Quantitatively, we may express this condition as:

$$e^{\alpha L} \geq \frac{1}{\sqrt{R_1 R_2}} = \frac{1}{R} \quad (2.1.4)$$

where

$$R = \sqrt{R_1 R_2} = \text{geometric mean reflectivity of the two end reflectors whose reflectivities are } R_1 \text{ and } R_2. \quad (2.1.5)$$

L = Length of Laser

The gain per round-trip passage (two traverses) through the laser is given by:

$$F = e^{2(\alpha L - \xi)} \quad (2.1.6)$$

where we define:

$$\xi = - \ln R \quad (2.1.7)$$

In order to have photon multiplication, the exponent in (2.1.6) must be larger than zero. Thus, the condition for laser action may be expressed by the Critical Laser Equation:

$$\alpha \geq \frac{\xi}{L} \quad (2.1.8)$$

or substituting Equations (2.1.3) and (2.1.8):

$$K_1 \geq K_a + K_r + K_s + K_d - \frac{\ln R}{L} \quad (2.1.9)$$

If R is close to unity, $\ln \left(\frac{1}{R} \right) \approx 1 - R = 1 - \sqrt{R_1 R_2}$, and:

$$K_1 \geq K_a + K_r + K_s + K_d + \frac{1 - \sqrt{R_1 R_2}}{L} \quad (2.1.10)$$

Most of the interaction processes discussed above take place between centers or impurities and photons. In this case, the K factors can be expressed in terms of cross-sections:

$$K = N \sigma, \left(\frac{1}{\text{cm}} \right) \quad (2.1.11)$$

where

N = Concentration of centers of impurities per cm^3

σ = Interaction cross-section of center or impurity, cm^2 .

It is the object of a large portion of the remainder of this report to determine quantitatively the magnitude of the various K factors and how they are related to pressure, temperature, and microscopic properties of the laser medium. The most important factor is K_1 , the constant that causes photon multiplication by stimulated emission. The value of K_1 depends in a complicated way on the pumping energy that is provided to maintain a population inversion of excited luminescent centers and on the various mechanisms which effect the population inversion.

After relations for the various K factors have been derived, it will be possible to determine from Equation (2.1.9) or (2.1.10) whether a given laser medium (in conjunction with a certain pumping technique) can be lased, and what the "threshold pump energy" must be. This will be done in Section 8 for a number of selected liquid lasers.

2.2 Geometric Considerations

So far, we only considered the material or physical effects of the laser medium on a photon and under what conditions the medium becomes multiplicative. In addition to these effects, one must also consider the laser's geometry before a complete determination can be made of what photons will lase and in what manner.

In the previous section, we identified a lasing photon by its energy, phase, etc. Actually the quantum of energy emitted due to the stimulated jump of an electron from the upper lasing level to the lower lasing level, has an uncertainty $\Delta(h\nu)$ associated with it which defines a small band of photon energies rather than one. This frequency width $\Delta\nu$ or associated linewidth $\Delta\lambda$ is primarily due to the vibration or motion of the lasing center while emitting the photon. In the case of a gas, for example, it can approximately be expressed as

$$\left(\frac{\Delta\nu}{\nu}\right)_L = \left(\frac{\Delta\lambda}{\lambda}\right)_L = \underbrace{\left[\frac{1.19 \times 10^{-8}}{\lambda(\text{micron})}\right]}_{\text{(Natural Linewidth)}} + \underbrace{\left[1.43 \times 10^{-6} \left(\frac{T(^{\circ}\text{K})}{A_{\text{amu}}}\right)^{\frac{1}{2}}\right]}_{\text{(Doppler Broadening)}} + \underbrace{\left[7.19 \times 10^{11} \frac{\sigma(\text{cm}^2) \lambda(\text{micron}) P(\text{atm})}{T(^{\circ}\text{K})^{\frac{1}{2}} m(\text{amu})^{\frac{1}{2}}}\right]}_{\text{(Pressure Broadening)}} \quad (2.2.1)$$

where

- λ = Photon wavelength (center), microns
- T = Temperature of laser gas, $^{\circ}\text{K}$
- A = Atomic Mass Number of lasing center, amu
- P = Pressure of laser gas, atm

$$m = \text{Reduced mass} = \left(\frac{A_a A_b}{A_a + A_b} \right)^{1/2} \text{ of lasing}$$

centers a with atomic mass A_a and other gas
atoms b with atomic mass A_b , amu

$$\sigma = \text{Gas - kinetic collision cross-section between}$$

other atoms (ions, molecules) of the gas and the
lasing centers, cm^2 .

In solids and liquids, no general relations describing the broadening processes have been derived yet. The subject is presently under intensive investigation. Most $(\frac{\Delta\nu}{\nu})$ values of lasing rare earth ions in solids show a linear temperature dependence, but others show very little dependence on temperature. The outer electrons apparently shield the lasing levels which lie in the unfilled shells from extra-atomic disturbances.

Since the lasing resonances have a finite linewidth, it is of interest to determine if photons of all energies within this width are equally excitable. At this point, it is necessary to examine the constraints of the laser geometry on the resonating lasing photon waves.

We shall assume that the laser geometry will be cylindrical as shown in Figure 2.2.1, and that the reflectors are confocal. This is in many cases the most practical and advantageous shape for a laser

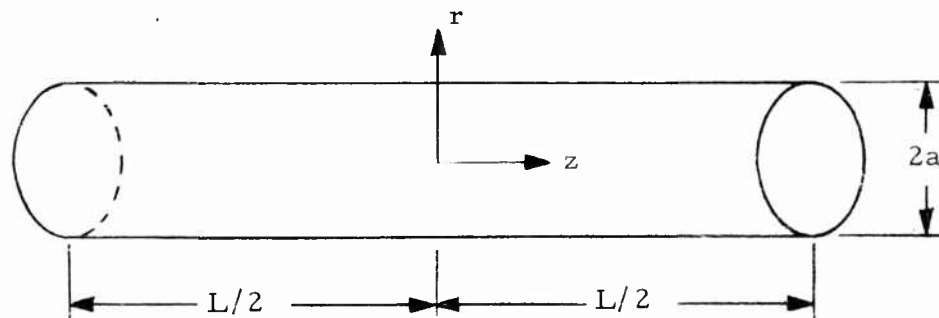


Figure 2.2.1 Basic Laser Geometry

For a cylindrical cavity, resonant electromagnetic modes are given by the following solution of the wave equation:

$$\left(\frac{K_{nm}}{r}\right)^2 + \left(\frac{\pi q}{L}\right)^2 = \frac{4\pi^2 X^2}{\lambda^2} \quad (2.2.2)$$

where $q = 0, 1, 2, 3, \dots$, and K_{nm} is the m^{th} zero of the Bessel function of order n . X is the refractive index and λ is the wavelength. The axial modes obtain when $K_{nm} = 0$ or

$$\lambda = \frac{2LX}{q} \quad (2.2.3)$$

These relations apply strictly for free space, but are still quite accurate if the cavity is filled with a material whose refractive index X is in the neighborhood of 1 - 2.

Two consecutive axial-mode resonances ($q_{m+1} - q_m = 1$) are separated by the wave number:

$$\Delta\left(\frac{1}{\lambda}\right) = \frac{1}{2LX} \quad (2.2.4)$$

or

$$\left(\frac{\Delta\lambda}{\lambda}\right)_c = \frac{\lambda}{2LX} = \frac{1}{q} \quad (2.2.5)$$

Values of $\left(\frac{\Delta\lambda}{\lambda}\right)_c$ of typical geometries are on the order of $\left(\frac{\Delta\lambda}{\lambda}\right)_c \approx 10^{-6}$ for the visible and near-infrared. The relative width of the lasing lines of most rare earth luminescent centers is on the other hand $\left(\frac{\Delta\lambda}{\lambda}\right)_L \approx 10^{-4}$ at $T = 300^\circ\text{K}$. Thus the frequencies of the lasing photons are determined by the geometrically allowable modes and not by the physically allowable frequencies. Figure 2.2.2 illustrates this situation.

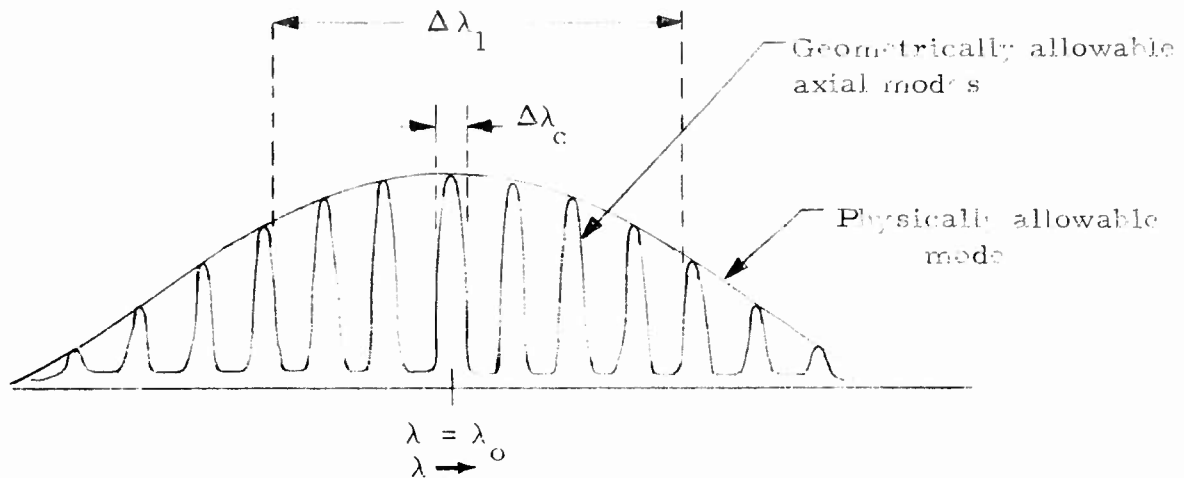


Figure 2.2.2 Comparison of Geometrical and Physical Modes
for Geometry-Controlled Lasing

When laser action occurs, the geometrical mode nearest the center of the physical resonance peak will be the first to deplete the physically available inverted centers, causing so-called "hole-burning" in this center mode and effecting a change in the relative peaks of the geometrical modes. For our present discussion these effects are secondary however.

In gaseous lasers at pressures of a few Torr and at room temperatures, the relative linewidth of the lasing resonance is $\left(\frac{\Delta\lambda}{\lambda}\right)_L \approx 10^{-6}$ and thus of the same order as the geometrically allowable distribution. This situation is depicted in Figure 2.2.3.

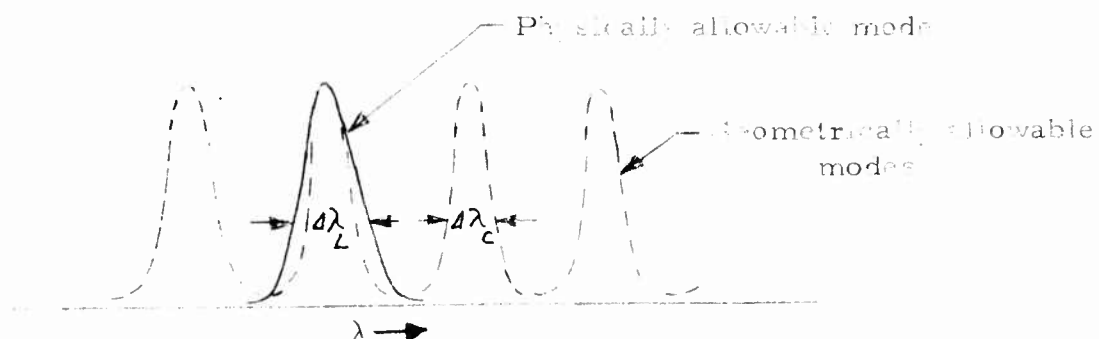


Figure 2.2.3 Comparison of Geometrical and Physical Modes
for Physics-Controlled Lasing

In this case, the distribution of lasing photon frequencies is determined by the physics of photon emission of the luminescent centers.

Aside from the allowable modes, the geometry of the laser also determines the spatial distribution of the amplitude of the oscillating laser beam. Boyd and Gordon (B1) showed that the transverse distribution of the amplitude follows approximately a gaussian distribution given by:

$$A(r, z) = A_o \exp\left(-\frac{r^2}{w^2}\right) \quad (2.2.6)$$

where:

$$w = \frac{L\lambda}{2\pi} \left\{ 1 + \left(\frac{2z}{L}\right)^2 \right\} \quad (2.2.7)$$

The center of the cylindrical laser is assumed to be at $z = 0$, $r = 0$, and the confocal reflectors are at $z = L/2$.

3. DIFFRACTION LOSSES

3.1 Plane Reflectors

In earlier lasers, plane reflectors were used at the ends of a cylindrical laser rod. For plane reflectors, it was determined by Fox and Li that for values of $N_F \lesssim 50$, diffraction losses will become appreciable. Here N_F is defined as:

$$N_F = \frac{a^2 X}{\lambda L} \quad (3.1.1)$$

where:

- a = reflector diameter
- X = refractive index of laser medium
- L = length of laser
- λ = lasing photon wavelength

For ruby and rare-earth lasers, $N_F \sim 1000$, and diffraction losses may be neglected. The Helium (Neon) laser on the other hand $N_F \sim 50$, and a diffraction loss of about 0.1% per pass will occur for the axial mode. Figure 3.1.1 shows the calculations of Fox and Li of diffraction losses for other values of N_F .

Most recent lasers employ confocal reflectors instead of plane reflectors. These are discussed in the next section.

3.2 Confocal Reflectors

For confocal reflectors, the diffraction loss was calculated by Boyd and Gordon (B1). For axial modes they found that the diffraction loss per transit is approximately given by the equation:

$$K_d L \approx 1 - \eta_d = 10.9 \times 10^{-4.94 N_F} \quad (3.2.1)$$

or:

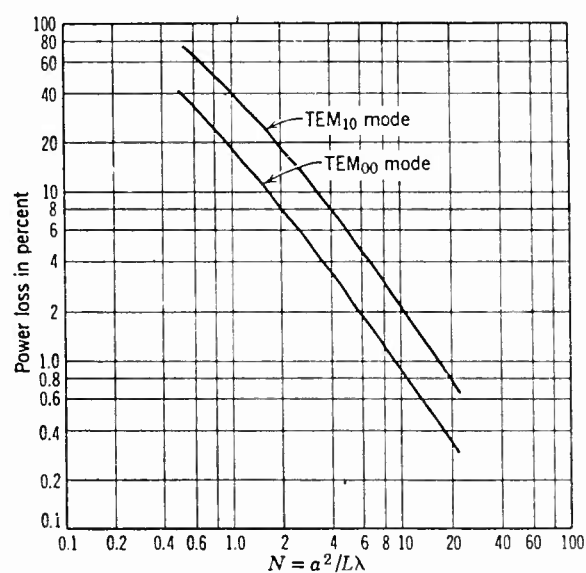
$$\overline{K}_d = \frac{10.9}{L} \times 10^{-4.94 N_F} \quad (3.2.2)$$

where N_F is given by (3.1.1), \overline{K}_d is the average diffractive loss factor discussed in Section 2, and η_d is the efficiency of "non-diffraction" per laser transit. Since in nearly all practical lasers, $N_F > 1$, we find that diffraction losses are negligible in confocally reflected lasers, that $K_d = 0$ and $\eta_d = 1$.

4. ABSORPTION

4.1 General Discussion

The absorption of photons by atoms and molecules of the host liquid is best treated by modern dispersion theory (M1). In this theory, two types of absorption are considered, namely that due to resonances of bound valence electrons and that due to the dissipation by free conduction band electrons. The first type of absorption shows large maxima for certain bands of photon wavelengths, whereas the second



Diffraction loss per transit versus $N = a^2/L\lambda$ for circular plane mirrors.
(Reproduced from the *Bell System Technical Journal* with the permission of the American Telephone and Telegraph Company.)

FIGURE 3.1.1

effect increases quadratically with the wavelength. The two types of absorption are most conveniently treated separately.

In addition to absorption of photons by the liquid medium, absorption of laser photons by the lasing luminescent centers occurs also. However, we shall treat this type of lasing absorption separately in Section 6, under photon multiplication. The net balance of stimulated emission and absorption of lasing photons by lasing centers, constitutes the laser multiplication coefficient.

In general, resonant absorption can occur through three types of interactions between photons and the medium:

1. Electronic
2. Ionic
3. Dipolar

The electronic interaction is one in which a bound electron is set into oscillation by the photon's electromagnetic field. The atom or molecule to which the electron belongs remains stationary in this interaction. In ionic interactions, negative and positive ions oscillate relative to each other, while in dipolar interactions, molecules with permanent dipoles are directed along the photon's electromagnetic field from previously random orientations.

The energies and frequencies that are required to effect electronic interactions lie in the near-infrared to ultraviolet portion of the electromagnetic spectrum. Ionic interactions take place in the far infrared regime while dipolar effects play a role for photons in the UHF to microwave portion of the spectrum. In most ordinary lasers, we have thus only to consider electronic interactions.

In the following, we shall first treat resonant absorption by valence electrons, and then absorption due to conduction electrons. Since in dielectrics only the first type of absorption occurs, and the latter is predominant in conductors, they are commonly referred to as dielectric and conductor absorption. Since the liquid host media that we are considering are semi-conductors, both types of absorption must be examined.

4.2 Dielectric Absorption

Upon solving the equation of motion of a bound electron in the photonic electromagnetic field, one finds for non-conducting (dielectric) media (M1) that:

$$n^2 - \kappa^2 - 1 = \sum_j \frac{(Ne^2 f_j / m \epsilon_0) (\omega_j^2 - \omega^2)}{(\omega_j^2 - \omega^2)^2 + \omega^2 g_j^2} \quad (4.2.1)$$

$$2n\kappa = \sum_j \frac{(Ne^2 f_j / m \epsilon_0) \omega g_j}{(\omega_j^2 - \omega^2)^2 + \omega^2 g_j^2} \quad (4.2.2)$$

where:

$$\begin{aligned} \kappa &= n - ik = \text{Complex Refractive Index} & (4.2.3) \\ \omega &= 2\pi\nu = \text{Angular Photon Frequency} \\ \omega_j &= \text{Resonant Frequency of } j^{\text{th}} \text{ electronic oscillator} \\ N &= \text{Scattering Molecules or Atoms per cm}^3 \\ e &= \text{Electronic Charge} \\ m &= \text{Electron Mass} \\ \epsilon_0 &= \text{Dielectric Constant of Free Space} \\ g_j &= \text{Damping force constant for } j^{\text{th}} \text{ electronic oscillator} \\ f_j &= \text{Oscillator strength of } j^{\text{th}} \text{ electronic oscillator} \end{aligned}$$

$\omega_j = \omega_0$, the other terms of the summation in (4.2.2) are often negligible, and we may write approximately:

$$n^2 - \kappa^2 - 1 = \left(\frac{Ne^2 f_0}{m \epsilon_0} \right) \left(\frac{\omega_0^2 - \omega^2}{(\omega_0^2 - \omega^2)^2 + \omega^2 g_0^2} \right) \quad (4.2.4)$$

$$2n\kappa = \left(\frac{Ne^2 f_0}{m \epsilon_0} \right) \left(\frac{\omega g_0}{(\omega_0^2 - \omega^2)^2 + \omega^2 g_0^2} \right) \quad (4.2.5)$$

The absorption coefficient K_a (see Section 2.1) is related to the complex portion of the refractive index by the relation (M1):

$$K_a = 2 \omega k / c = 4\pi k / \lambda \quad (4.2.6)$$

If the refractive index n is known, we may obtain K_a directly from Equations (4.2.5) and (4.2.6):

$$\begin{aligned} \left(K_a\right)_v &= \frac{\omega c}{n} \left(\frac{e^2}{mc^2 \epsilon_0} N f_o \right) \left(\frac{\omega g_o}{(\omega_o^2 - \omega^2)^2 + \omega^2 g_o^2} \right) = \\ &= 8.45 \times 10^{-3} \left(\frac{f_o N}{n} \right) \left(\frac{\omega g_o}{(\omega_o^2 - \omega^2)^2 + \omega^2 g_o^2} \right), \text{ cm}^{-1} \end{aligned} \quad (4.2.7)^*$$

For frequencies away from resonance ($\omega \ll \omega_o$), where $k \ll n$ and $g_o \ll \omega_o$, we find from (4.2.4):

$$n^2 - 1 = \left(\frac{N e^2 f_o}{m e_o} \right) \frac{1}{\omega_o^2} \quad (4.2.8)$$

Thus if n is given we may calculate ω_o or λ_o from (4.2.8), and vice versa. It turns out experimentally that (4.2.8) gives values for λ_o that are too high by a factor of about 5.4 for most halides. Good agreement with experiment is obtained if one uses the semi-empirical formula

$$\lambda_o = 2.2 \times 10^6 \left(\frac{n^2 - 1}{N f_o} \right)^{\frac{1}{2}}, \text{ cm} \quad (4.2.9)$$

* We use the subscript v on K_a to indicate absorption by valence electron.

which is lower by a factor of 5.4 than the relation obtainable from (4.2.8).

The value of g_o is approximately equal to the width $\Delta\nu$ of the resonance peak at half-maximum. Typical values of $\Delta\nu / \nu_o$ in the resonance region are on the order of 10^{-4} , so that approximately $g_o \approx 10^{-4} \omega_o$. For f_o we may take approximately the number of valence electrons that can be excited in the resonance.

We shall be interested in AsCl_3 as a liquid host for lasable rare earth ions. The structure of AsCl_3 is similar to liquid NH_3 , that is it consists of a triangle with chlorine ions centered on the corners and an arsenic ion at the center, approximately 0.69 \AA above the plane of the triangle as shown in Figure 4.2.1. From (4.2.15), and the measured value of $n = 1.621$, we obtain $\lambda_o = 2600 \text{ \AA}$ corresponding to an energy of 4.76 ev. The gap between the valence and conduction band of the Cl^- ions is estimated to be $E_g \approx 9 \text{ ev}$, so that the first excited level appears to lie half-way between the band-gap, as is reasonable to expect.

For the passage of neodymium-lased photons of 1.06 microns through AsCl_3 we calculate from (4.2.7), using $g_o = 7.26 \times 10^{11} \text{ sec}^{-1}$, $\omega_o = 7.26 \times 10^{15} \text{ cps}$, $N = 7.19 \times 10^{21} \text{ cm}^{-3}$, and $f_o = 3$, that $(K_a)_v = 0.114 \text{ cm}^{-1}$.

4.3 Conduction-band Absorption

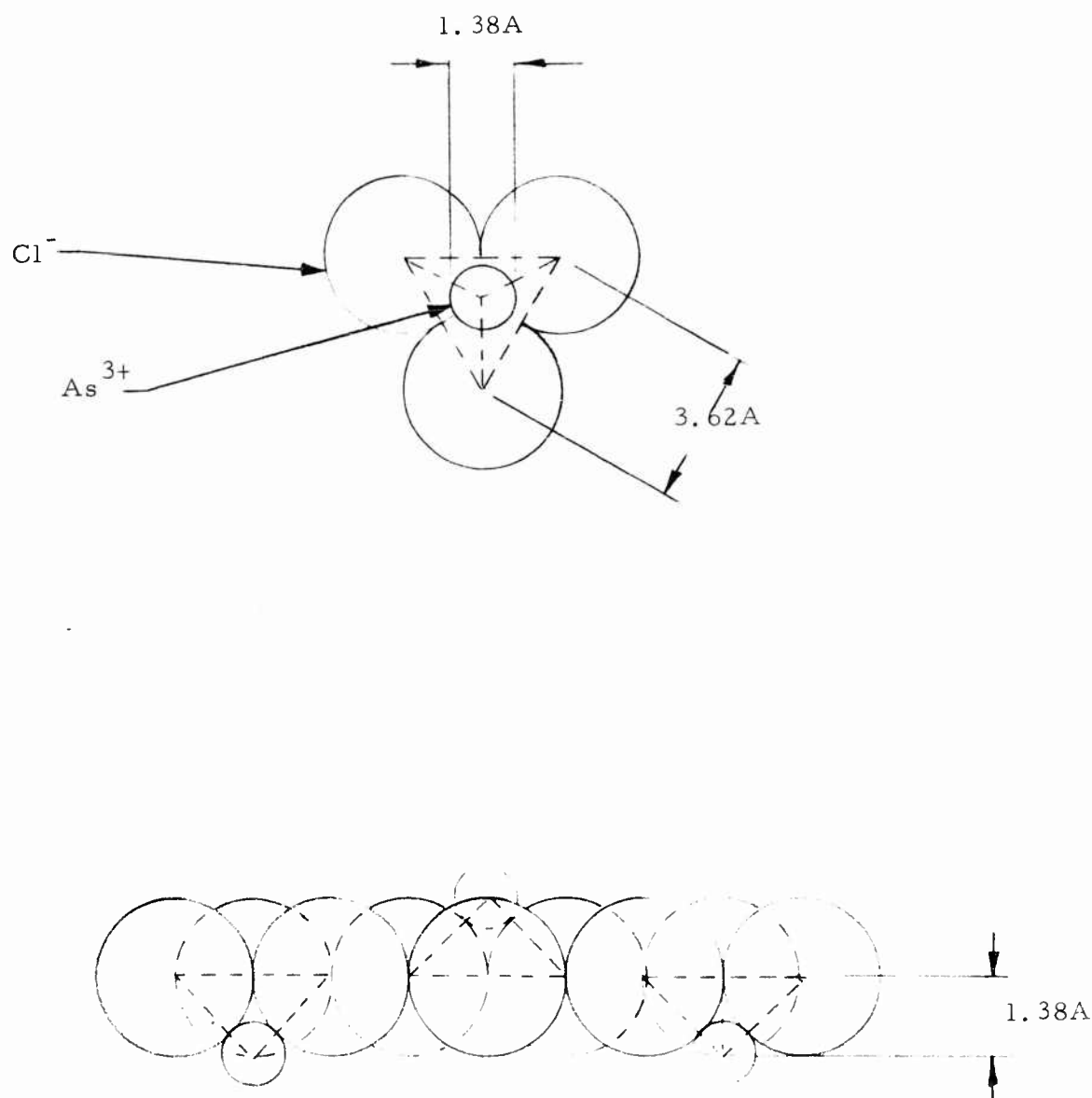
Absorption losses due to photon interactions with conduction electrons may be expressed by Drude's relation (M1):

$$(K_a)_c = \left(\frac{\lambda^2 e^3}{4\pi^2 c n \epsilon_o} \right) \left(\frac{N_n}{m_n^2 \mu_n} + \frac{N_p}{m_p^2 \mu_p} \right), \text{ cm}^{-1} \quad (4.3.1)^*$$

where:

$$N_n = \text{density of negative carriers, } \frac{1}{\text{cm}^3}$$

*The subscription c on K_a indicates absorption by conductor electrons.



Dipole Moment = 1.97 Debye
 Density = 2.163 gms/cm^3 at 20°C
 Refractive Index = 1.621

Figure 4.2.1. Structure and Aggregation of Liquid AsCl_3

- N_p = Density of positive carriers, $\frac{1}{\text{cm}^3}$
 μ_n = Mobility of negative carriers, $\frac{\text{cm}}{\text{sec esu}}$
 μ_p = Mobility of positive carriers, $\frac{\text{cm}}{\text{sec esu}}$
 m_n = Effective mass of negative carriers, gms
 m_p = Effective mass of positive carrier, gms
 n = Positive part of the refractive index for photons of frequency ω .

For laser photon wavelengths away from resonances, the refractive index n may be calculated from (M1):

$$n = \left[1 + \frac{Ne^2 f_0}{m\epsilon_0} \left(\frac{1}{\omega_0^2 - \omega^2} \right) \right]^{\frac{1}{2}} \quad (4.3.2)$$

The mobility of charge carriers in non-polar (covalent) crystals such as diamond, silicon or germanium has been calculated by Seitz:

$$\mu = \frac{2^{1/2} 6^{1/3}}{4\pi} \frac{N^{1/3} e \hbar^2 M}{(m_*)^{5/2} C^2} \frac{k\Theta^2}{(kT)^{3/2}} \quad (4.3.3)$$

where:

- Θ = Debye temperature = $\frac{\hbar \nu_0}{k} (6\pi^2 N)^{1/3}$
 ν_0 = Velocity of sound
 k = Boltzmann constant
 N = Number of atoms per cm^3
 M = Atomic mass
 m_* = Effective mass = $\frac{\hbar^2}{d^2 W / dk^2}$
 W = Carrier energy
 k = Wave number of carrier

$$C = \frac{\hbar^2}{2m} \int |\text{grad} \mu|^2 d\tau = \text{Bloch constant.}$$

Table 4.3.1 shows some experimentally measured values of μ in units of ($\text{cm}^2/\text{sec volt}$).

TABLE 4.3.1

Material	Room Temp.		Arbitrary Temp.		$W_g(\text{ev})$	$C(\text{ev})$
	μ_n	μ_p	μ_n	μ_p		
Si (polycryst)	300	100	$1.5 \times 10^6 T^{-3/2}$	$5 \times 10^5 T^{-3/2}$	1.1	~5
Si (single crystal)	1200	250			1.1	
Ge	3600	1700	$1.9 \times 10^7 T^{-3/2}$	$9 \times 10^6 T^{-3/2}$	0.7	
PbTe (single crystal)	2100	840			0.63	
Diamond					6-7	

Typical effective mass ratios m^*/m vary from 1 (for the alkaline metals) to 30 (Nickel, Platinum). Here m is the actual electron mass.

Values of $(K_a)_c$ for InSb, with carrier concentrations of $N_n = 3.5 \times 10^7$ per cm^3 are shown in Figure 4.3.1. Though AsCl_3 does not quite fall in the same class as the semiconductors, we may estimate its conduction band **absorption** coefficient from some of the values given for semiconductors. We estimate on this basis that $(K_a)_c$ for AsCl_3 is approximately:

$$(K_a)_c \approx 1.5 \times 10^{-17} \lambda^2 (N_n + 3N_p), \text{ cm}^{-1}$$

(4.3.4)

where λ is in microns and N_n, N_p in carriers/ cm^3 .

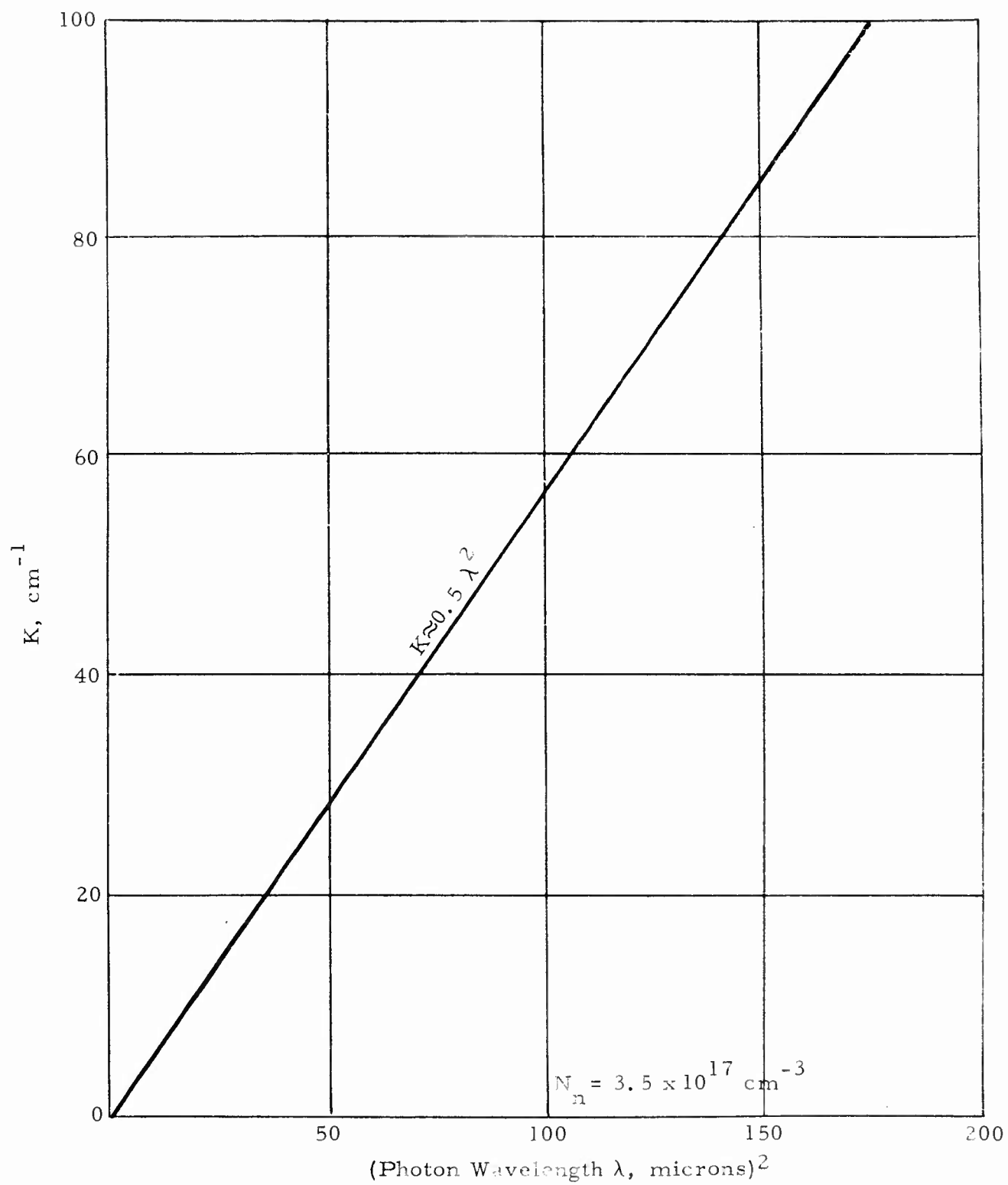


Figure 4.3.1. Absorption Coefficient of InSb

5. SCATTERING

5.1 Discussion

If scattering centers are present in the host medium, photons will be removed from the laser beam by the scattering process. Scattering centers are in general discontinuities in the homogeneous host medium. The luminescent rare-earth halide centers dissolved in AsCl_3 for example present discontinuities which can scatter laser photons. Of course, these same centers absorb and re-emit the lasing photons very strongly also. It is important to determine the scattering effect, however, and establish whether it is excessive relative to the multiplication effect.

In addition to the luminescent centers, macromolecular and other impurities might be present which will cause scattering losses.

The scattering laws change considerably in going from photon wavelengths less than the dimensions of the scattering center to wavelengths larger than the scatterer, as shown in Figure 5.1.1. For large macromolecular scatters, the cross section is equal to the scatterer's geometric projection perpendicular to the laser beam, provided that the scatterer is not transparent to the photon. For scatterers of the same dimensions as the photon wavelength, Mie showed that (VI) the cross-section changes rapidly through successive maxima and minima (see Figure 5.1.1), while for sub-wavelength dimensions the cross-section is given by Rayleigh's scattering laws.

We shall assume that great care is taken in removing all impurities from the liquid host medium and that the primary source for scattering will be the presence of the luminescent centers. The dimensions of various rare earth ions are given in Table 5.1.1.

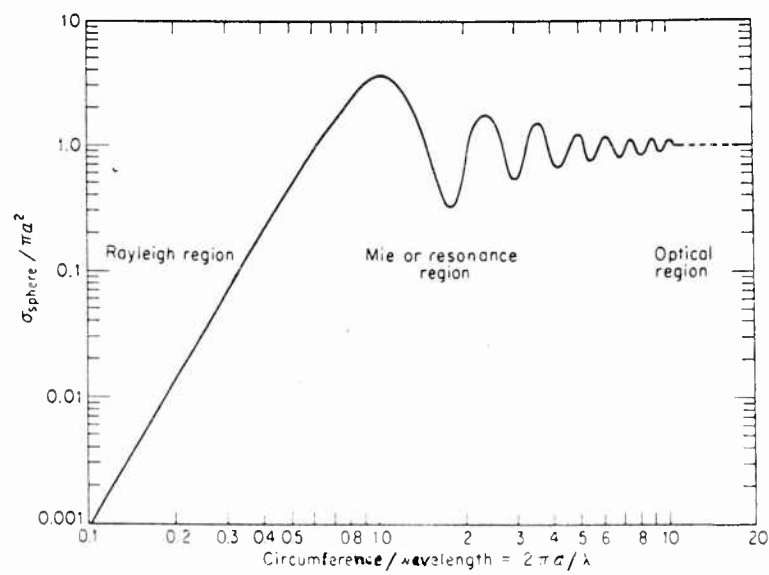


FIGURE 5.1.1 Scattering Cross-Section for Spherical Particle of Radius a ; λ = Photon Wavelength

TABLE 5.1.1 Ionic Radii

ION	RADIUS (Å)	ION	RADIUS (Å)
Cl ⁻	1.81	Nd 3+	1.15
As ³⁺	0.69	Dy ²⁺	1.27
B ³⁺	0.26	Dy ³⁺	1.07
U ³⁺	1.12	Tm ²⁺	1.24
Sm ²⁺	1.33	Tm ³⁺	1.04
Sm ³⁺	1.13	Ho ³⁺	1.05
Pr ³⁺	1.16	Er ³⁺	1.04

It is clear from the table that for lasing Neodymium photons of 10,6000 Angstroms, for example, Rayleigh scattering will apply, and the same situation holds true for nearly all photons in ordinary lasers. We shall limit therefore our remaining discussions to Rayleigh scattering.

5.2 Rayleigh Scattering

For Rayleigh scattering in which the scatterer's dimensions are much smaller than the photon wavelength, Lord Rayleigh calculated for the scattering coefficient:

$$K_s = \frac{1}{6\pi\epsilon_o^2} \frac{Nf_o^4 e^4}{m^2 c^4} \frac{\lambda_o^4}{\lambda^4} = \quad (5.2.1)$$

$$= 0.421 \times 10^{26} Nf_o^4 (\lambda_o/\lambda)^4, \text{ cm}^{-1}$$

where:

- N = Number of scattering centers/cm³
- ρ = Density of scattering centers, gms/cm³
- f_o = Number of oscillating electrons per scatterer ≈ Z of scatterer
- A = Atomic mass number of scatterer
- m = Electron mass

c = Velocity of light

λ_o = Fundamental Resonant Wavelength

λ = Photon wavelength

For a solution of mole fraction y of Nd Cl_3 in AsCl_3 , assuming that $\lambda_o \approx 1000 \text{ \AA}$, $f_o = 3$, and with a AsCl_3 density of $7.19 \times 10^{21} \text{ molecules/cm}^3$, we obtain for 1.06 micron photons:

$$K_s = 2.45 \times 10^{-7} y \text{ cm}^{-1} \quad (5.2.2)$$

From (5.2.2) we see that scattering by luminescent centers won't be a serious problem even for theoretical mole fractions up to 100%.

6. REFRACTIVE LOSSES

6.1 General Discussion

When pumping heat is deposited in the host liquid of a laser, thermal and density gradients will be set up which will cause variations in the refractive index. This will cause laser beam photons to bend away from the axial direction and consequently produce losses.

Aside from inhomogeneities produced by heat, other inhomogeneities may exist due to the formation of domains or clusters in the host liquid. For example AsCl_3 is a pyramid-shaped symmetric-top molecule with a dipole moment. These molecular dipoles may form domains in which all dipoles are aligned in a certain direction. From an examination of the liquid structure, it appears more likely however that successive neighboring molecular pyramids have their tops alternatively up and down. The base triangles (with a Cl^- ion on each corner) form close-packed hexagonal layers between which the As^{3+} ions are nestled. In this case dipole domain formation will be suppressed. At present no experimental data are available which will verify either one of these liquid structure models.

In the following we shall make an estimate of the refractive losses due to uniform heat generation in the host liquid.

6.2 Refractive Losses Due to Laser Heating

Heat deposited in the laser medium will in general be transferred by the three mechanisms of conduction, convection and radiation. The laser liquid may be convectively cooled by continuous circulation or the liquid may be stagnant and heat is transferred by conduction and gravity-induced convection. The latter situation is undesirable since it creates irregular inhomogeneities. Only in pulsed operation is it possible that laser action takes place before thermal convective effects disturb lasing conditions.

We are only interested here in obtaining an estimate of the effects of heating on laser action. We shall take, therefore, a simple steady-state temperature distribution for volumetrically heated media, and determine the refractive losses caused by the density gradient. More complex cooling and heating distributions can best be analyzed on a case-for-case basis; the present analysis can serve as a guide for more complicated situations.

The radial steady-state temperature distribution in a pure conduction-cooled cylindrical internally-heated medium is given by

$$T(r) - T_a = \frac{Q}{4K}(a^2 - r^2), \text{ for } 0 \leq r \leq a \quad (6.2.1)$$

where

$T(r)$ = temperature at point r from the center of the cylinder, $^{\circ}\text{K}$

T_a = temperature at boundary of cylinder, $^{\circ}\text{K}$

Q = heat source, $\frac{\text{cal}}{\text{sec} \times \text{cm}^3}$

K = thermal conductivity of cylinder, cal/cm
x sec $^{\circ}\text{K}$

a = radius of cylinder, cm

r = radial distance from center of cylinder, cm

The temperature distribution will induce a density distribution given by:

$$\begin{aligned} N(r) &= N_a \left[\frac{1}{1 + \beta(T(r) - T_a)} \right] = \\ &= N_a \left[\frac{1}{1 + \gamma(a^2 - r^2)} \right] = \\ &N_a \left(1 - \gamma(a^2 - r^2) \right) \end{aligned} \quad (6.2.2)$$

where

$$\gamma = \frac{Q\beta}{4K}, \text{ cm}^{-2} \quad (6.2.3)$$

β = volumetric coefficient of expansion, $1/^{\circ}\text{K}$

N = atoms or molecules per cm^3

The subscript a refers to values at $r = a$. In the above it is assumed that the liquid is free to expand. In other words the pressure remains constant in the liquid.

To calculate refractive losses due to the inhomogeneous distribution given by (6.2.2), consider a cross-sectional slab of the laser medium of thickness dz , as shown in Figure 6.2.1.

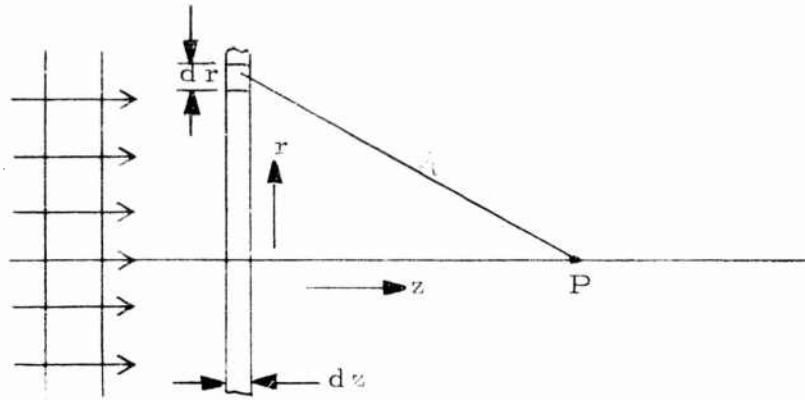


Figure 6.2.1 Geometry of Scattering by Thin Layer

Let the electric vector of the incident wave have unit amplitude so that $E_i = \sin(2\pi z / \lambda)$, and let the fraction of the scattered wave that reaches point P be E_s . Then if the fraction of the incident wave that is scattered* is small, we have that the total electric vector at P is approximately:

$$E_{\text{tot}} = E_i + E_s. \quad (6.2.4)$$

Now the scattered energy is proportional to the scattering cross-section σ of the scattering atoms or molecules, and therefore $E_s \propto \sigma^{1/2}$. If there are N scatterers per cm^3 , the scattering contribution at P by scattering events in the annulus $2\pi r dr dz$ is given by:

$$dE_s = N \sigma^{1/2} \cdot \sin\left(\frac{2\pi R}{\lambda}\right) \cdot \frac{2\pi r dr dz}{R} \quad (6.2.5)$$

Now the density of scatterers varies in accordance with Equation (6.2.2), so that the total scattering contribution at P from the slab of thickness dz is given by:

$$E_s = N_a \sigma^{1/2} dz \int_{r=0}^a \frac{1 - \gamma(a^2 - r^2)}{R} \sin\left(\frac{2\pi R}{\lambda}\right) 2\pi r dr =$$

(continued)

*In this section we mean by "scattering," coherent elastic scattering.

$$\begin{aligned}
&= N_a \sigma^{\frac{1}{2}} \lambda dz \left[\left\{ (1 - \gamma (a^2 + z^2) + \frac{\gamma \lambda^2}{4\pi^2} \left(\frac{4\pi^2 z^2}{\lambda^2} - 2 \right) \right\} \cdot \right. \\
&\quad \cdot \cos \left(\frac{2\pi z}{\lambda} \right) - \left\{ 1 - \gamma (a^2 + z^2) + \frac{\gamma \lambda^2}{4\pi^2} \left(\frac{4\pi^2 (z^2 + a^2)}{\lambda^2} - 2 \right) \right\} \cdot \\
&\quad \cdot \cos \left(\frac{2\pi \sqrt{z^2 + a^2}}{\lambda} \right) + \frac{\gamma \lambda}{\pi} \sqrt{z^2 + a^2} \sin \left(\frac{2\pi \sqrt{z^2 + a^2}}{\lambda} \right) + \\
&\quad \left. - \frac{\gamma \lambda}{\pi} z \sin \left(\frac{2\pi z}{\lambda} \right) \right]
\end{aligned}$$

(6.2.6)

We shall be interested below in obtaining the differential losses by a slab dz at $z = 0 + dz$. We have then that $z = 0 + dz \ll a$, so that we may neglect sine and cosine terms of $\sqrt{z^2 + a^2}$ since one must assume some damping; scattered waves arriving at $(r = 0; z = 0 + dz)$ from $r = a$ are much weaker than those coming from scattering centers closer by. Doing this, Equation (6.2.6) simplifies to:

$$E_s = N_a \sigma_a^{\frac{1}{2}} \lambda dz \left[\left\{ (1 - \gamma (a^2 + z^2)) + \frac{\gamma \lambda^2}{4\pi^2} \left(\frac{4\pi^2 z^2}{\lambda^2} - 2 \right) \right\} \cdot \right. \\ \left. \cdot \cos \left(\frac{2\pi z}{\lambda} \right) - \frac{\gamma \lambda}{\pi} z \sin \left(\frac{2\pi z}{\lambda} \right) \right] \quad (6.2.7)$$

A similar analysis in which the index of refraction or N is constant, yields:

$$\left(\frac{E_s}{N = \text{const.}} \right) = N \sigma^{\frac{1}{2}} \lambda dz \cdot \cos \frac{2\pi z}{\lambda} \quad (6.2.8)$$

Since $\sin(A + B) = \sin A \cos B + \cos A \sin B \cong \sin A + B \cos A$, if B is assumed small, we have that the amplitude at P of a photon wave in a homogeneous medium ($N = \text{const.}$) is:

$$(E + E_s) = \sin \frac{2\pi z}{\lambda} + N \sigma^{\frac{1}{2}} \lambda dz \cos \frac{2\pi z}{\lambda} = \\ \approx \sin \left(\frac{2\pi z}{\lambda} + N \sigma^{\frac{1}{2}} \lambda dz \right) \quad (6.2.9)$$

which shows that the amplitude is unchanged (no power loss) but that the phase is shifted by $N \sigma^{1/2} \lambda dz$.

In the non-homogeneous medium on the other hand we find from Equation (6.2.7) that:

$$E + E_s = \sin \left(\frac{2\pi z}{\lambda} \right) - \frac{\gamma \lambda}{\pi} z \sin \left(\frac{2\pi z}{\lambda} \right) + \\ \text{(continued)}$$

$$\begin{aligned}
& + N_a \sigma_a^{\frac{1}{2}} \lambda dz \left\{ (1 - \gamma a^2) - \frac{\gamma \lambda^2}{2\pi^2} \right\} \cos \frac{2\pi z}{\lambda} = \\
& = \left(1 - \frac{\gamma \lambda}{\pi} z \right) \sin \frac{2\pi z}{\lambda} + \left(1 - \frac{\gamma \lambda}{\pi} z \right) N_a \sigma_a^{\frac{1}{2}} \lambda dz \cdot \\
& \cdot \left(\frac{1 - \gamma a^2}{1 - \frac{\gamma \lambda}{\pi} z} \right) \cos \left(\frac{2\pi z}{\lambda} \right), \text{ or:}
\end{aligned}$$

$$E + E_s \approx \left(1 - \frac{\gamma \lambda}{\pi} z \right) \sin \left(\frac{2\pi z}{\lambda} + (1 - \gamma a^2) N_a \sigma_a^{\frac{1}{2}} \lambda dz \right),$$

(6.2.10)

where we neglected some terms on the basis that $\lambda \ll a$ in practical laser systems.

Comparing (6.2.10) with 6.2.9) we see that in addition to a changed phase shift, a change in amplitude (power loss) occurs when the medium is not homogeneous. Since the power is proportional to the square of the amplitude, we have:

$$\frac{d\varphi}{\varphi_0} = \frac{1 - \left(1 - \frac{\gamma \lambda}{\pi} z \right)^2}{1} = \frac{2\gamma \lambda}{\pi} z \quad (6.2.11)$$

or since we did our analysis at $z = 0 + dz$:

$$\frac{d\varphi}{\varphi_0} = \frac{2\gamma \lambda}{\pi} dz \quad (6.2.12)$$

We find thus from this zero-order analysis that:

$$K_r = \frac{2\gamma\lambda}{\pi} = \frac{Q\beta\lambda}{2\pi K} \quad (6.2.13)$$

For As Cl_3 , we have that $\beta = 4 \times 10^{-4} (\text{°K})^{-1}$, $K = 0.017$ cal/cm · sec. °K , so that for Neodymium-lased photons of 1.06 microns:

$$K_r = 3.97 \times 10^{-7} Q, \text{ cm}^{-1} \quad (6.2.14)$$

where Q is in calories/cm³ · sec. For laser action it is estimated that on the order of 1 KW per cm³ of input pump energy is required, or $Q = 239$ cal/sec · sec³. From (6.2.14), we find then that $K_r = 0.95 \times 10^{-4} \text{ cm}^{-1}$. It was assumed that $\gamma < 1/a^2$ in the above analysis. For lasers of radius $a \leq 0.5$ cm, the result should be fair, since $\gamma = 1.4 < 4$.

7. PHOTON MULTIPLICATION BY STIMULATED EMISSION

7.1 General Considerations

In this report we are interested in luminescent liquid lasers. Semiconductor liquid lasers will be discussed in Part B. We shall furthermore restrict our analysis to inorganic lasers. Organic liquid lasers are subject of intensive studies elsewhere.

For inorganic laser liquids the most suitable luminescent centers that can be incorporated in the liquid lattice appear to be the rare earth ions. Suitable inorganic host media are the liquid halides. The halide liquids have some degree of structure and it is expected that the internal electromagnetic fields are similar to those in solids of which a large body of knowledge already exists. If direct nuclear pumping is considered, one has the further advantage that little or no radiolysis occurs in halides.

A list of promising liquid halides is given in Table 7.1.1. Of these AsCl_3 and BCl_3 look convenient as hosts. The rare earth halides NdCl_3 , UCl_3 , SmCl_3 , EuCl_3 , GdCl_3 , ErCl_3 , etc., may be dissolved in them as luminescent centers. Lasing photons from rare earth centers are created by electron transitions between the inner ion-filled levels. These levels are strongly screened from extra-atomic disturbances by the outer electrons of the rare earth ion, which explains the line sharpness of the emitted photons. Since the rare earth ions in liquid halides experience a field which is not much different from that in glasses, it is expected that the lines emitted by them should be approximately the same as that in glass.

The effect of the lattice fields on the linewidth of an inner shell electron transition is very complicated to treat theoretically. G. H. Dicke (D1) discusses some of the various effects qualitatively but concludes that reliable information concerning these effects can only be obtained experimentally. It was thought for a while that laser action in liquids would be difficult to achieve due to the high internal electric field fluctuations which would widen the lines considerably. However, several liquids have been lased now and these arguments appear to have been exaggerated. It is important that the luminescent centers are in a relatively constant field as evidenced by the fact that in the first liquid laser that operated, the luminescent center was anchored in a large organic clathrate molecule which shielded the center from outside field fluctuations. It may be necessary to employ solutions of complex rare earth molecules rather than the simple rare earth chlorides mentioned above in order to achieve laser action. Experiments will be necessary to settle these questions. We shall assume in all of the following that the rare earth chlorides will be lasable and that the linewidths are comparable to those of the rare earth ions in solids. Should it be found experimentally that this is not so, then all of the following analysis is still valid if one finds a rare earth complex molecule instead of a chloride that will lase, and one substitutes the former for the latter.

The method by which the electrons in the unfilled shells of the luminescent centers are excited to lasable states can be either through the absorption of a photon of the right energy, or by excitation through energy

HALIDE ELEMENT	IODIDE (GMS/CC)	BROMIDE (GMS/CC)	CHLORIDE (GMS/CC)	FLUORIDE (GMS/CC)
	M.P. ; B.P. (°C) (°C)	M.P. ; B.P. (°C) (°C)	M.P. ; B.P. (°C) (°C)	M.P. ; B.P. (°C) (°C)
Antimony	SbI ₃ (4.77) 167 ; 401	SbBr ₃ (4.15) 96.6 ; 280	SbCl ₃ (3.14) 73.4 ; 223	SbF ₃ (4.38) 292 ; subl.
Arsenic	AsI ₃ (4.39) 146 ; 403	AsBr ₃ (3.54) 32.8 ; 221	AsCl ₃ (2.16) -18 ; 130	AsF ₃ (2.67) -8.5 ; 63
Boron	BI ₃ (3.35) 43 ; 210	BBr ₃ (2.65) -46 ; 90.1	BCl ₃ (1.43) -107 ; 12.5	Gas
Carbon	Decomp.	CBr ₄ (3.42) 48.4 ; 189.5	CCl ₄ (1.595) -23.0 ; 76.8	Gas
Gallium	GaI ₃ (4.15) 212 ; 345	Ga Br ₃ (3.69) 121.5 ; 279	GaCl ₃ (2.36) 77.9 ; 201	—
Germanium	GeI ₄ (4.33) 144 ; dec.	GeBr ₄ (3.13) 26.1 ; 185.5	GeCl ₄ (1.88) -49.5 ; 83.1	Gas
Phosphor	PI ₃ () 61 ; dec.	PBr ₃ (2.85) -40 ; 173	PCl ₃ (1.57) -91 ; 75.5	Gas
Silicon	SiI ₄ () 120.5 ; 290	SiBr ₄ (2.81) 5 ; 153	SiCl ₄ (1.48) -70 ; 57.6	Gas
Sulphur		S ₂ Br ₂ (2.64) -40 ; 54	S ₂ Cl ₂ (1.68) -80 ; 136	SCl ₂ (1.62) -78 ; 59
Tin		SnBr ₄ (3.34) 31 ; 202	SnCl ₄ (2.23) -33 ; 114	
Titanium			TiCl ₄ (1.73) -30 ; 136.4	
Vanadium τ			VC1 ₄ (1.82) -20 ; 148.5	
Aluminum	AlI ₃ (3.98) 191 ; 360	AlBr ₃ (3.01) 97.5 ; 263	AlCl ₃ (1.31) 190 ; 183 2 atom	
Molybdenum			MoCl ₅ (2.93) 194 ; 268	MoF ₆ (2.55) 17 ; 35
Niobium		NbBr ₅ 150 ; 362	NbCl ₅ (2.75) 194 ; 254	NbF ₅ (3.92) 72 ; 220

TABLE 7.1.1

Low Temperature Halide Liquids

exchange with a free (conduction-band) electron. In the first technique a flashlamp is used as pump source whose output spectrum peaks at the desired pumping energy level. In the second technique, electrons are excited from the balance state to an excited state or to the conduction band of the host medium by energetic particles or radiation from a nuclear source. The electrons then collide with the luminescent centers and transfer their energy to the center resulting in the excitation of one of the electrons of the unfilled shells to a lasable state. The latter mechanism is one that takes place in scintillators of radiation counters. It will be discussed in more detail in the next section.

In order that the mechanisms described result in the efficient formation of lasable states and in a lasable population inversion, many conditions must simultaneously hold. We shall examine these conditions in the following sections.

7.2 Spectroscopic Data of the Rare Earth Ions

In order to calculate the multiplication constant K_1 defined in Section 2, certain spectroscopic constants of the lasing transition must be known. We shall investigate these parameters in this section.

In Figure 7.2.1 (composed by G. H. Dieke), the observed energy levels of the trivalent rare-earth ions are shown. Lasing action takes place for jumps between lower-lying metastable states as shown for Nd^{3+} .

By absorption of a quantum or by excitation during a free electron - luminescent center interaction, the electron is excited to one of the upper states or bands from where it rapidly cascades downwards till it is trapped in a metastable state, which constitutes the upper lasing level. Little theoretical work has been done to determine what fraction η_c of the pumped-up higher levels cascades to the upper lasing level of interest. The problem is rather complicated and varies from case to case. The selection rules $\Delta l = \pm 1$, etc., are of some help, but most information to date has been obtained experimentally. In our analysis below we shall arbitrarily assume

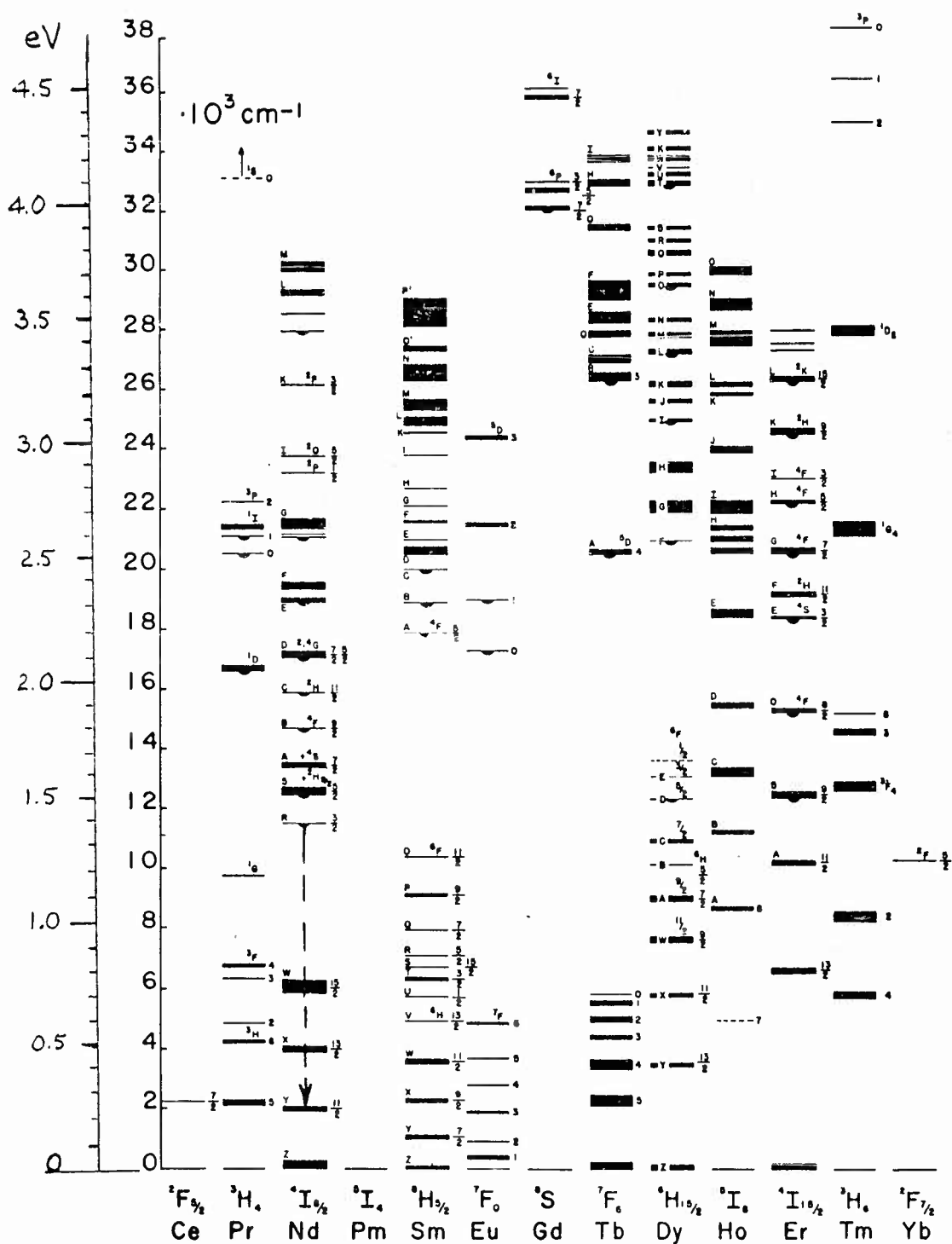


FIGURE 7.2.1 Observed energy levels of the trivalent rare earth ions

The width of the levels indicates the total separation of the Stark components in the anhydrous trichlorides (with a few exceptions). A pendant circle means fluorescence observed from this state.

that $\eta_c = 0.2$, that is 20% of the pumped electrons will cascade to the desired upper lasing level.

In Section 4, we determined that the fundamental resonance in AsCl_3 was 4.76 ev. This is the energy that can be absorbed by a valence electron of the Cl^- ions of the host medium. Thus if these electrons are excited to this level and the exciton is passed on till it collides with a rare earth center, 4.76 ev can be absorbed by the center which is of the right magnitude for pumping (see Figure 7.2.1). Energy absorbed by electrons that are boosted to the (estimated) 9 ev conduction band, can also be conveniently disposed of at the centers through the dropping of the electron from the conduction band to the excitation level with the transfer of $9 - 4.76 = 4.24$ ev to the center for excitation. The remaining 4.76 ev is transferred as an exciton and can activate a second luminescent center.

Dieke (D1) has studied a large number of rare earth salts and finds that the chlorides of the rare earths exhibit many fluorescent lines and more so than nearly all other salts. This finding seems to support the idea that excited electrons from Cl^- ions have the proper energies in lattice structures to efficiently induce fluorescence in the rare earth ions. It appears, therefore, prudent to choose a chloride as the host medium.

Kittle (K1) cites a lot of evidence that excitons in halides can diffuse over distances of at least 1000 lattice constants and transfer their energy upon encountering a center. In Copper-doped Zinc Sulphide, a similar mechanism transfers 10% of the incident energy of nuclear radiation (which boosts electrons of sulphur ions into the excitation state and into the conduction band) into emitted light from the luminescing Copper centers.

If the pump source is photonic rather than nuclear, it is expected that the electrons from the Cl^- ions will also aid in exciting the luminescent centers. The source's photon energy distribution will peak somewhere in the neighborhood of 2 - 4 ev in order to pump effectively. A considerable number of photons of energy above 4.76 ev will, therefore,

also be present and these will excite the Cl^- valence electrons to excited states. The resulting excitons will then pump the centers as before.

Three important spectroscopic quantities which are needed in addition to n_c , are the spontaneous lifetimes of the upper and lower lasing level, τ_2 and τ_1 , and the spontaneous relaxation time for the particular $2 \rightarrow 1$ transition, which we shall designate by τ . For U^{3+} a value for $\tau = 130 \mu\text{sec}$ has been measured. Based on this value, it is estimated that $\tau_2 \approx 125 \mu\text{sec}$ and $\tau_1 \approx 8 \mu\text{sec}$. It was found further that above 90°K , de-excitation by phonons becomes important and it was determined that $\tau = 15 \mu\text{sec}$ at 300°K . The phonon-assisted de-excitation rate constant is thus:

$$K_p (T = 300) = \frac{1}{15} - \frac{1}{130} = \frac{1}{17} = 0.059 \text{ sec}^{-1},$$

for Uranium.

For Neodymium and the other rare earth ions, little data on τ , τ_1 , and τ_2 have been published. For lack of anything better, we shall use the values for the Uranium laser transition in calculations aimed at estimating laser action by rare earth ions.

7.3 The Laser Multiplication Coefficient

When a photon of lasing frequency encounters a luminescent center in the upper lasing state(2), it will stimulate the de-excitation of this state to the lower lasing level (1) and produce a second photon of the same frequency coherent with itself. Thus multiplication takes place. When such a photon encounters a center in the lower lasing state (1) however, the inverse process takes place, and the photon is absorbed. It is clear that if photon multiplication is to take place, there should be more centers present in the medium in the upper lasing state(2) than in the lower state (1).

Schawlow (S1) shows that for excited state densities N_1 and N_2 , the laser multiplication constant K_1 is given by:

$$K_1 = \frac{2}{\Delta\nu} \sqrt{\frac{\ln^2}{\pi}} \left(\frac{\lambda^2}{8\pi} \right) \left(\frac{g_2}{g_1} \right) \left(\frac{N_2 - N_1}{\tau} \right) \quad (7.3.1)$$

where:

- $\Delta\nu$ = Spectral linewidth of the $2 \rightarrow 1$ spontaneous transition, cps
- λ = Wavelength of photons emitted by $2 \rightarrow 1$ transition, cm
- N_1, N_2 = Population densities of active atoms in state 1 and 2 respectively, atoms/cm³
- g_1, g_2 = Statistical weights (multiplicity) of lower (1) and upper (2) states
- τ = Mean life for spontaneous emission of photons from state 2 to state 1, sec.

The reason why physical constants for spontaneous emission enter in Equation (7.3.1) is that the absorption and stimulated emission probabilities for a photon-excited center encounter are related to the intrinsic properties of the $2 \rightarrow 1$ transition, the latter being most easily expressed in terms of constants that can be measured from spontaneous $2 \rightarrow 1$ emissions. Einstein first derived the basic relations between the rate constants or probabilities for absorption, stimulated emission, and spontaneous emission.

We next define the "critical laser ratio" C_{12} :

$$C_{12} = \frac{N_1}{N_2} \quad (7.3.2)$$

For laser action to be possible at all, C_{12} must always be less than 1, that is:

$$C_{12} < 1, \text{ for laser action.} \quad (7.3.3)$$

Substituting C_{12} in (7.3.1), we obtain:

$$K_1 = \frac{2}{\Delta \nu} \sqrt{\frac{\ln 2}{\pi}} \left(\frac{\lambda^2}{8\pi} \right) \left(1 - C_{12} \right) \frac{g_2}{g_1} \frac{N_2}{\tau} \quad (7.3.4)$$

The parameter C_{12} depends strongly on the kinetics of the densities of states 1 and 2 and will be discussed in detail in Section 7.5. It depends on temperature, pressure, chemical kinetics and a number of other effects.

In Section 7.5, a kinetics analysis is made yielding expressions for N_2 and N_1 under steady state conditions. Substituting these values for N_2 and N_1 into (7.3.4) and simplifying, yields:

$$K_1 = 0.431 c_s Q \frac{f_2 B \tau_2}{\Phi} \bullet \left[\frac{(1 - \gamma_{12}) B \tau_1 + 1 + K_{p1} \tau_1}{(1 + B \tau_1 + K_{p1} \tau_1) (1 + B \gamma_{12} \tau_2 + K_{p2} \tau_2) - \gamma_{12} B^2 \tau_1 \tau_2} \right], \text{ cm}^{-1} \quad (7.3.5)$$

where:

c_s = constant defined by Equation (7.4.4).

Q = Pumping power density

Φ = Photon flux inside cavity, $\frac{\text{photons}}{\text{cm}^2 \text{ sec}}$

$$f_2 = \tau_2 / \tau \quad (7.3.6)$$

$$\gamma_{12} = g_1 / g_2 \quad (7.3.7)$$

$$B = 0.0867 \frac{g_2}{g_1} \frac{\lambda^2 \Phi}{\tau \Delta \nu}, \frac{1}{\text{sec}} \quad (7.3.8)$$

K_{pi} = Rate constant for de-excitation of level
i by phonon interaction; sec^{-1} .

(All parameters are in cgs units.)

If phonon de-excitation is negligible, Equation (7.3.5) reduces
to:

$$K_1 = 0.431 c_s Q \frac{f_2 B \tau_2}{\Phi} \left[\frac{1 - \gamma_{12}) B \tau_1 + 1}{1 + B (\tau_1 + \gamma_{12} \tau_2)} \right] \quad (7.3.9)$$

With neglect of phonon-assisted de-excitation, we have that

$$\left(\frac{dN_2}{dt} \right)_{\text{pumping}} = \left(\frac{dN_2}{dt} \right)_{\substack{\text{stimul.} \\ \text{emission} \\ \text{(lasing)}}} + \left(\frac{N_2}{\tau_2} \right)_{\substack{\text{spont.} \\ \text{emission}}} \quad (7.3.10)$$

Now, under steady-state conditions, the loss of laser photons from the
system must equal the rate of stimulated emissions, and so:

$$\left(\frac{dN_2}{dt} \right)_{\substack{\text{stim.} \\ \text{emission}}} e^{\alpha L} = \frac{T_r \Phi}{L} \quad (7.3.11)$$

where:

α = Laser "absorption" coefficient defined by
Equation (2.1.3)
 L = Length of laser, cm
 T_r = Transmission coefficient of laser reflectors

From (7.3.11) and (7.3.10), we then have for Φ :

$$\Phi = \frac{L}{T_r} e^{\alpha L} \left(c_s Q - \frac{N_2}{\tau_2} \right). \quad (7.3.12)$$

Substituting Equation (7.5.3) for N_2 , we get:

$$\Phi = \frac{Le^{\alpha L}}{T_r} c_s Q \frac{\gamma_{12} B \tau_2}{1 + B(\tau_1 + \gamma_{12} \tau_2)} \quad (7.3.13)$$

Substituting this value for Φ in (7.3.8) and solving for B , we get:

$$B = \frac{0.0867 f_2^2 \lambda^2}{(\tau_1 \gamma_{12} \tau_2) \Delta \nu} \frac{Le^{\alpha L}}{T_r} c_s Q \quad (7.3.14)$$

Also Φ is solved explicitly now:

$$\Phi = \left(\frac{\gamma_{12} \tau_2}{\tau_1 + \gamma_{12} \tau_2} \right) \frac{Le^{\alpha L}}{T_r} c_s Q \quad (7.3.15)$$

With (7.3.14) and (7.3.15), Equation (7.3.9) reduces to:

$$K_1 = 0.0374 \frac{f_2^2 \lambda^2}{\gamma_{12} \Delta \nu} c_s Q \left[\frac{1 + (1 - \gamma_{12}) B \tau_1}{1 + B(\tau_1 + \gamma_{12} \tau_2)} \right] \quad (7.3.16)$$

Equation (7.3.16) with (7.3.14) completely specifies K_1 in terms of pumping power and laser parameters. The factor $e^{\alpha L}$ which appears in the expression for B , has α in it which contains K_1 . Thus expression (7.3.16) does not give K_1 explicitly. However, in nearly all cases, $e^{\alpha L} \sim 1$, so that K_1

may be calculated directly from (7.3.16) and (7.3.14).

Finally, we need an expression for the pumping power density Q in terms of laser parameters. Inverting (7.3.16) we get:

$$Q = 11.52 \frac{\Delta \nu}{c_s f_2 \lambda^2} \left\{ \left[\left(\frac{0.431/\gamma_{12} - K_1^h}{h\theta} \right)^2 + \frac{2K_1}{h\theta} \right]^{\frac{1}{2}} + \left[\frac{0.431/\gamma_{12}}{h\theta} - \frac{K_1}{\theta} \right] \right\}, \frac{\text{Watts}}{\text{cm}^3} \quad (7.3.17)$$

where:

$$\theta = \frac{0.862}{\gamma_{12}} \frac{(1 - \gamma_{12}) \tau_1}{\tau_1 + \gamma_{12} \tau_2} \quad (7.3.18)$$

$$h = \frac{Le^{\alpha l}}{T_r} \quad (7.3.19)$$

7.4 Nuclear Chemogenics

Though photonic pumping is also of interest and most of the analysis presented applies to the case of photonic pumping as well, we shall make a special study of nuclear pumping, since it appears to be particularly suited for the activation of liquid halide lasers. The advantages of direct nuclear pumping over photonic or electronic pumping have been discussed elsewhere and will not be entered into here (E1).

The concept of nuclear pumping involves using the energy of fission fragments directly to pump lasers and the design of integrated laser rod/fuel elements to form a compact lasing nuclear reactor in which the reactor's energy is directly converted into lasing light.

The simplest design of such a nuclear-fueled laser element would consist of a tube filled with a liquid halide such as AsCl_3 in which UCl_3 is dissolved. The latter would simultaneously serve as nuclear fuel and luminescent center. Should other frequencies be desired, other rare earth halides such as NdCl_3 or CrCl_3 may be added to the solution.

When a fission fragment passes through a liquid, it transfers energy to and is stopped by the electrons in the liquid, resulting in ionization. Each fission fragment starts out with an energy of about 100 Mev and produces on the order of 10^7 ions in its track. The mean free path of a fission fragment is on the order of ten microns in a liquid, so that for a volumetrically distributed source nearly all the energy of fission is deposited in the liquid.

In reference E2, the detailed theory is given of the formation of the various chemical species, termed "chemogenes" by fission fragments. In liquids such as AsCl_3 , the dominating energy transfer process will be the excitation of the valence electrons of Cl^- into the conduction band. The kinetic energy of the electron in the conduction band is usually on the order of the band gap energy. Thus for liquid AsCl_3 with $E_g = 9$ ev, the energy transferred per electron is approximately $\Delta E = 18$ ev. If the nuclear fission

source amounts to Q watts per cm^3 , we have then that the production of chemogenes C_i or electron-hole pairs per cm^3 per second is given by

$$\frac{dC_i}{dt} = 6.23 \times 10^{18} \frac{Q}{\Delta E} = 3.46 \times 10^{17} Q, \frac{\text{electrons}}{\text{cm}^3 \text{-sec}} \quad (7.4.1)$$

Equation (7.4.1) is only a crude estimate, as the probabilities for the formation of other states have all been equated to zero and only the valence to conduction band excitation is assumed to take place. After the conduction electrons have diffused through the lattice and lost most of their kinetic energy the electron hole pair will recombine at a luminescent center site where the recombination energy causes the excitation of the center. The recombination will probably take place in two steps as described in Section 7.2, the overall result being the excitation of two centers per recombination.

We shall conservatively assume the excitation of one center per electron-hole recombination, and assume further that 20% of the excited states will cascade into the upper lasing level. With these assumptions, we finally obtain:

$$\frac{dN_2}{dt} = 0.20 \frac{dC_i}{dt} = 6.92 \times 10^{16} Q, \frac{\text{states 2}}{\text{cm}^3 \text{-sec}} \quad (7.4.2)$$

For liquid lasers in general, we may write:

$$\frac{dN_2}{dt} = c_s Q, \quad (7.4.3)$$

where c_s is a constant and Q is the nuclear power density (watts/cm^3).

The constant c_s is defined by:

$$c_s = 6.23 \times 10^{18} \frac{\eta_c}{\Delta E}, \left(\frac{\text{atoms}}{\text{joule}} \right) \quad (7.4.4)$$

where:

$$\eta_c = \text{cascade efficiency}$$

$$\Delta E = \text{average energy dissipated to excite host electron.}$$

If absorptive losses can be neglected and if lasing is well above threshold, the efficiency of the nuclear-energy to lasing-light conversion for rare-earth chlorides dissolved in AsCl_3 is:

$$\eta_{\text{overall}} = \frac{0.2 h\nu_1}{18} = 1.11 h\nu_1 \%, \quad (7.4.5)$$

where $h\nu_1$ is the energy of the emitted laser photons in ev. For Neodymium-lased photons of 1.06 micron wavelength, $h\nu_1 = 1.168$ ev, and the efficiency is thus 1.3%. In general, the efficiency is given by:

$$\eta_{\text{overall}} = \eta_c \frac{h\nu_1}{\Delta E} \quad (7.4.6)$$

7.5 The Critical Laser Ratio

The critical laser ratio C_{12} was defined by Equation (7.3.2). Its value is determined by the rate equations which govern the production and depletion of the upper and lower lasing levels.

For the upper lasing level (state 2) we may write:

$$\frac{dN_2}{dt} = c_s Q - \frac{c_2}{8\pi\nu_1^2 \tau} \frac{(\pi \ln 2)^{\frac{1}{2}} \Phi}{\Delta \nu_1} (N_2 - \frac{g_2}{g_1} N_1) +$$

(continued)

$$- \frac{N_2}{\tau_2} - K_{P_2} (T) N_2 \quad (7.5.1)$$

and for the lower level:

$$\frac{dN_1}{dt} = \frac{c^2}{8\pi\nu_1^2 \tau} \frac{(\pi \ln 2)^{\frac{1}{2}} \Phi}{\Delta \nu_1} \left(N_2 - \frac{g_2}{g_1} N_1 \right) +$$

$$- \frac{N_1}{\tau_1} - K_{P_1} (T) N_1 \quad (7.5.2)$$

where:

- Φ = Laser beam photon flux inside cavity,
photons/cm²
- ν_1 = Laser photon frequency
- $\Delta \nu_1$ = Linewidth of lasing transition
- τ = Time constant for spontaneous $2 \rightarrow 1$
transition
- τ_2 = Natural lifetime of upper state 2.
- τ_1 = Natural lifetimes of lower state 1.
- c_s = Constant defined by Equation (7.4.4)
- Q = Nuclear power density, watts/cm³
- c = Velocity of light

g_2, g_1 = Statistical weights of upper and lower state respectively

$K_{p_i}(T)$ = Temperature-dependent rate constant for phonon-assisted de-excitation of an excited state i .

For steady-state conditions, $\frac{dN_2}{dt} = \frac{dN_1}{dt} = 0$, and

we obtain

$$N_2 = \frac{c_s Q (B + \frac{1}{\tau_1} + K_{p_1})}{\left(\frac{g_1}{g_2} B + \frac{1}{\tau_2} + K_{p_2}\right) \left(B + \frac{1}{\tau_1} + K_{p_1}\right) - \frac{g_1}{g_2} B^2} \quad (7.5.3)$$

$$N_1 = \frac{c_s Q \frac{g_1}{g_2} B}{\left(\frac{g_1}{g_2} B + \frac{1}{\tau_2} + K_{p_2}\right) \left(B + \frac{1}{\tau_1} + K_{p_1}\right) - \frac{g_1}{g_2} B^2} \quad (7.5.4)$$

where:

$$B = \frac{(\pi \ln 2)^{\frac{1}{2}} c^2 (g_2/g_1)}{8\pi \nu_1^2 \tau} \frac{\Phi}{\Delta \nu_1} =$$

$$= 0.0867 \frac{\lambda_1^2 \Phi}{\tau \Delta \nu_1} \frac{g_2}{g_1} \quad (7.5.5)$$

where all parameters must be in cgs units. ..

The critical laser ratio is then obtained by dividing (7.5.4) into (7.5.3) and we get:

$$C_{12} = \frac{g_1/g_2 \ B}{B + \frac{1}{\tau_1} + K_{p_1}} \quad (7.5.6)$$

If, as is usual, the spontaneous emission rates at the lower level are high compared to phonon-assisted loss rates so that K_{p_1} may be neglected in (7.5.6), we get that:

$$C_{12} = \frac{g_1/g_2}{1 + \frac{1}{B\tau_1}} \quad (7.5.7)$$

It is clear from (7.5.7) that for strong laser action we must have the conditions:

$$B < \frac{1}{\tau_1} \left(\frac{1}{g_1/g_2 - 1} \right) \quad (7.5.8)$$

From Equation (7.5.5) we may write this as:

$$0.0867 \frac{\lambda^2 \Phi}{\Delta\nu_1} < \frac{\tau}{\tau_1} \left(\frac{1}{1 - g_2/g_1} \right) \quad (7.5.9)$$

Thus, the photon flux in the laser beam should not be too high, otherwise the stimulated emission it induces will "flood" the lower laser level which cannot depopulate any faster than at the rate $1/\tau_1$.

7.6 Threshold Conditions

For laser action, Equation (2.1.9) must hold. At threshold $\beta = 0$, so that:

$$\alpha = \xi/L \quad (7.6.1)$$

and

$$K_1 = K_a + K_r + K_s + K_d - \frac{\xi}{L} = \alpha_a - \frac{\xi}{L} \quad (7.6.2)$$

where for convenience we lump all losses into one factor:

$$\alpha_a = K_a + K_r + K_s + K_d \quad (7.6.3)$$

From Equation (7.3.17), we find then that at threshold power, we have:

$$\begin{aligned} Q_{\text{threshold}} &= \frac{11.52 \Delta \nu}{c_s f_2 \lambda^2 L \theta} \left\{ \left[\left((1-R) \left(1 + \frac{0.431R}{\gamma_{12}} \right) - \alpha_a L \right)^2 + \right. \right. \\ &\quad \left. \left. + 2\theta R (1-R) \left(\alpha_a L - (1-R) \right) \right]^{\frac{1}{2}} - \left[(1-R) \left(1 + \frac{0.431R}{\gamma_{12}} \right) - \alpha_a L \right] \right\} = \\ &= \frac{11.52 \Delta \nu}{c_s f_2 \lambda^2 L \theta} \left[(1-R) \left[1 + \frac{0.431R}{\gamma_{12}} \right] - \alpha_a L \right]. \end{aligned} \quad (7.6.4)$$

$$\cdot \left\{ \sqrt{1 + \frac{2\theta R (1-R) (\alpha_a L - (1-R))}{\left((1-R) \left[1 + \frac{0.431R}{\gamma_{12}} \right] - \alpha_a L \right)^2 - 1}} - 1 \right\}$$

where we used relation (7.3.19) at threshold conditions:

$$h_{\text{threshold}} = \frac{L}{R T_r} \approx \frac{L}{R (1 - R)} , \quad (7.6.5)$$

and further used the approximations:

$$T_r = 1 - R , \quad (7.6.6)$$

and:

$$\xi = -\ln R \approx 1 - R , \quad (7.6.7)$$

which are not bad for most reflectors.

The parameter θ was defined by Equation (7.3.18):

$$\theta = \frac{0.862}{\gamma_{12}} \frac{(1 - \gamma_{12}) \tau_1}{\tau_1 + \gamma_{12} \tau_2}$$

By inspection of (7.6.4), we find that if θ is positive, a minimum occurs in the bracketed quantity when:

$$L = \frac{1-R}{\alpha_a} \left(1 + \frac{0.431R}{\gamma_{12}} \right) \quad (7.6.8)$$

In this case $Q_{\text{threshold}}$ becomes:

$$Q_{\text{threshold}} = \frac{10.7 \Delta \nu R (1-R)}{c_s f_2 \lambda^2 L \theta} \left(\frac{\theta}{\gamma_{12}} \right)^{\frac{1}{2}} = \frac{10.7 \Delta \nu R \alpha_a (\gamma_{12}/\theta)^{\frac{1}{2}}}{c_s f_2 \lambda^2 (\gamma_{12} + 0.431R)} \quad (7.6.9)$$

If θ is negative, the minimum occurs when:

$$L = \frac{2(1-R)}{\alpha_a} \left[1 + \frac{0.431R}{\gamma_{12}} + \theta R + 2 \sqrt{\theta^2 R^2 + \theta R \left(1 + \frac{0.215R}{\gamma_{12}} \right)} \right] \quad (7.6.10)$$

The threshold energy is then:

$$Q_{\text{threshold}} = \left\{ \frac{11.52 \Delta\nu (1-R) \left[1 + \frac{0.431R}{\gamma_{12}} \right]}{c_s f_2 \lambda^2 L (-\theta)} \right\} \cdot \left\{ 1 - 2 \left[1 + \frac{\gamma_{12} \theta R \left(1 + 2 \sqrt{1 + \frac{\gamma_{12} + 0.215R}{\gamma_{12} \theta R}} \right)}{\gamma_{12} + 0.431R} \right] \right\} \quad (7.6.11)$$

8. THE AsCl_3 (NdCl_3) AND AsCl_3 (UCl_3) LASER SYSTEMS

8.1 Conditions for Lasing

In the previous sections expressions were obtained for the cross-sections of lossy and multiplicative processes important to laser action. We are interested to apply all this information to the AsCl_3 (NdCl_3) and AsCl_3 (UCl_3) systems, and determine whether laser action can take place, and what the threshold power requirements are.

In Table 8.1.1, calculated values of the various physical parameters which determine laser action are tabulated for AsCl_3 (UCl_3) and AsCl_3 (NdCl_3). Substituting these values in Equation (7.6.4), we find for the required threshold power levels:

$$Q_{(\text{U}^{3+})} = \frac{1952}{L} \left\{ \left[\left((1-R) (0.517R) - 0.026L \right)^2 + \right. \right. \\ \left. \left. + 0.0246R(1-R) \left(0.026L - (1-R) \right) \right]^{\frac{1}{2}} + \right. \\ \left. - \left[(1-R) (0.517R + 1) - 0.026L \right] \right\} \frac{\text{Watts}}{\text{cm}^3}$$

(8.1.1)

$$Q_{(Nd^{3+})} = \frac{33,940}{L} \left\{ \left[(1-R) (0.251 R + 1) - 0.114 L \right] + \right. \\ \left. - \left[\left((1-R) (0.251 R + 1) - 0.114 L \right)^2 + \right. \right. \\ \left. \left. - 0.0258 R (1-R) (0.114 L - (1-R)) \right]^{\frac{1}{2}} \right\}, \frac{\text{Watts}}{\text{cm}^3} \quad (8.1.2)$$

TABLE 8.1.1 Calculated Laser Constants for $AsCl_3 (U^{3+})$
and $AsCl_3 (Nd^{3+})$

Parameters	$AsCl_3 (UCl_3)$	$AsCl_3 (NdCl_3)$
g_2	12	7
g_1	10	12
γ_{12}	0.833	1.714
τ_2 (sec)	125×10^{-6}	$\sim 125 \times 10^{-6}$
τ_1 (sec)	8×10^{-6}	$\sim 8 \times 10^{-6}$
τ (sec)	130×10^{-6}	$\sim 130 \times 10^{-6}$
f_2	0.96	0.96
c_s	$6.92 \times 10^{16} \frac{\text{atoms}}{\text{Joule}}$	$6.92 \times 10^{16} \frac{\text{atoms}}{\text{Joule}}$
$\Delta\nu$ (cps)	1.20×10^{10}	2.83×10^{10}
λ (cm)	2.49×10^{-4}	1.06×10^{-4}
K_a (cm ⁻¹)	0.026	0.114
K_r (cm ⁻¹)	$3.97 \times 10^{-7} Q$	$3.97 \times 10^{-7} Q *$
K_s (cm ⁻¹)	$0.9 \times 10^{-8} y$	$2.45 \times 10^{-7} y *$
K_d (cm ⁻¹)	Very small	Very Small
α_a (cm ⁻¹)	0.026	0.114
η overall	0.58%	1.30%

*Note: y = Mole Fraction of Rare Earth Chloride in Host Chloride.
 Q = Input Power, Watts/cm³.

For the (U^{3+}) laser, $\theta > 0$, so that when

$$L = 38.45 (1-R) (0.517 R + 1), \text{ cm} \quad (8.1.3)$$

we have from (7.6.9):

$$Q_{\text{threshold}} = \frac{221.6 R (1-R)}{L} = \frac{5.76 R}{(0.517 R + 1)}, \quad \frac{\text{Watts}}{\text{cm}^3} \quad (8.1.4)$$

For the (Nd^{3+}) laser, $\theta < 0$, so that when:

$$L = 17.54 (1-R) \left(1 + 0.238 R + 0.0258 R \sqrt{10.72 + \frac{77.5}{R}} \right), \text{ cm} \quad (8.1.5)$$

we have a minimum in required threshold power given by:

$$Q_{\text{threshold}} = \frac{33,940 (1-R) (1 + 0.251 R)}{L} \left[1 - 2 \left\{ 1 - \frac{0.022 R (1 + \sqrt{10.72 + \frac{77.5}{R}})}{1.714 + 0.431 R} \right\} \right]$$

$$= \frac{1933 (1 + 0.251 R) \left[1 - 2 \left\{ 1 - \frac{0.022 R (1 + \sqrt{10.72 + 77.5/R})}{1.714 + 0.431 R} \right\} \right]}{1 + 0.238 R + 0.0258 R \sqrt{10.72 + 77.5/R}}, \quad (8.1.6)$$

$$\frac{\text{Watts}}{\text{cm}^3}$$

For $R = 0.99$, we finally get:

$$(Q_{\text{thr}})_{\text{U}^{3+}} = 3.77 \text{ watts/cm}^3$$

$$(Q_{\text{thr}})_{\text{Nd}^{3+}} = 1280 \text{ watts/cm}^3$$

$$(L)_{\text{U}^{3+}} = 5.81 \text{ cm}$$

$$(L)_{\text{U}^{3+}} = 2.59 \text{ cm}$$

9. REFERENCES

- B1 G.D. Boyd and J.P. Gordon, "Confocal Multi-mode Resonator for Millimeter through Optical Wavelength Masers", Bell System Tech Journal, 40, 489-508, 1961.
- C1 P. Connes, "L'etalon de Fabry - Perot Spherique", J. Phys. Radium, 19, 262-269, 1958.
- D1 G.H. Dieke, "Spectroscopic Observations of Maser Materials", p. 164 ff, Advances in Quantum Electronics, Columbia Univ. Press, 1961.
- E1 J. W. Eerkens, "Feasibility Investigation of Nuclear-Pumped Lasers", Terra Nova Report No. 752.
- E2 J. W. Eerkens, "On the Physical Theory of Chemical Species Formation by Fission Fragments", Paper given at Conference on Ionization Phenomena in Gases, Munchen, Germany, 1961.
- F1 A.G. Fox and Tingye Li, "Resonant Modes in a Maser Interferometer", Bell Systems Tech. Journal, 40, 453-488, 1961.
- K1 C. Kittel, "Introduction to Solid State Physics", Wiley, 1953.
- M1 T.S. Moss, "Optical Properties of Semiconductors", Butterworths (London), 1961.
- S1 A.L. Schawlow, "Infrared and Optical Masers", Solid State Journal, June 1961, p. 21 ff.
- V1 H.C. Van de Hulst, "Light Scattering by Small Particles", Wiley, 1957.

SCATTERING LOSSES IN LIQUID LASERS

by

Paul G. Thiene

9 August 1963

59

ABSTRACT

Light scattering loss in liquids due to thermal density fluctuations is briefly treated. Starting with the differential scattering cross section for a single molecule, the cross section for the bulk material is obtained by summing over all the molecules in a given region of the material. The contribution to the cross section due to density fluctuations is then used to obtain the desired extinction coefficient for scattering. An order-of-magnitude calculation of the extinction coefficient for a typical liquid is made. The result is compared with mirror losses and is found to be relatively small.

TABLE OF CONTENTS

- I. INTRODUCTION
- II. SCATTERING CROSS SECTION
- III. CORRELATION FUNCTION
- IV. THERMAL FLUCTUATIONS

SCATTERING LOSSES IN LIQUID LASERS

I. INTRODUCTION

Calculations of the threshold condition for lasing commonly equate the induced power to the resonator losses due to absorption and transmission at the mirrors. In addition to mirror losses there are other losses to be considered. There are losses due to scattering from mirror imperfections. There is diffraction loss at the mirror apertures. Within the laser medium there are absorption losses and losses due to scattering by optical inhomogeneities. According to Kaiser and Keck⁽¹⁾ losses due to scattering by optical inhomogeneities in laser crystals can greatly exceed the mirror losses.

In general the scattering losses in solid media arise from inhomogeneities in density and anisotropy.⁽²⁾ The local inhomogeneities may be "frozen" in the material.⁽³⁾ There are, however, always fluctuations due to thermal agitation.^(4, 5)

The liquid presents a somewhat different situation in that the frozen inhomogeneities are absent, but the scattering due to thermal fluctuations in density and anisotropy may be greater than that in a solid.⁽⁶⁾ Rudimentary analysis shows that the extinction coefficients due to density fluctuations is

-
- (1) W. Kaiser and M. J. Keck, J. Appl. Phys. 33, 762 (1962)
 - (2) M. Goldstein and E. R. Michalik, J. Appl. Phys 26, 1450 (1955)
 - (3) P. Debye and A. M. Bueche, J. Appl. Phys. 20, 518 (1959)
 - (4) R. D. Mauer, J. Chem. Phys. 25, 1206 (1956)
 - (5) G. Oster, Chem. Revs. 43, 319 (1948)
 - (6) J. Frenkel, "Kinetic Theory of Liquids," p 294, Dover, N. Y., 1955

proportional to the isothermal compressibility of the material. By way of comparison, the room temperature compressibility of most glasses⁽⁴⁾ is on the order of 10^{-12} cm²/dyne, while the compressibility of liquids may be 50 to 100 times larger.⁽⁷⁾

The following is an introductory treatment of the simple case of coherent scattering due to density fluctuations in a pure liquid composed of non-polar spherically symmetric molecules. The discussion is developed in a form which is intended to provide a basis for later inquiry into the more complicated questions including scattering caused by anisotropy fluctuations, cybotactic clustering⁽⁶⁾ and macroscopic inhomogeneity due to pump heating. Starting with the differential scattering cross section for a single molecule, the cross section for the bulk material is obtained by summing over all the molecules in a given region of the material. The contribution to the cross section due to density fluctuations is then used to obtain the desired extinction coefficient for scattering. An order-of-magnitude calculation of the extinction coefficient for a typical liquid is made. The result is compared with mirror losses and is found to be relatively small.

(7) D. Gray, "Amer. Inst. of Physics Handbook," p 2-164, McGraw-Hill, N. Y., 1957

II. SCATTERING CROSS SECTION

From a classical point of view the scattering process is described simply as follows. When a beam of light traverses matter, the electric field causes periodic oscillations of the electrons in the material. These oscillating electrons reradiate the incident energy in the form of scattered radiation. The intensity, angular distribution and polarization of the scattered radiation is determined by the distribution, orientation and polarizabilities of the molecules of which the material is comprised.

Quantum mechanically, the description is somewhat different.⁽⁸⁾

The scattering process consists in the absorption by a molecule of the incident photon of propagation vector \underline{k}_0 and the simultaneous emission of a photon \underline{k} . The process is of second order in that two quanta are involved. If the final and initial states of the molecule are the same, the scattering is "coherent" (Rayleigh scattering); the wave length of the scattered quantum is the same as that of the incident quantum. If, however, the final state differs from the initial state the wave length of the scattered quantum is not equal to the wave length of the incident quantum (Raman scattering).

Consider first the coherent scattering of a beam of photons with a propagation vector \underline{k}_0 along the polar axis of a spherical coordinate system and polarized in the $\varphi=0, \theta=\pi/2$ direction. The differential cross section for scattering of the photon into a solid angle $d\Omega'$ in a direction θ with

(8) W. Heitler, "The Quantum Theory of Radiation," p 189, Oxford Univ. Press, London, 1954

respect to the direction of \underline{k}_0 is

$$d\Phi_j = k_0^4 \alpha^2 / e^{-i(\underline{k}_0 - \underline{k}) \cdot \underline{r}_j} / (1 - \sin^2 \theta \cos^2 \varphi) d\Omega_j. \quad (1)$$

In (1) α is the molecular polarizability which is a scalar for spherically symmetric molecules. The azimuthal angle of the direction of polarization of the scattered photons is φ . The cross section for N identical molecules is then

$$d\Phi = k_0^4 \alpha^2 / \sum_{j=1}^N e^{-i(\underline{k}_0 - \underline{k}) \cdot \underline{r}_j} / (1 - \sin^2 \theta \cos^2 \varphi) d\Omega, \quad (2)$$

where $d\Omega$ is the solid angle seen by an observer at a large distance away from the region of scattering.

The sum over phases in (2) can be transformed to an integral involving the actual number density of the molecules over the volume of the material. By the actual number density is meant the discontinuous distribution of the instantaneous positions of all the molecules, and not the local volume average usually implied. Regarding the molecules as point particles the number density can be written as

$$n(\underline{r}) = \sum_{j=1}^N \delta(\underline{r} - \underline{r}_j). \quad (3)$$

It follows that

$$\begin{aligned} \sum_{j=1}^N e^{-i(\underline{k}_0 - \underline{k}) \cdot \underline{r}_j} &= \sum_{j=1}^N \int \delta(\underline{r} - \underline{r}_j) e^{-i(\underline{k}_0 - \underline{k}) \cdot \underline{r}} d\underline{r} \\ &= \int n(\underline{r}) e^{-i(\underline{k}_0 - \underline{k}) \cdot \underline{r}} d\underline{r}. \end{aligned} \quad (4)$$

The instantaneous number density now can be expressed conveniently as the sum of a statistical average value $\langle n(r) \rangle$ and the fluctuation $\delta n(r)$ from the average:

$$n(r) \equiv \langle n(r) \rangle + \delta n(r) . \quad (5)$$

Letting $\underline{k} \equiv \underline{k}_0 - \underline{k}$ for brevity and substituting (5) into (4) yields

$$\sum_{j=1}^N e^{-i\underline{k} \cdot \underline{r}_j} = \langle n_{\underline{k}} \rangle + \delta n_{\underline{k}} , \quad (6)$$

where

$$\langle n_{\underline{k}} \rangle \equiv \int n(r) e^{-i\underline{k} \cdot \underline{r}} d\underline{r} \quad (7)$$

and

$$\delta n_{\underline{k}} \equiv \int \delta n(r) e^{-i\underline{k} \cdot \underline{r}} d\underline{r} \quad (8)$$

are the Fourier components of the average density and the density fluctuation.

In terms of the Fourier components the statistical average of the differential cross section given by (2) is found to be

$$\langle d\Phi \rangle = k_0^4 \alpha^2 \left[\langle n_{\underline{k}} \rangle^2 + \langle |\delta n_{\underline{k}}|^2 \rangle \right] (1 - \sin^2 \theta \cos^2 \varphi) d\Omega , \quad (9)$$

noting that $\langle \delta n_{\underline{k}} \rangle = 0$.

At this point it is useful to introduce a correlation function for the density.

III. CORRELATION FUNCTION

In a homogeneous isotropic material each molecule is equally likely to be at any point in space provided that all other molecules can have arbitrary positions. Because of the interaction forces, however, there must be some correlation between the relative positions of different molecules. In other words, given the position of one molecule, different positions of a neighboring molecule are not equally probable.

A measure of the correlation between a density fluctuation at \underline{r} given by (5) and a density fluctuation at a point a vector distance \underline{s} from \underline{r} is

$$\langle \delta n(\underline{r}) \delta n(\underline{r} + \underline{s}) \rangle = \langle n(\underline{r}) n(\underline{r} + \underline{s}) \rangle - \langle n(\underline{r}) \rangle \langle n(\underline{r} + \underline{s}) \rangle. \quad (10)$$

If there were no interaction between the molecules, as in an ideal gas, the average of the product of the number densities would be simply the product of the averages; the right side of expression (10) would vanish. The magnitude of the correlation is conveniently expressed by a correlation function $\chi(\underline{s})$ defined by

$$\langle \delta n(\underline{r}) \delta n(\underline{r} + \underline{s}) \rangle = \langle n(\underline{r}) \rangle [\chi(\underline{s}) + \delta(\underline{s})]. \quad (11)$$

For a region of material consisting of a very large number of molecules it is reasonable to suppose that the correlation function falls

rapidly to zero in a distance small compared with the macroscopic dimensions of the region.

Several useful results readily follow from (11). Multiplying (11) by $d\mathbf{r}d\mathbf{s}$ and integrating over some volume V of the material yields

$$\langle (\Delta N)^2 \rangle = \langle N \rangle \left[\int_V v(\mathbf{s}) d\mathbf{s} + 1 \right], \quad (12)$$

where

$$\Delta N = \int_V \delta n(\mathbf{r}) d\mathbf{r} \quad (13)$$

and

$$\langle N \rangle = \int_V \langle n(\mathbf{r}) \rangle d\mathbf{r}. \quad (14)$$

Expression (12) states that the mean square fluctuation of the number of particles in a given volume is proportional to the average number of particles in the volume.

Multiplying (11) by $e^{-i\mathbf{k}\cdot\mathbf{s}} d\mathbf{r}d\mathbf{s}$ and performing a double integration results in a relation between the mean square of the Fourier components of the density fluctuations and the Fourier components of the correlation function:

$$\langle |\delta n_{\mathbf{k}}|^2 \rangle = \langle N \rangle [v_{\mathbf{k}} + 1], \quad (15)$$

where

$$v_{\mathbf{k}} = \int_V v(\mathbf{s}) e^{-i\mathbf{k}\cdot\mathbf{s}} d\mathbf{s} \quad (16)$$

The contribution of density fluctuations to the differential cross section given by (9) can now be simply written in terms of the Fourier components of the correlation function. Substituting result (15) into (9) gives

$$d\sigma(\theta) = k_0^4 \alpha^2 [\nu_k + 1] (1 - \sin^2 \theta \cos^2 \varphi) d\varphi \quad (17)$$

for the differential cross section per molecule.

IV. THERMAL FLUCTUATIONS

It is now straightforward to estimate the scattering loss in pure liquids due to density fluctuations of a thermal nature. While the correlation function can be expressed in terms of the interaction potential between the molecules, it is convenient for the present to relate it to the phenomenological parameter of isothermal compressibility.

According to statistical mechanics⁽⁹⁾ the mean square fluctuation of the number of molecules at temperature T in a volume V is

$$\langle (\Delta N)^2 \rangle = \langle N \rangle^2 \frac{\beta k T}{V}, \quad (18)$$

where

$$\beta \equiv - \frac{1}{V} \left(\frac{\partial V}{\partial P} \right)_T$$

is the isothermal compressibility.

Combining (18) and (12) gives

$$1 + \int v(\underline{s}) d\underline{s} \equiv 1 + v_0 = \beta \bar{n} k T, \quad (19)$$

in which $\bar{n} \equiv \langle N \rangle / V$ is the mean number density of molecules.

If now consideration is restricted to conditions for which the wave length of the radiation is large compared with the range of correlation, $k \cdot s \ll 1$ in (16). Thus, as a first approximation only the zero-order Fourier component

(9) R. Tolman, "The Principles of Statistical Mechanics," p 647, Oxford Univ. Press, 1938

of the correlation function need be considered. To this approximation then, the differential cross section (17) is

$$\begin{aligned} d\sigma(\theta) &\approx k_0^4 \alpha^2 (1 + \frac{2}{3}) (1 - \sin^2 \theta \cos^2 \varphi) d\Omega \\ &\approx k_0^4 \alpha^2 \beta \bar{n} kT (1 - \sin^2 \theta \cos^2 \varphi) d\Omega. \end{aligned} \quad (20)$$

It should be noted that the foregoing derivation tacitly assumed that the local electric field of the incident radiation in the material is equal to the free-space field. An approximate relation between the local field \underline{F} and the free-space field \underline{E} is⁽¹⁰⁾

$$\underline{F} = \underline{E} + \frac{4\pi}{3} \bar{n} \alpha \underline{F}. \quad (21)$$

With this correction expression (20) is altered to

$$d\sigma(\theta) \approx k_0^4 \frac{\bar{n} \alpha}{(1 - \frac{4\pi}{3} \bar{n} \alpha)^2} \beta kT (1 - \sin^2 \theta \cos^2 \varphi) d\Omega \quad (22)$$

In laser application the practical parameter of interest is the extinction coefficient in paraxial directions, that is, in a small solid angle around $\theta = 0$. In a cone of half angle θ_0 the extinction coefficient for scattering due to thermal fluctuation in density is obtained by integrating (22) from θ_0 to π

(10) P. Debye, "Polar Molecules," p 11, Dover, New York, 1945.

averaging over φ , and multiplying the result by the number density \bar{n} :

$$K_s(\theta_0) \approx \frac{128\pi^5}{3} \left(\frac{\bar{n}\alpha}{1 - \frac{4\pi}{3}\bar{n}\alpha} \right)^2 \frac{\beta kT}{\lambda^4} F(\theta_0) \quad (23)$$

where

$$F(\theta_0) \equiv \frac{1}{2} \left[1 + \frac{3}{4} \cos \theta_0 + \frac{1}{4} \cos^3 \theta_0 \right].$$

The free-space wave length of the radiation is $\lambda = 2\pi/k_0$. The function $F(\theta_0)$ ranges from 1 to 0 as θ_0 goes from 0 to π . Formula (23) gives the extinction coefficient in a cone of half angle θ_0 due to thermal fluctuations in density.

As an example, consider a typical liquid for which $\bar{n} = 10^{22}/\text{cm}^3$, $\alpha = 10^{-23} \text{ cm}^3$, (11) $\beta = 10^{-10} \text{ cm}^2/\text{dyne}$ and $T = 300^\circ\text{K}$. The extinction coefficient for $\lambda = 8000^\circ\text{\AA}$ is estimated by (23) to be

$$K_s(\theta_0) \approx 4 \times 10^{-5} F(\theta_0) \text{ cm}^{-1}.$$

For comparison, the extinction coefficient corresponding to loss in laser mirrors of reflectivity $R = 99\%$ separated by a distance $L = 10 \text{ cm}$ is

$$K_m = \frac{1-R}{L} = 10^{-3} \text{ cm}^{-1}.$$

Thus, the tentative conclusion is reached that scattering losses due to thermal fluctuations in non-polar liquids are negligible compared with mirror losses. It should be noted, however, that near a resonance of the molecule, the polarizability may be considerably larger than the value assumed for illustration.

(11) Landolt-Bornstein, "Zahlenwerte und Funktionen", 1 3 510 Springer 1951

PART B

NUCLEAR PUMPING OF SEMICONDUCTOR LASERS

BY: DR. FRANCIS H. WEBB, JR.
DR. PAUL H. LEVINE

1. INTRODUCTION

1.1 General Preface

The second major part of this report is a discussion of the pumping of semiconductors with nuclear radiation to create laser light.

Laser action in semiconductors by excess free carrier injection into the junction region of forward biased diodes is well established experimentally. Even more fully explored is the generation of such excess free carriers by the passage of nuclear radiation through semiconducting materials, a process which underlies the operation of solid-state nuclear particle detectors.

We have considered the question, "Can these two well-established phenomena be fruitfully combined to produce intense laser radiation?" On the basis of our analysis, we conclude that it indeed appears possible to achieve such a synthesis. We have investigated in some detail the requisite conditions and, within the limitations of time and the present theoretical and experimental understanding of these phenomena, have carried the program through to the design of a demonstration experiment.

Our results are naturally far from definitive, as further study of the many relevant physical processes is required. Nor do we attempt to compare the relative merits of nuclear-pumped and injection semiconductor lasers, aside from an observation that with the former, higher optical power outputs due to increased active volume and degree of inversion appear to be possible.

On balance, we conclude that there are sufficient reasons, both from the standpoint of basic physical understanding and with respect to possible systems application of the phenomenon, to amply justify further theoretical and experimental exploration in this direction.

1.2 Background

The lasability of certain direct-gap semiconductors, most notably GaAs and related III-V compounds, has been recently experimentally established by several groups.⁽¹⁻⁴⁾ In essence, this capability stems from the fact that in direct-gap materials, a photon with energy approximately equal to that of the gap is much more likely to stimulate band-to-band (or band to impurity level) recombination of excess carriers than to be absorbed by these carriers, since the latter process requires a short wavelength phonon to conserve momentum whereas the former does not. (A more elaborate description of this distinction is given in Appendix II). To date, laser action in these materials has been obtained only in forward biased p-n junction diodes, where the requisite inversion of carriers is obtained by electrical injection in the junction region. Below the laser threshold, fluorescent experiments have been performed using both electrical and optical injection.⁽⁵⁾ The entire field of semiconductor lasers is, as the references indicate, a new one, and comprehensive review articles are not as yet available.

A theoretical understanding of injection lasers is currently evolving along lines laid down by Bernard and Duraffourg⁽⁶⁾ who, on the basis of detailed balancing arguments similar to those which we exploit in Section 2, pointed out that near-degenerate bands are a necessary prerequisite to lasing action. As such, laser action in semiconductors can be understood as a process brought about by the existence of a sufficient number of excess charge carriers (i. e., "inversion" in conventional laser terminology) regardless of the means whereby this non-equilibrium situation is achieved. The question of how such excess carriers are created in an injection laser constitutes a separate problem which has been investigated, for example, by Mayburg⁽⁷⁾ who, by combining his results with

an approximation to the Bernard-Duraffourg criterion, could explain some features of the thresholds observed for the occurrence of laser action. (8)

Whereas the foregoing studies are based on somewhat general arguments and can indicate necessary conditions for lasability, the sufficiency of these criteria hinges upon an examination of the relative probabilities of intra-band and inter-band radiation processes as was carried out by Dumke. (9) His work gave quantitative justification to the expectation that direct-gap semiconductors, GaAs in particular, are likely to be favorable for laser action, whereas indirect-gap materials are not.

Having noted that laser action is an intrinsic capability of direct-gap semiconductors when a sufficient number of excess carriers are present, one may reasonably inquire whether these carriers can be produced by means other than electrical injection. If such alternatives could be found, several fundamental and practical advantages would accrue. For one thing, stimulated emission in injection lasers occurs only in the neighborhood of the narrow ($\sim 10^{-4}$ cm) junction region which places severe restrictions on the optical power output. To be sure, higher outputs can be obtained by passing more current through the junction, but this in turn leads to ohmic heating problems, especially if operation at liquid nitrogen temperature or below is desired. At the basic level, the fact that one deals with a junction rather than bulk homogeneous material introduces some uncertainty as to where recombination is actually taking place, and thus renders difficult an experimental study of the finer details of the fundamental radiative processes.

Optical injection appears out of the question with present sources due, in part, to the opacity of GaAs at these wavelengths. If one goes to higher energies, however, the situation appears

more favorable. We are fortunate here in being able to draw on a vast literature concerning the interaction of X and gamma radiations as well as charged and uncharged energetic particles with semiconductors. This background work, far too extensive to catalog here, has come about as a result of the development of semiconductor nuclear detectors as well as the interest in the effects of radiation environments on semiconductor behavior. The result of these studies which is of paramount importance is that a substantial fraction ($\sim 30\%$ in Ge, for example) of the energy lost by such radiations in a semiconductor goes into the production of the very same excess carriers which are required for laser action. We are thus led inescapably to the attractive possibility that nuclear radiation can be used to "pump" a semiconductor laser. This report constitutes a first look into this possibility. While our imminent concern is understandably one of the feasibility of this basic concept, we cannot resist the temptation of looking prematurely ahead and suggesting that the direct efficient conversion of the abundant power of a nuclear reactor into coherent narrow-band light would have technological implications of some importance.

1.3 Outline of Study

The question of the feasibility of a nuclear-pumped semiconductor laser (NPSL) is attacked by degrees. In Section 2, we present an analysis (somewhat more detailed than has hitherto been published) of the detailed balance of absorption, spontaneous emission and induced emission in a bulk, direct-gap semiconductor, and deduce therefrom the threshold density of excess carriers above which laser action would take place. This analysis, similar to those of Barnard and Duraffourg⁽⁶⁾ and Mayburg⁽⁷⁾, neglects boundary and geometrical effects and assumes merely that, by some means, an inverted electron-hole population has been achieved. The dependence of the threshold excess carrier concentration on temperature and impurity concentration is derived. Particular attention throughout is focussed on GaAs since it has one of the largest gap energies (and hence highest frequency photon emission) of the direct-gap materials. At inversion levels above threshold, the photon gain per cm of the "pumped" semiconductor is obtained as a function of carrier concentration, temperature, impurity concentration, etc. from which the central frequency of the laser line and a measure of its bandwidth can be derived. The specific example of heavily doped p-type GaAs operating at 77°K is numerically considered.

The basic theory of Section 2 is based on certain approximations and simplifications which are examined further in Section 3. Here, we go beyond the static analysis of Section 2 and write down the coupled dynamical equations governing the time rate of change of the excess carrier density and photon population.

The transition from infinite bulk material to a finite sample with partially reflecting ends is made. Dumke's⁽⁹⁾ arguments concerning the relative importance of free carrier absorption

and induced emission are reviewed and cited in support of assumptions made in Section 2. Since we are not at this point overly concerned with the detailed characteristics of the laser radiation - only whether or not laser action can take place - the content of this section is largely qualitative, its main function being to indicate the lines along which a more detailed study should follow. We, therefore, consider in many places the overidealization of completely degenerate filling of the conduction and valence bands which, while admittedly somewhat unrealistic in most cases, nevertheless gives some insight into the physical processes involved.

In Section 4, we return to the mainstream of the analysis. Having derived the requisite excess carrier concentration for laser action in Section 2, and indicated albeit approximately what rates of generation of excess carriers would be required to attain such values (Section 3.6), we turn in Section 5 to the question of free carrier generation by nuclear particles. After an examination of the physical processes involved in the interaction of energetic charged particles with a semiconductor, we compute the rate of generation of excess carriers as a function of particle flux and energy. Particular attention is given to the case of a beam of 80 MeV α particles, for reasons to be given shortly. The possibility of using neutrons and fission products from a reactor to generate inversion is briefly examined due to its practical significance, but reservations concerning radiation damage of the semiconductor raise unanswered questions.

The problem of radiation damage in general is briefly discussed in Section 5. Lack of adequate detailed data on damage effects in GaAs precludes an evaluation of its possible bearing on the feasibility of the NPSL, and thus defines a major area of further study. Some attention is therefore given to the possible use of liquid

semiconductors, since radiation damage would be a less severe restriction in this case.

In Section 6, we apply the results of our study to the preliminary design of a demonstration experiment. The experiment is designed to employ a cyclotron such as the 88 inch high flux machine at the University of California (Berkeley), whose beam of 80 MeV α particles appears ideally suited to this experiment. The demonstration experiment was in the beginning stages of preparation at the expiration of contractual effort covered by this report.

The final section presents our conclusions.

2. Threshold Criteria for Semiconductor Lasers

2.1 Photon Detailed Balance

Consider a spatially infinite medium in which electrons can occupy a series of levels with energy $E_1 < E_2 < E_3 < \dots$. Denoting the group velocity of an electromagnetic wave of frequency ν as $c'(\nu)$, we write the number of photons $Q(\nu, t)$ per unit volume with frequency between ν and $\nu + d\nu$ in the form:

$$Q(\nu, t) \equiv \frac{8\pi\nu^2}{c'^3(\nu)} \left(\frac{1 + q(\nu, t)}{\exp(h\nu/kT) - 1} \right) \quad (2.1)$$

This form is chosen because if $q = 0$, we have the black body spectrum appropriate to temperature T . The rate of change of $q(\nu, t)$ (and hence of $Q(\nu)$) due to electron transitions between levels i and j ($j > i$) is then given by the usual quantum mechanical expression

$$\begin{aligned} \frac{8\pi\nu^2}{c'^3(\nu) [\exp(h\nu/kT) - 1]} \left(\frac{\partial q(\nu, t)}{\partial t} \right)_{ij} &= n(E_j, t) \rho(E_i, t) \left[\frac{2\pi}{h} |M_{ij}|^2 \right] \cdot \\ &\quad \begin{array}{c} \text{spontaneous} \\ \text{emission} \end{array} \quad \begin{array}{c} \text{induced} \\ \text{emission} \end{array} \\ &\quad \delta(E_j - E_i - h\nu) \frac{8\pi\nu^2}{c'^3(\nu)} \left[1 + \frac{1 + q(\nu, t)}{\exp(h\nu/kT) - 1} \right] \\ &\quad - n(E_i, t) \rho(E_j, t) \left[\frac{2\pi}{h} |M_{ji}|^2 \right] \cdot \\ &\quad \delta(E_j - E_i - h\nu) \frac{8\pi\nu^2}{c'^3(\nu)} \underbrace{\left[\frac{1 + q(\nu)}{\exp(h\nu/kT) - 1} \right]}_{\text{Absorption}} \\ &\quad (2.2) \end{aligned}$$

where $n(E_i, t)$ is the number of electrons/unit volume in level E_i , and $\rho(E_j, t)$ is the number of final states/unit volume at energy E_j into which an electron can go. Equation (2.2) indicates how the photon density changes due to the three processes: spontaneous emission, induced emission and absorption. Note that all three terms have the common factor $|M_{ij}|^2$ (which by Hermiticity equals $|M_{ji}|^2$), the square of the matrix element of the electromagnetic field Hamiltonian between states i and j :

$$|M_{ij}|^2 = \left| \langle i | \tilde{J} \cdot \tilde{A}(\nu) | j \rangle \right|^2$$

$$\tilde{J} = \text{current operator} \rightarrow \frac{e}{m} \tilde{p}$$

$$\tilde{A} = \text{vector potential} \quad (2.3)$$

Since we are interested in semiconductors, we consider the general energy level scheme shown in Figure 1.

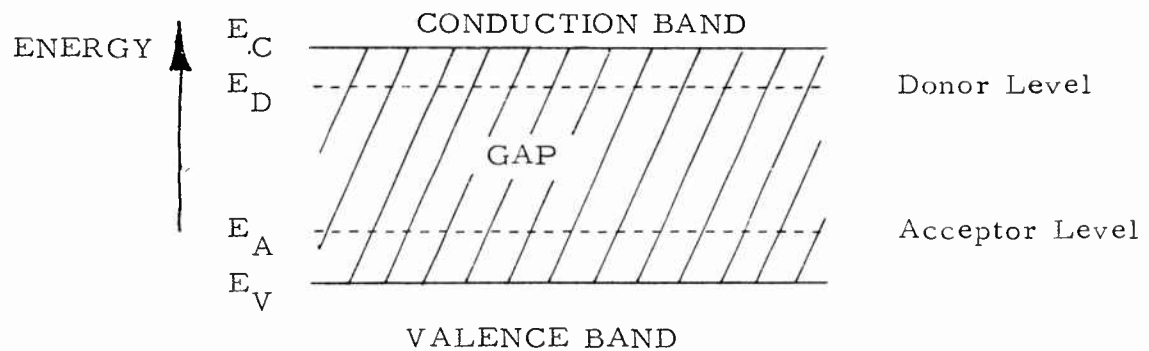


Figure 1. Semiconductor Level Scheme

Of particular interest is the situation in which electrons in both the conduction band (and donor level) and holes in the valence band (and acceptor level) are respectively in thermal equilibrium with the lattice at temperature T , but not necessarily in equilibrium with each other. This circumstance would occur if, by some means, electron and hole densities in excess of their equilibrium values are artificially maintained for times long compared to the quite short ($\sim 10^{-10}$ sec) electron-lattice and hole-lattice relaxation times.

A situation of this sort is conveniently described by assigning different Fermi levels to the electrons and holes. Thus, we write for the number of conduction electrons/unit volume with energies between E and $E + dE$.

$$\begin{aligned}
 n(E)dE &= \frac{1}{1 + \exp\left(\frac{E - \phi_n}{kT}\right)} D_C(E)dE \\
 &\equiv \frac{4\pi \left(\frac{2m_c}{h^2}\right)^{\frac{3}{2}} (E - E_C)^{\frac{1}{2}} dE}{1 + \exp\left(\frac{E - \phi_n}{kT}\right)} \quad (2.4)
 \end{aligned}$$

where $E \geq E_C$ and

where $D_C(E)$ is the conduction electron density of states, m_c the effective mass in the conduction band, and ϕ_n the electron Fermi energy.

Similarly the number of holes/unit volume in the valence band with energies between E and dE is given by

$$\begin{aligned}
 p(E) dE &= \frac{1}{1 + \exp\left(\frac{\phi_p - E}{kT}\right)} D_V(E) dE \\
 &\equiv \frac{4\pi \left(\frac{2m_v}{h^2}\right)^{\frac{3}{2}} (E_v - E)^{\frac{1}{2}} dE}{1 + \exp\left(\frac{\phi_p - E}{kT}\right)} \quad (2.5)
 \end{aligned}$$

where $E \leq E_v$ and

where $D_V(E)$ is the density of states function for holes in the valence band, m_v the hole effective mass, and ϕ_p the hole Fermi energy. It is easily shown that $\phi_n = \phi_p$ only if the electrons and holes are mutually in thermodynamic equilibrium and further that if excess carriers are present, then $\phi_n > \phi_p$.

2.2 Interband and Intraband Transitions

Referring back to equation (2.2), we consider three cases:

- (i) i and j are in conduction band
- (ii) i and j are in valence band
- (iii) j in c.b., i in v.b.

Case (i): Free Electron Absorption

For case (i), we have

$$\begin{aligned}
 \eta(E_j) \rho(E_i) &= \eta(E_j) \left[1 - \frac{1}{1 + \exp\left(\frac{E_i - \phi_n}{kT}\right)} \right] D_c(E_i) \\
 &= \frac{D_c(E_j) D_c(E_i) \exp\left(\frac{E_i - \phi_n}{kT}\right)}{\left[1 + \exp\left(\frac{E_i - \phi_n}{kT}\right) \right] \left[1 + \exp\left(\frac{E_j - \phi_n}{kT}\right) \right]} \quad (2.6)
 \end{aligned}$$

so that (2.2) becomes

$$\left(\frac{\partial g(\nu, t)}{\partial t} \right)_{\substack{ij \\ in \\ c.b.}} = \frac{D_c(E_i) D_c(E_j) \left[\frac{2\pi}{\hbar} |M_{ij}^{c0}|^2 \right]}{\left[1 + \exp\left(\frac{E_i - \Phi_n}{kT}\right) \right] \left[1 + \exp\left(\frac{E_j - \Phi_n}{kT}\right) \right]} \delta(E_j - E_i - h\nu) \cdot$$

$$\left[\exp\left\{ \frac{E_i - \Phi_n}{kT} \right\} \right] \left(\exp\left\{ \frac{h\nu}{kT} \right\} + g(\nu, t) \right) -$$

$$\left(\exp\left\{ \frac{E_j - \Phi_n}{kT} \right\} \right) \left(1 + g(\nu, t) \right) \Bigg]$$

(2.7)

Since the delta function insures $h\nu = E_j - E_i$, (2.7) simplifies to

$$\left(\frac{\partial g(\nu, t)}{\partial t} \right)_{\substack{ij \\ in \\ c.b.}} = -g(\nu, t) \left[\exp\left(\frac{h\nu}{kT}\right) - 1 \right] \cdot$$

$$\frac{\exp\left(\frac{E_i - \Phi_n}{kT}\right) D_c(E_i) D_c(E_i + h\nu)}{\left[1 + \exp\left(\frac{E_i - \Phi_n}{kT}\right) \right] \left[1 + \exp\left(\frac{h\nu + E_i - \Phi_n}{kT}\right) \right]} \cdot$$

$$\left[\frac{2\pi}{\hbar} |M_{ij}^{c0}|^2 \right] \delta(E_j - E_i - h\nu)$$

(2.8)

Equation (2.8) is just the net rate of loss of photons due to absorption by free electrons between states i and j . The matrix element, $M_{ij}^{c.b.}$, for this process thus involves a phonon to conserve momentum and is therefore expected to be both temperature dependent and small compared to the non-phonon processes to be introduced presently.

Summation of (2.8) over all i and j in the conduction band yields the contribution to the total rate of change of q due to absorption by free electrons:

$$\left(\frac{dq}{dt}\right)_{CB \leftrightarrow CB} = -q(\nu) \left[\exp\left(\frac{h\nu}{kT}\right) - 1 \right] \cdot \quad (2.9)$$

$$\int_{E_c}^{\infty} dE \left[4\pi \left(\frac{2m_c}{h\nu} \right)^{\frac{3}{2}} \right]^2 \frac{(E-E_c)^{\frac{1}{2}} (E+h\nu-E_c)^{\frac{1}{2}} \exp\left(\frac{E-\phi_n}{kT}\right)}{\left[1 + \exp\left(\frac{E-\phi_n}{kT}\right) \right] \left[1 + \exp\left(\frac{E-\phi_n+h\nu}{kT}\right) \right]} A_{cc}(E, \nu, T)$$

where we have introduced the appropriate density of states as well as the abbreviation:

$$A_{cc}(E, \nu, T) \equiv \frac{2\pi}{\hbar} \left| \langle E_j T | \tilde{J} \cdot \tilde{A}(\nu) | E + h\nu_j T \rangle \right|^2 \quad (2.10)$$

E in conduction band

for the matrix element (squared).

Case (ii): Free Hole Absorption

In a precisely analogous fashion, we find for case (ii) that the contribution to the total rate of change of q due to absorption by free holes is given by

$$\left(\frac{dq}{dt} \right)_{vB \leftrightarrow vB} = -g(v) \left[\exp\left(\frac{h\nu}{kT}\right) - 1 \right] \cdot \quad (2.11)$$

$$\int_{-\infty}^{E_v} dE \left[4\pi \left(\frac{2m_v}{h^2} \right)^{\frac{3}{2}} \right]^2 \frac{(E_v - E)^{\frac{1}{2}} (E_v - E + h\nu)^{\frac{1}{2}} \exp\left(\frac{\phi_p - E}{kT}\right)}{\left[1 + \exp\left(\frac{\phi_p - E}{kT}\right) \right] \left[1 + \exp\left(\frac{\phi_p - E + h\nu}{kT}\right) \right]} A_{vv}(E, \nu, T)$$

where

$$A_{vv}(E, \nu, T) \equiv \frac{2\pi}{h} \left| \langle E_j T | \tilde{J} \cdot \tilde{A}(\nu) | E - h\nu_j T \rangle \right|^2 \quad (2.12)$$

E in valence band

Case (iii): Interband Transitions

Whereas the intra-band processes (i) and (ii) have thus been shown to lead to a net photon absorption, this is not always the case for the inter-band process (iii) as we now demonstrate.

For j in the conduction band, i in the valence band, we have

$$n(E_j) p(E_i) = \frac{D_c(E_j) D_v(E_i)}{\left[1 + \exp\left(\frac{E_j - \phi_n}{kT}\right) \right] \left[1 + \exp\left(\frac{\phi_p - E_i}{kT}\right) \right]} \quad (2.13)$$

$$E_j \geq E_c \quad ; \quad E_i \leq E_v$$

that is, the density at electrons at E_j times the density of holes at E_i . On the other hand,

$$\begin{aligned} n(E_i) p(E_j) &= D_v(E_i) \left[1 - \frac{1}{1 + \exp\left(\frac{\phi_p - E_i}{kT}\right)} \right] D_c(E_j) \left[1 - \frac{1}{1 + \exp\left(\frac{E_j - \phi_n}{kT}\right)} \right] \\ &= \frac{D_c(E_j) D_v(E_i)}{\left[1 + \exp\left(\frac{E_j - \phi_n}{kT}\right) \right] \left[1 + \exp\left(\frac{\phi_p - E_i}{kT}\right) \right]} \exp\left(\frac{E_j - E_i - (\phi_n - \phi_p)}{kT}\right) \end{aligned} \quad (2.14)$$

Inserting (2.13) and (2.14) into (2.2) we obtain

$$\begin{aligned} \left(\frac{\partial q(\nu, t)}{\partial t} \right)_{\substack{j \text{ in CB} \\ i \text{ in VB}}} &= \frac{D_c(E_j) D_v(E_i) \left[\frac{2\pi}{h} |M_{ij}|^2 \right] \delta(E_j - E_i - h\nu)}{\left[1 + \exp\left(\frac{E_j - \phi_n}{kT}\right) \right] \left[1 + \exp\left(\frac{\phi_p - E_i}{kT}\right) \right]} \cdot \\ &\quad \left\{ \exp\left(\frac{h\nu}{kT}\right) + q(\nu, t) - \left[\exp\left(\frac{E_j - E_i - (\phi_n - \phi_p)}{kT}\right) \right] \left[1 + q(\nu, t) \right] \right\} \end{aligned} \quad (2.15)$$

since $h\nu = E_j - E_i$, a little algebra reduces (2.15) to:

(cf (2.8) and (2.9))

$$\left(\frac{dg(\nu, t)}{dt} \right)_{\substack{j \leftrightarrow cB \\ i \leftrightarrow vB}} = \frac{D_c(E_j) D_v(E_i) \left[\frac{2\pi}{\hbar} |M_{ij}|^2 \right] \delta(E_j - E_i - h\nu)}{\left[1 + \exp\left(\frac{E_j - \phi_n}{kT}\right) \right] \left[1 + \exp\left(\frac{\phi_p - E_j + h\nu}{kT}\right) \right]} \cdot \left\{ \left[\exp\left(\frac{h\nu}{kT}\right) \right] \left[1 - \exp\left(\frac{-(\phi_n - \phi_p)}{kT}\right) \right] - g(\nu, t) \left[\exp\left(\frac{h\nu - (\phi_n - \phi_p)}{kT}\right) - 1 \right] \right\} \quad (2.16)$$

Summation of (2.16) over states in the conduction and valence bands, we obtain the contribution to the total rate of change of q due to band to band transitions:

$$\left(\frac{dq(\nu, t)}{dt} \right)_{vB \leftrightarrow cB} = \left\{ \left[\exp\left(\frac{h\nu}{kT}\right) \right] \left[1 - \exp\left(\frac{-(\phi_n - \phi_p)}{kT}\right) \right] - g(\nu, t) \left[\exp\left(\frac{h\nu - (\phi_n - \phi_p)}{kT}\right) - 1 \right] \right\} \cdot \int_{E_c}^{\infty} dE \left(4\pi \left(\frac{2m_c}{\hbar^2} \right)^{\frac{3}{2}} \right) \left(4\pi \left(\frac{2m_v}{\hbar^2} \right)^{\frac{3}{2}} \right) \frac{(E - E_c)^{\frac{1}{2}} (E_v - E + h\nu)^{\frac{1}{2}}}{\left[1 + \exp\left(\frac{E - \phi_n}{kT}\right) \right] \left[1 + \exp\left(\frac{\phi_p - E + h\nu}{kT}\right) \right]} A_{cv}(E, \nu, T) \quad (2.17)$$

where the interband matrix element is designated by

$$A_{cv}(E, \nu, T) \equiv \frac{2\pi}{\hbar} \left| \langle E - h\nu, T | \hat{J} \cdot \hat{A}(\nu) | E, T \rangle \right|^2$$

E in conduction band
E - hν in valence band

(2.18)

Equation (2.17) has an interesting structure which we will presently explore in more detail. For the time being, we wish to call attention to the inhomogeneous (i. e. independent of q) term which is positive and corresponds to a net spontaneous emission tending to drive the electron and hole subsystems back to equilibrium (i. e. $\phi_n \rightarrow \phi_p$). Even more significant is the fact that the coefficient of q can be negative or positive depending on ν . Specifically, if $h\nu > \phi_n - \phi_p$ then it is negative and corresponds to an exponential attenuation of q with time. On the other hand, if $h\nu < \phi_n - \phi_p$ the coefficient changes sign and corresponds to an exponential amplification $q(\nu)$ due to stimulated emission. Deferring further exploration of this point until later, we make the final observation that for a direct-gap semiconductor, inter-band transitions can occur without the assistance of phonons (or, more precisely, with the aid of relatively plentiful low momentum phonons). Hence the matrix element A_{CV} is thus both weakly temperature dependent and much larger in magnitude than the intraband matrix elements A_{VV} and A_{CC} appearing in (2.9) and (2.11).

2.3 Transitions Involving Impurity Levels

The remaining processes which must be considered are transitions where i or j or both are an impurity level. We distinguish the five remaining cases:

- (iv) i a donor level, j in conduction band
- (v) i in valence band, j an acceptor level
- (vi) i in acceptor level, j in conduction band
- (vii) i in valence band, j a donor level
- (viii) i in acceptor level, j a donor level

Making the reasonable assumption that the energy difference between each impurity level and the nearest band edge is small compared to the band gap energy ($E_c - E_v$), then the occupation of the donor level is determined by the electron Fermi energy ϕ_n , whereas the occupation of the acceptor level is determined by ϕ_p . Specifically, the number of electrons/unit volume in the donor level at temperature T is given by

$$n(E) = \frac{N_D}{1 + \beta_D^{-1} \exp\left(\frac{E_D - \phi_n}{kT}\right)} \delta(E - E_D) \quad (2.19)$$

where N_D is the concentration of donor atoms/unit volume. β_D is the "spin-degeneracy" of the donor⁽¹⁾ which for a monovalent impurity, is generally taken to be 2.

Similarly, the hole concentration in the acceptor level is (in analogous notation)

$$p(E) = \frac{N_A}{1 + \beta_A^{-1} \exp\left(\frac{\phi_p - E_A}{kT}\right)} \delta(E - E_A) \quad (2.20)$$

The evaluation of the various partial transition rates as given by (2.2) then proceeds as before with the exception of a slightly subtle point occasioned by the impurity "spin degeneracy," β : when the final state (say i) is an impurity level, the density-of-final-states $\rho(E_i)$ is given by the hole density at i times the spin degeneracy of the level. A little reflection will indicate why this is so. Thus, for example, in process (iv) cited above we would have

$$\eta(E_j) e(E_i) = \left(\frac{D_c(E_j)}{\left[1 + \exp\left(\frac{\phi_n - E_j}{kT}\right) \right]} \right) \cdot \left(\delta(E_i - E_0) \left[1 - \frac{1}{1 + \beta_D^{-1} \exp\left(\frac{E_D - \phi_n}{kT}\right)} \right] \right) \beta_D \quad (2.21)$$

E_j in conduction band

E_i a donor level

whereas for the inverse process (which does not involve an impurity level in the final state)

$$\eta(E_i) e(E_j) = \left(\frac{\delta(E_i - E_0)}{1 + \beta_D^{-1} \exp\left(\frac{E_D - \phi_n}{kT}\right)} \right) \cdot \left(D_c(E_j) \left[1 - \frac{1}{1 + \exp\left(\frac{\phi_n - E_j}{kT}\right)} \right] \right) \quad (2.22)$$

etc.

Carrying out the calculations we obtain for the various processes:

(iv)

$$\left(\frac{dq}{dt} \right)_{\text{DONOR} \leftrightarrow \text{CB}} = \left\{ -q(\nu) \left[\exp\left(\frac{h\nu}{kT}\right) - 1 \right] N_D \left[4\pi \left(\frac{2m_e}{h^2} \right)^{\frac{3}{2}} \right] \right\} \cdot \left\{ \frac{\left[\exp\left(\frac{E_D - \phi_n}{kT}\right) \right] [E_D + h\nu - E_c]^{\frac{1}{2}}}{\left[1 + \beta_D^{-1} \exp\left(\frac{E_D - \phi_n}{kT}\right) \right] \left[1 + \exp\left(\frac{E_D - \phi_n + h\nu}{kT}\right) \right]} A_{DC}(\nu, T) \right\} \quad (2.23)$$

where

$$A_{DC}(\nu, T) \equiv \frac{2\pi}{h} \left| \langle E_{Dj} T | \hat{J} \cdot \hat{A}(\nu) | E_D + h\nu_j T \rangle \right|^2$$

$$(v) \left(\frac{dq}{dt} \right)_{VB \leftrightarrow \text{ACCEPTOR}} = \left\{ -q(\nu) \left[\exp\left(\frac{h\nu}{kT}\right) - 1 \right] N_A \left[4\pi \left(\frac{2m_v}{h^2} \right)^{\frac{3}{2}} \right] \right\}.$$

$$\left\{ \frac{\left[\exp\left(\frac{\phi_p - E_A}{kT}\right) \right] \left[E_v - E_A + h\nu \right]^{\frac{1}{2}}}{\left[1 + \beta_A^{-1} \exp\left(\frac{\phi_p - E_A}{kT}\right) \right] \left[1 + \exp\left(\frac{\phi_p - E_A + h\nu}{kT}\right) \right]} A_{AV}(\nu, T) \right\}$$

where

$$A_{AV}(\nu, T) \equiv \frac{2\pi}{h} \left| \langle E_{A_j} T | \tilde{J} \cdot \tilde{A}(\nu) | E_A - h\nu_j T \rangle \right|^2$$

$$(vi) \left(\frac{dq}{dt} \right)_{\text{ACCEPTOR} \leftrightarrow CB} = \left\{ \left[\exp\left(\frac{h\nu}{kT}\right) \right] \left[1 - \exp\left(\frac{-(\phi_n - \phi_p)}{kT}\right) \right] - q(\nu, T) \left[\exp\left(\frac{h\nu - (\phi_n - \phi_p)}{kT}\right) - 1 \right] \right\}.$$

$$\left\{ N_A \left[4\pi \left(\frac{2m_c}{h^2} \right)^{\frac{3}{2}} \right] \frac{(E_A + h\nu - E_c)^{\frac{1}{2}} A_{AC}(\nu, T)}{\left[1 + \exp\left(\frac{E_A + h\nu - \phi_n}{kT}\right) \right] \left[1 + \beta_A^{-1} \exp\left(\frac{\phi_p - E_A}{kT}\right) \right]} \right\}$$

where

$$A_{AC}(\nu, T) \equiv \frac{2\pi}{h} \left| \langle E_{A_j} T | \tilde{J} \cdot \tilde{A}(\nu) | E_A + h\nu_j T \rangle \right|^2$$

(vii)

$$\left(\frac{dq}{dt} \right)_{VB \leftrightarrow \text{DONOR}} = \left\{ \left[\exp\left(\frac{h\nu}{kT}\right) \right] \left[1 - \exp\left(\frac{-(\phi_n - \phi_p)}{kT}\right) \right] - q(\nu, T) \left[\exp\left(\frac{h\nu - (\phi_n - \phi_p)}{kT}\right) - 1 \right] \right\}.$$

$$\left\{ N_D \left[4\pi \left(\frac{2m_v}{h^2} \right)^{\frac{3}{2}} \right] \frac{(E_v - E_D + h\nu)^{\frac{1}{2}} A_{VD}(\nu, T)}{\left[1 + \beta_D^{-1} \exp\left(\frac{E_D - \phi_n}{kT}\right) \right] \left[1 + \exp\left(\frac{\phi_p - E_D + h\nu}{kT}\right) \right]} \right\}$$

where

$$A_{VD}(\nu, T) \equiv \frac{2\pi}{h} \left| \langle E_{D_j} T | \tilde{J} \cdot \tilde{A}(\nu) | E_D - h\nu_j T \rangle \right|^2$$

and

$$(viii) \quad \left(\frac{dq}{dt} \right)_{\text{ACCEPTOR} \leftrightarrow \text{DONOR}} = \left\{ \left[\exp\left(\frac{h\nu}{kT}\right) \right] \left[1 - \exp\left(\frac{-(\phi_n - \phi_p)}{kT}\right) \right] - q(\nu, T) \left[\exp\left(\frac{h\nu - (\phi_n - \phi_p)}{kT}\right) - 1 \right] \right\}.$$

$$\left\{ \frac{N_D N_A A_{AD}(T) \delta(h\nu - E_D + E_A)}{\left[1 + \beta_D^{-1} \exp\left(\frac{E_D - \phi_n}{kT}\right) \right] \left[1 + \beta_A^{-1} \exp\left(\frac{\phi_p - E_A}{kT}\right) \right]} \right\}$$

where

$$A_{AD}(T) \equiv \frac{2\pi}{h} \left| \langle E_{Aj} T | \tilde{J} \cdot \tilde{A} \left(\frac{E_D - E_A}{h} \right) | E_{Dj} T \rangle \right|^2$$

2.4 The Threshold Condition

We now sum the partial rates due to all processes and obtain the net result which can be concisely written in the form

$$\frac{dq(\nu)}{dt} = -\alpha(\nu) q + \left\{ \left[1 - \exp\left(\frac{-(\phi_n - \phi_p)}{kT}\right) \right] + \left[\exp\left(\frac{h\nu}{kT}\right) - \exp\left(\frac{-(\phi_n - \phi_p)}{kT}\right) \right] q \right\} \beta(\nu) \quad (2.24)$$

The coefficients α and β are obtained quite simply by comparing (2.24) with the sum of (2.9), (2.11), (2.17) and (2.23). Since there is little point in repeating all these terms for the general case, we will not do so. Later in the development, when specific cases are considered, α and β will be examined in detail.

Nevertheless, much can be learned from (2.24) using only the following properties of α and β (which can be trivially established from their definitions):

- (1) $\alpha > 0$ for all ν
- (2) $\beta = 0$ for photon energies less than a threshold value $(h\nu_0)$ approximately equal to the band gap energy, $E_c - E_v$. In the absence of impurities, this threshold would be exactly that of the band gap.
- (3) Above, but near, this threshold energy, $\beta > 0$ and rises rapidly with increasing frequency. Since the matrix elements on which β depends involve the cooperation of considerably lower momentum phonons in direct-gap semiconductors than do those determining α , $\beta \gg \alpha$ for photon energies in the neighborhood of threshold in such materials.

Turning to (2.24), we observe that for frequencies ν such that

$$\alpha(\nu) - \left[\exp\left(-\frac{h\nu}{kT}\right) - \exp\left(\frac{-(\phi_n - \phi_p)}{kT}\right) \right] \beta(\nu) > 0 \quad (2.25)$$

q has become asymptotically constant at large times with the value

$$q(\nu) = \frac{[1 - \exp(\frac{-(\phi_n - \phi_p)}{kT})] \beta(\nu)}{\alpha(\nu) - \left[\exp\left(-\frac{h\nu}{kT}\right) - \exp\left(\frac{-(\phi_n - \phi_p)}{kT}\right) \right] \beta(\nu)} \quad (2.26)$$

Thus, below the frequency threshold (ν_0) of β , $q \rightarrow 0$ and the spectrum is that of a black-body. Also, as one would expect, when the electron and hole subsystems are in equilibrium so that $\phi_n = \phi_p$, q again is zero. For those frequencies above ν_0 where the inequality (2.25) holds, (2.26) and the definition (2.1) determine the alteration of

the photon spectrum occasioned by the non-equilibrium between electrons and holes. In finite semiconductor samples which are optically thick at frequency ν , (2.26) and (2.1) should give the emission spectrum at such frequencies. Thus, for example, injection luminescence below the laser threshold in GaAs is determined by these equations for optically thick samples.

Our interests, however, lie with laser action which occurs for those frequencies at which the inequality (2.25) is reversed, viz.

$$\alpha(\nu) - \left[\exp\left(-\frac{h\nu}{kT}\right) - \exp\left(-\frac{(\phi_n - \phi_p)}{kT}\right) \right] \beta(\nu) < 0 \quad (2.27)$$

in which case $q(\nu)$ increases in time without limit.

A necessary, though not sufficient, condition for (2.27) to hold is that

$$h\nu_0 < h\nu < \phi_n - \phi_p \quad (2.28)$$

as is readily established from the properties of α and β cited above. Furthermore, since $\beta \gg \alpha$ for frequencies even slightly above ν_0 , we are led to the remarkably simple result that to a good approximation the criterion for the onset of laser action is that the difference between the electron and hole Fermi energies should exceed $h\nu_0$. When the significance of the threshold frequency is explored in somewhat more detail, we can write this criterion specifically as (see Figure 1).

$$\phi_n - \phi_p > \begin{cases} E_C - E_V & \text{intrinsic} \\ E_D - E_V & \text{heavily doped n type} \\ E_C - E_A & \text{heavily doped p type} \\ E_D - E_A & \text{heavily doped but fully compensated} \end{cases} \quad (2.29)$$

Influence of Unequal Electron and Hole Effective
Masses On Threshold Carrier Density

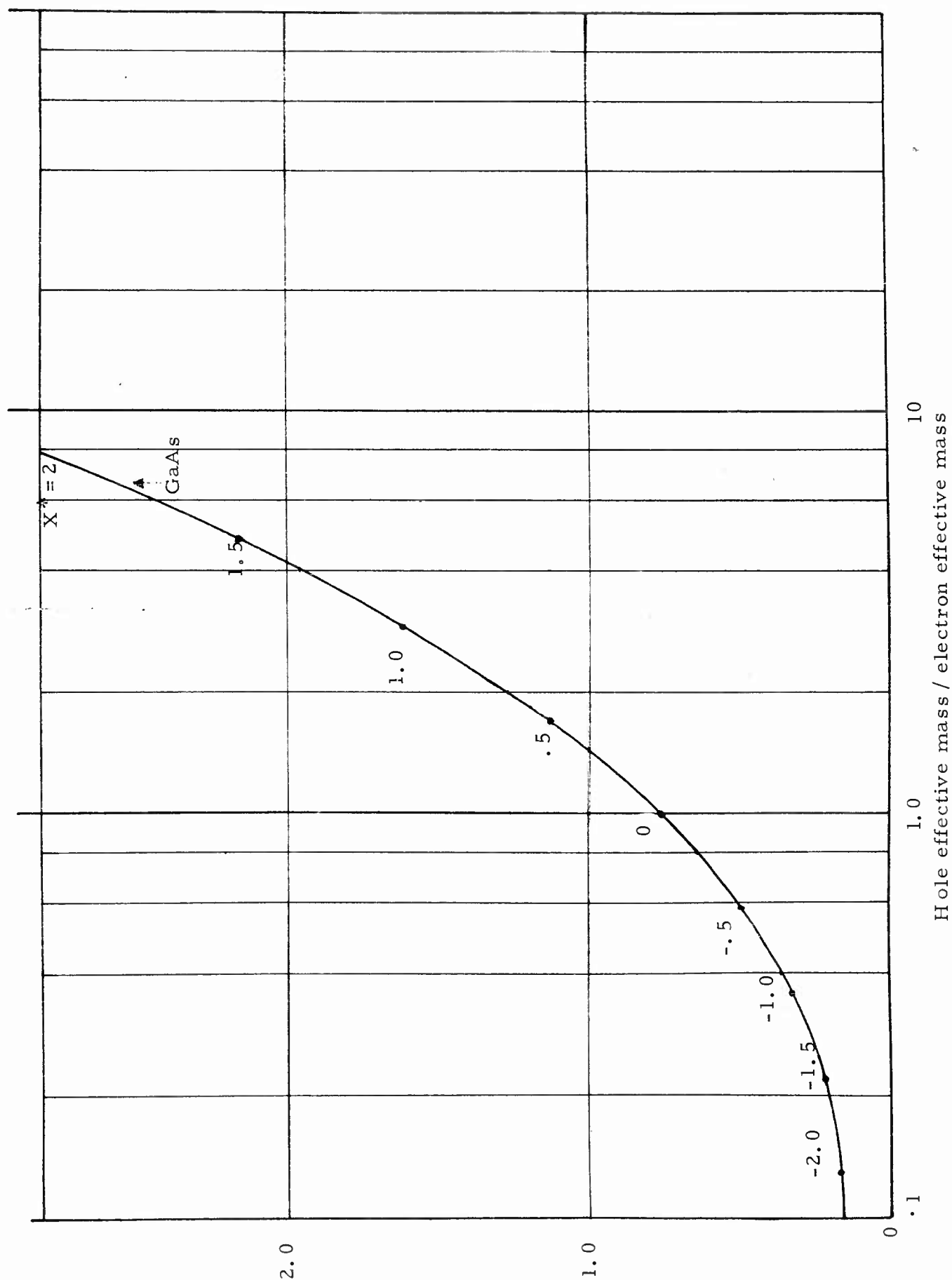


Figure 1a 102

The reason for the various categories in (2.29) is that at low impurity concentrations, only the band-to-band transition component of β is large enough to overcome α whereas at higher concentrations impurity level-to-band transitions (which have lower threshold frequencies) can also contribute sufficiently to β to achieve (2.27). In any event suppose that (2.27) is satisfied for frequencies in the range

$$h\nu_0 < h\nu_1 \leq h\nu \leq h\nu_2 \leq \phi_n - \phi_p \quad (2.30)$$

Then the central frequency of the laser line is at that frequency, ν^* , in this interval where the function

$$\left[\exp\left(-\frac{h\nu}{kT}\right) - \exp\left(-\frac{(\phi_n - \phi_p)}{kT}\right) \right] \beta(\nu)$$

is a maximum.

2.5 Threshold Excess Carrier Densities - Intrinsic Semiconductor

Once the energy levels of Figure 1 and the impurity densities are given, the difference in Fermi energies, $\phi_n - \phi_p$, is uniquely determined by the density of excess carriers. In this subsection, we relate $\phi_n - \phi_p$ to this excess carrier density and can thus re-express the threshold criteria (2.29) in terms of the excess carriers. To this end, we note first that the density of electrons in the conduction band, n_c , is related to ϕ_n by

$$\begin{aligned} n_c &= 4\pi \left(\frac{2m_c}{h^2} \right)^{\frac{3}{2}} \int_{E_c}^{\infty} dE \frac{(E - E_c)^{\frac{1}{2}}}{1 + \exp\left(\frac{E - \phi_n}{kT}\right)} \equiv \\ &\equiv 2 \left(\frac{2\pi m_c kT}{h^2} \right)^{\frac{3}{2}} \mathcal{F}_{\frac{1}{2}} \left[\frac{\phi_n - E_c}{kT} \right] \end{aligned} \quad (2.31)$$

where the (tabulated) Fermi-Dirac integral $\mathcal{F}_{1/2}$ is defined by

$$\mathcal{F}_{1/2}(x) = \frac{2}{\sqrt{\pi}} \int_0^{\infty} \frac{\epsilon^{1/2} d\epsilon}{1 + \exp(\epsilon - x)} \quad (2.32)$$

The density of electrons in the donor level, n_D , is similarly given by

$$n_D = \frac{N_D}{1 + \beta_D^{-1} \exp\left(\frac{E_D - \phi_n}{kT}\right)} \quad (2.33)$$

Thus, the density of excess electrons, n_{ex} , contained in the donor level + conduction band is

$$\begin{aligned} n_{ex} &= n_c - (N_D - n_D) = \\ &= 2 \left(\frac{2\pi m_c kT}{h^2} \right)^{3/2} \mathcal{F}_{1/2} \left[\frac{\phi_n - E_c}{kT} \right] - \\ &\quad - \frac{N_D \beta_D^{-1} \exp\left(\frac{E_D - \phi_n}{kT}\right)}{1 + \beta_D^{-1} \exp\left(\frac{E_D - \phi_n}{kT}\right)} \end{aligned} \quad (2.34)$$

In a similar fashion, we obtain for the density of excess holes in the acceptor level + valence band

$$p_{ex} = 2 \left(\frac{2\pi m_v kT}{h^2} \right)^{\frac{3}{2}} \mathcal{F}_{\frac{1}{2}} \left[\frac{E_v - \phi_p}{kT} \right] - \frac{N_A \beta_A^{-1} \exp \left(\frac{\phi_p - E_A}{kT} \right)}{1 + \beta_A^{-1} \exp \left(\frac{\phi_p - E_A}{kT} \right)} \quad (2.35)$$

Charge neutrality demands that

$$n_{ex} = p_{ex} \quad (2.36)$$

Equations (2.34) - (2.36) then determine ϕ_n and ϕ_p in terms of n_{ex} .

Consider first the case of an ideal intrinsic semiconductor ($N_A = N_D = 0$), the threshold condition for which is

$$\phi_n - \phi_p = E_c - E_v \quad (2.37)$$

From the preceding equations we find for the threshold excess charge density, n^* , the expression

$$n^* = 2 \left(\frac{2\pi m_c kT}{h^2} \right)^{\frac{3}{2}} \mathcal{F}_{\frac{1}{2}} (\chi^*) \quad (2.38)$$

where

$$\left(\frac{m_v}{m_c} \right)^{\frac{3}{2}} = \frac{\mathcal{F}_{\frac{1}{2}} (\chi^*)}{\mathcal{F}_{\frac{1}{2}} (-\chi^*)} \quad (2.39)$$

Thus for this example, η^* is proportional to $T^{3/2}$, the constant of proportionality depending on the ratio of hole and electron effective masses. (2.38) and (2.39) are exhibited graphically in Figure 1 a

For GaAs, $m_v \approx 0.5 m_o$, $m_c = 0.08 m_o$ in which case we find \dagger

$$\chi_{\text{GaAs}}^* = 1.77 \quad \eta^* = 1.68 \left(\frac{m_o kT}{h^2} \right)^{\frac{3}{2}} \quad (2.40)$$

Evaluation of (2.40) at room temperature, liquid nitrogen temperature, and liquid helium temperature leads to the results in Table 1.

T =	4.2°	77°	300°	K
η^*	2.25 x 10 ¹⁵	1.77 x 10 ¹⁷	1.36 x 10 ¹⁸	electron-hole pairs/cc

Table 1. Temperature Dependence of Critical Excess Carrier Densities for Intrinsic GaAs

\dagger Mayburg⁽¹¹⁾, on the basis of a crude, heuristic analysis, obtains

$$\eta^* = 1.45 \left(\frac{m_o kT}{h^2} \right)^{3/2}$$

2.6 Threshold Excess Carrier Densities - Effects of Impurities

When impurities are present, we shall find that the threshold excess carrier densities derived in the previous subsection for intrinsic material (henceforth to be denoted by η_{int}^*) are lowered. The calculation of this lowering, however, is complicated by the fact that we must now consider the four possible transitions shown in Figure 2 rather than just band-band as before. The threshold frequency for each case is as shown.

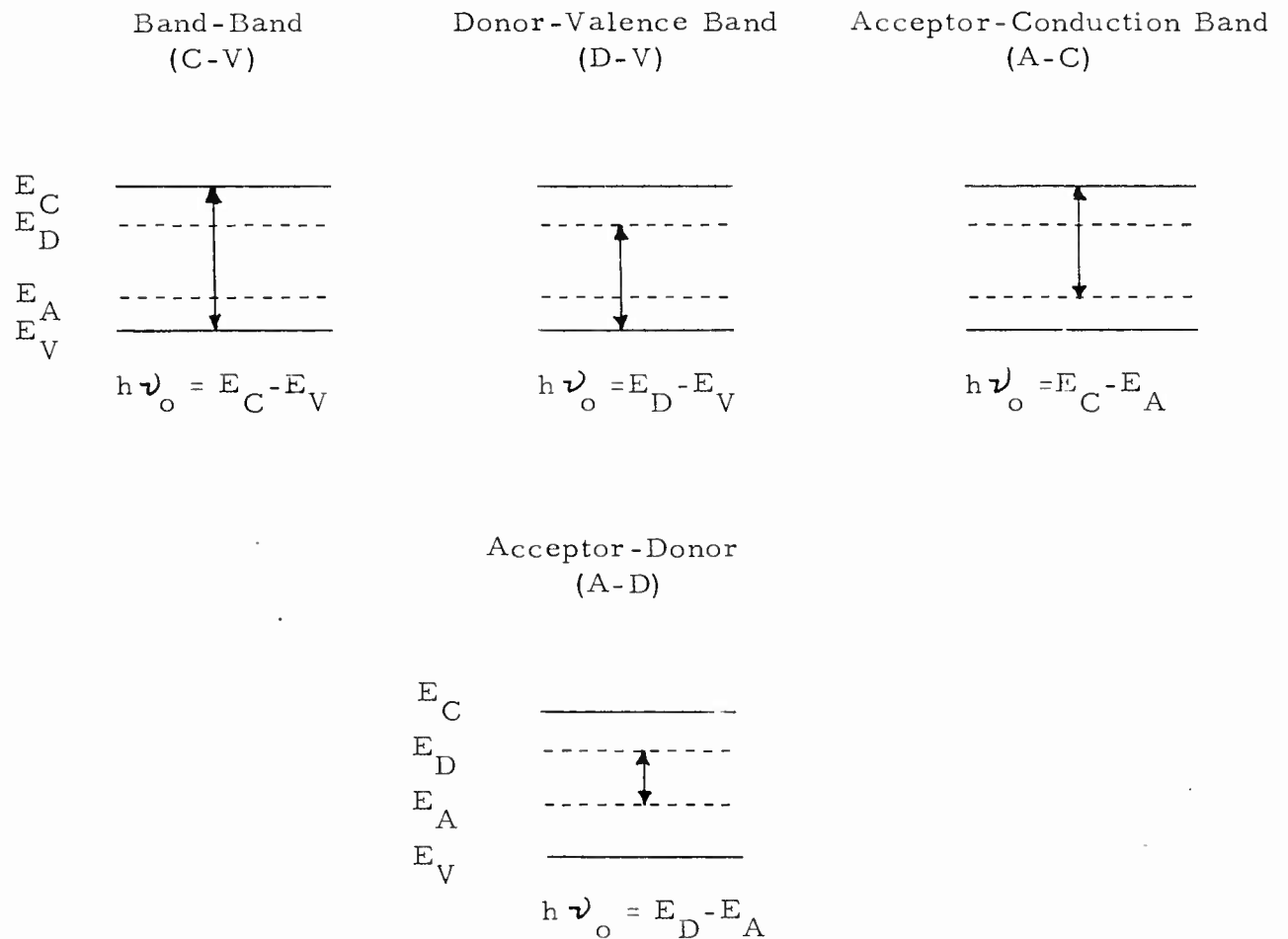


Figure 2 Possible Transitions When Impurities are Present

Although these distinctions can be shown to negligibly influence the threshold excess carrier density if the impurity levels differ in energy from the nearest band edge by much less than kT , this condition will not always hold--especially at very low temperatures. We should, therefore, consider all possibilities although it must be borne in mind that at sufficiently low impurity concentrations, induced transitions involving such levels will not favorably compete with free carrier absorption and laser action at such frequencies will be impossible. Since we cannot ascertain at what concentrations this occurs without a detailed calculation of the matrix elements involved, we will proceed as if laser action involving impurity levels can occur, relegating the consideration of the foregoing question to a future calculation.

Now, the solution of the relevant equations (2.34 - 2.36) can only be carried out numerically. In the interest of brevity, therefore, we will fix our attention on a specific material, GaAs, for which considerable experimental data on the behavior and effect of impurities is available. The donor is chosen to be Tellurium, the acceptor to be Zinc. From a variety of experimental evidence^(*) it has been found that for donor concentrations below about $5 \times 10^{17} \text{ cm}^{-3}$, the donor level lies very close ($\sim 0.003 \text{ eV}$) to the conduction band edge and merges with the conduction band at higher concentrations. We therefore can take $E_C - E_D = 0$ without appreciable error, a convenient circumstance indeed since we need then only consider the two processes C-V and A-C of Figure 2.

*Broom, R. F., Barrie, R. and Ross, I. M., Semiconductors and Phosphors, Proc. of Int'l Colloq. at Garmisch-Partenkirchen, p. 453, Friedr. Vieweg und sohn (1958); Emel'yanenko, O. V. and Nasledov, D. N., Zhur. Tekh. Fiz. 28, 1177 (1958).

Zinc is soluble in (

and leads to an acceptor level lying about 0.08 ev above the valence band for solution grown and diffused samples^{*}, or about 0.030 ev for diffused samples^{**}. We will take the latter value since diffused samples are more easily fabricated and more commonly used. Although, rigorously speaking, this energy difference is, to a certain extent, temperature and concentration dependent, we will ignore such complications. The "spin degeneracies" of both donor and acceptor are taken to be 2.

The numerical solution of equations 2.34 - 2.36 is straightforward. The results are given in Figure 3, where we plot the threshold excess carrier density as a function of impurity concentration for uncompensated donors (Te) and acceptors (Zn). We consider both the conduction-valence band and conduction band-acceptor level transitions. (The latter transition is not shown at 4.2° K since the computed threshold concentrations are essentially zero, even at low impurity concentrations. These unrealistically low values, while indicative that laser action at the 4.8 ev line should be easily attainable at 4.2° K, are somewhat misleading since the inclusion of donor-acceptor compensation as well as the nonzero separation of the donor level from the conduction band edge will markedly alter them).

* Weisberg, L. R., Rosi, F. D. and Herkart, P.G., Metallurgical Society Conferences, Vol. 5, Interscience, N. Y. (1959); Dousmanis, G.C., Mueller, C. W. & Nelson, H., Appl. Phys. Letters, 3, 133, 1963.

** Nathan, M. I. and Burns, G., Appl. Phys. Letters 1, 89 (1962).

Effect of Uncompensated Donors (Te) and Acceptors (Zn) on Threshold Excess Carrier Concentration for GaAs Laser

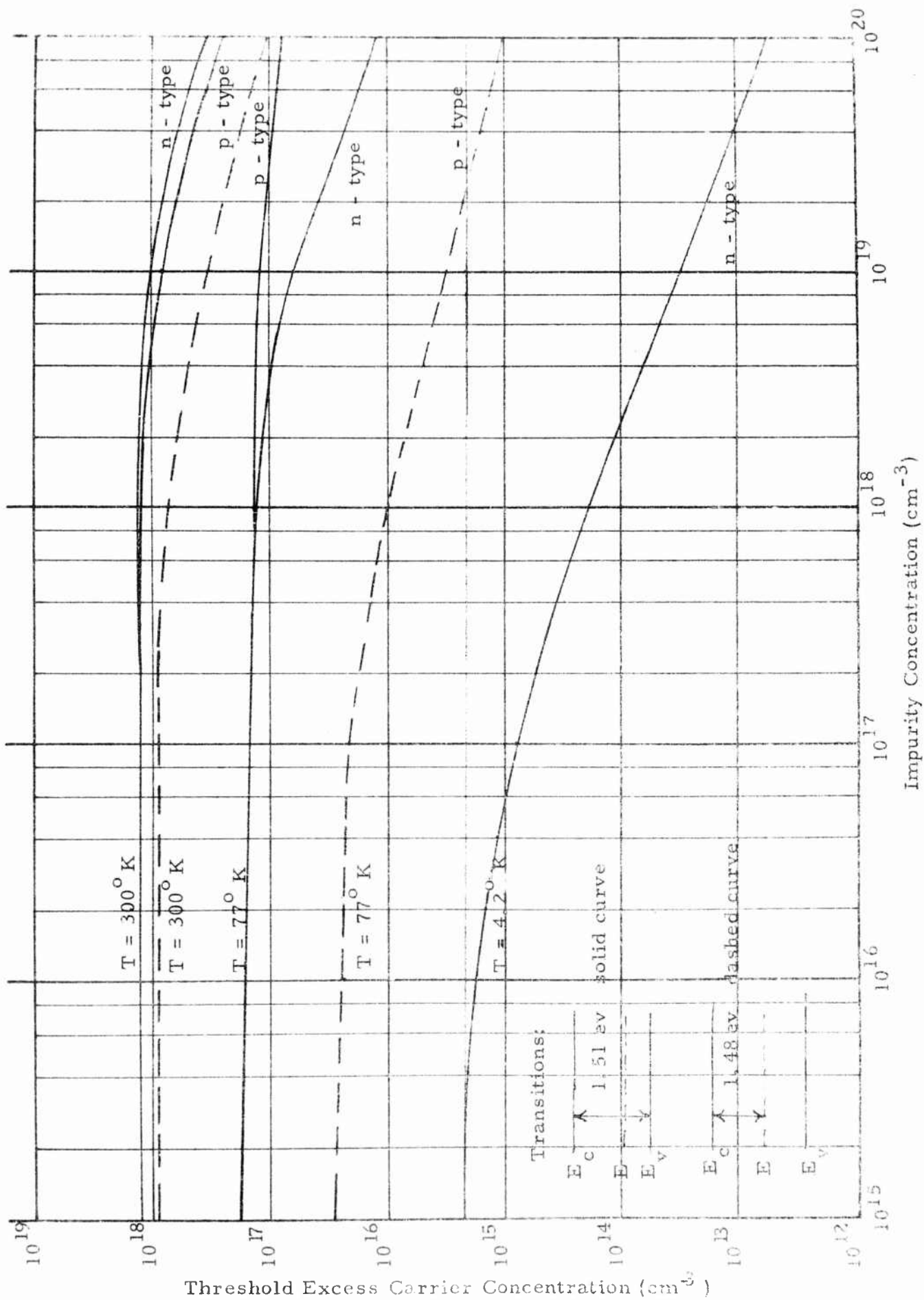


Figure 3

Several conclusions may be drawn from these results:

1. Whereas at room temperature n and p type GaAs have similar thresholds for the band-band transition, at significantly lower temperatures the n-type material is more favorable for laser action at this line. This is due to the freezing out of the acceptors.

2. In spite of the foregoing, laser action in heavily doped p-type GaAs is more easily achieved than in n-type, since the conduction-band to acceptor level transition has a much lower threshold than that of the band-band transition. This dominance of the 1.48 ev line over that at 1.51 ev in all but lightly doped n-type GaAs has been experimentally observed.*

3. At liquid nitrogen temperatures, laser action (at 1.48 ev) in heavily ($\sim 10^{20} \text{ cm}^{-3}$) doped p-type GaAs should be possible for excess carrier concentrations greater than 10^{15} cm^{-3} . At room temperature, this threshold is increased by about two orders of magnitude.

* Wilson, D. K., Appl. Phys. Letters 3, 127, 1963.

2.7 Frequency Dependence of Stimulated Emission

When the excess carrier concentration exceeds the threshold computed in the previous subsection, stimulated emission is the dominant process and laser action occurs. The strength, frequency, and band-width of the laser line is then controlled by the function $\beta(\nu)$ contained in equation 2.24. Specifically, $q(\nu)$ increases in time as

$$\frac{dq}{dt} \sim \exp \left\{ \left[\exp\left(-\frac{h\nu}{kT}\right) - \exp\left(-\frac{(\phi_n - \phi_p)}{kT}\right) \right] \beta(\nu) \right\} \quad (2.41)$$

so that the quantity

$$G(\nu) \equiv \frac{1}{C'(\nu)} \left[\exp\left(-\frac{h\nu}{kT}\right) - \exp\left(-\frac{(\phi_n - \phi_p)}{kT}\right) \right] \beta(\nu) \quad (2.42)$$

may be interpreted as the photon gain per cm of the material when in a lasable condition specified by a value of $\phi_n - \phi_p$ in excess of the frequency threshold $h\nu_0$. In this subsection, we wish to examine $G(\nu)$.

Since we have shown that the most favorable situation is when stimulated emission involves the participation of an acceptor level, we will limit our considerations to this case. Specifically, we focus attention on the conduction band-acceptor level transition, occurring in p-type GaAs at about 1.48 eV. Maximal doping, i. e. the solubility limit of 10^{20} cm^{-3} , will be assumed. (The fact that the gap energy, $E_C - E_V$, is lowered somewhat due to the heavy doping must be taken into account to locate the laser frequency. Since this gap shrinkage arises from causes unrelated to the radiative processes herein considered, we will treat the gap energy as an arbitrary, but fixed, quantity and will locate the laser line relative to this gap. We will, however, assume that the energy separation ($\sim .03 \text{ eV}$) between the acceptor level and valence band edge is unchanged).

Going back to equation 2.24, we find from equation 2.23 - (vi) that, for the c. b. - acceptor transition

$$\beta(\nu) = \left(\exp\left[\frac{h\nu}{kT}\right] \right) N_A \frac{(E_A + h\nu - E_c)^{\frac{1}{2}} \left[4\pi \left(\frac{2m_c}{h^2} \right)^{\frac{3}{2}} A_{Ac}(\nu, T) \right]}{\left[1 + \exp\left(\frac{E_A + h\nu - \phi_n}{kT}\right) \right] \left[1 + \beta_A^{-1} \exp\left(\frac{\phi_p - E_A}{kT}\right) \right]}$$

(2.43)

$$E_c - E_v > h\nu > E_c - E_A$$

As it is not our intention to compute the matrix element, A_{Ac} , we will consider it to be a given quantity and ignore its slight frequency variation over the narrow laser bandwidth. Thus

$$G(\nu) = \text{CONSTANT} \cdot N_A \frac{\left[1 - \exp\left(\frac{h\nu - (\phi_n - \phi_p)}{kT}\right) \right] [E_A + h\nu - E_c]^{\frac{1}{2}}}{\left[1 + \exp\left(\frac{E_A + h\nu - \phi_n}{kT}\right) \right] \left[1 + \beta_A^{-1} \exp\left(\frac{\phi_p - E_A}{kT}\right) \right]}$$

(2.44)

$$E_c - E_v > h\nu > E_c - E_A \equiv h\nu_0$$

Defining the reduced quantities

$$\frac{h\nu - h\nu_0}{kT} = \frac{h\nu - (E_c - E_A)}{kT} \equiv \omega \qquad \frac{\phi_n - E_c}{kT} \equiv \chi$$

$$\frac{\phi_n - \phi_p - h\nu_0}{kT} = \frac{\phi_n - \phi_p - (E_c - E_A)}{kT} \equiv \eta \qquad (2.45)$$

2.44 becomes

$$G(\omega) = \text{CONSTANT} \cdot N_A \frac{[1 - \exp(\omega - \eta)] (kT)^{\frac{1}{2}} \omega^{\frac{1}{2}}}{[1 + \exp(\omega - \chi)] [1 + \frac{1}{2} \exp(\chi - \eta)]} \quad (2.46)$$

where β_A has been given the value 2.

η and χ are determined by the excess carrier concentration, n_{ex} , via the relations.

$$n_{\text{ex}} = 2 \left(\frac{2\pi m_v kT}{h^2} \right)^{\frac{3}{2}} F_{\frac{1}{2}}(\chi) \quad (2.47)$$

$$n_{\text{ex}} = 2 \left(\frac{2\pi m_c kT}{h^2} \right)^{\frac{3}{2}} F_{\frac{1}{2}}(\eta - \chi - \Delta) - \frac{N_A}{1 + 2\exp(\eta - \chi)} \quad (2.48)$$

where $\Delta = E_A - E_v/kT$

To fix ideas, we have computed $G(\omega)$ for heavily zinc doped ($N_A = 10^{20} \text{ cm}^{-3}$) GaAs at $T = 77^\circ \text{ K}$ for excess carrier concentrations (n_{ex}) of 2×10^{15} , 10^{16} and 10^{17} cm^{-3} , i.e. 2, 10 and 100 times the threshold value, n_{ex}^* . The results are shown in Figure 4. The frequency of maximum gain, that at which the laser line would be centered, is seen to shift to higher energies as the excess carrier concentration is increased. The line width and intensity also are seen to increase.

Photon Gain for Conduction Band - Acceptor Level Laser Transition in p-type GaAs

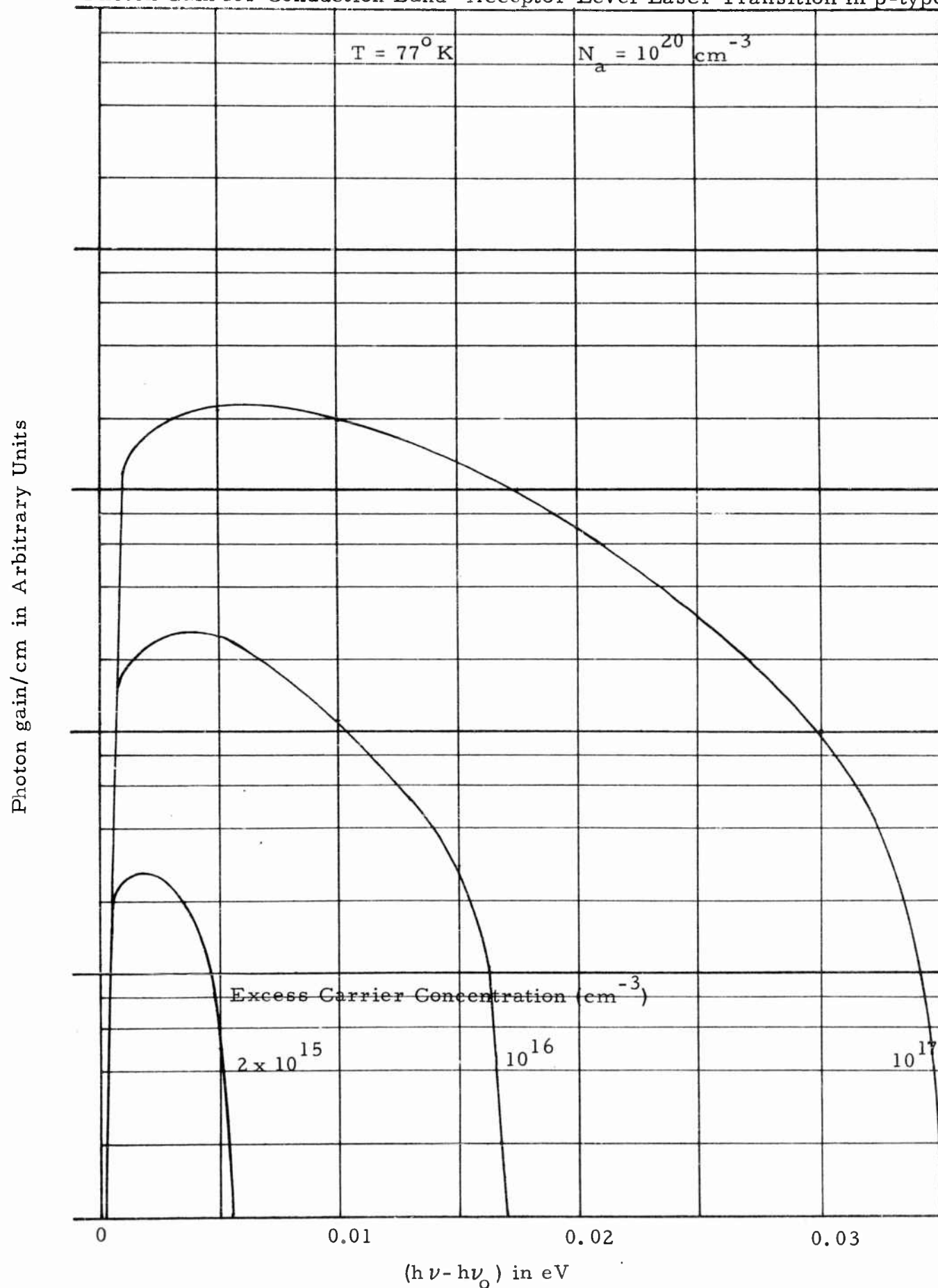
 $(h\nu - h\nu_0)$ in eV

Figure 4 115

3. FURTHER CHARACTERISTICS OF LASER ACTION3.1 Laser Action

Laser action occurs when the photon field of a given electromagnetic mode induces a greater amount of photon emission than absorption. The photon population builds up until it is limited by the finite rate at which excited states are produced. Conditions for lasing have been obtained by Combrisson, Honig and Townes^(1,2) for the case of a single pair of levels radiating into a Lorentzian shaped line.

The typical equations describing the population inversions of the upper laser level, n , in the presence of a driving photon field, q , can be written:

$$dn/dt = aP - An - Anq$$

$$dq/dt = \alpha Anq - \beta q$$

where A is the transition probability for decay from the upper state, αAnq is the rate of increase of stimulated photons, losses are accounted for in the β term, n is the inversion level and aP is the rate of exciting the upper state.

The equations appropriate for population inversion in a semiconductor have the same general form but they differ in detail.

Three equations can be written corresponding to the population of electrons, hole and photons. Only two of the equations are written here. In this case the assumption is made that radiation occurs in only one electromagnetic mode which propagates perpendicular to reflective surfaces in an optical laser structure.

The time rate of change of electrons is given by

$$\frac{dn}{dt} = \left(\frac{dn}{dt}\right)_{\text{Formation}} + \left(\frac{dn}{dt}\right)_{\text{Recombination}} + \left(\frac{dn}{dt}\right)_{\text{Other Absorption}}$$

And the photon flux by

$$dq/dt = \left(\frac{dq}{dt}\right)_{\text{Inducted}} + \left(\frac{dq}{dt}\right)_{\text{Free Carrier}} + \left(\frac{dq}{dt}\right)_{\text{End Losses}} + \left(\frac{dq}{dt}\right)_{\text{Other}}$$

where

dn/dt	= rate of change of electrons in the conduction band
$(dn/dt)_F$	= rate of generation of degenerate electrons in conduction band
$(dn/dt)_R$	= rate of electron change due to recombination radiation
$(dn/dt)_O$	= rate of electron change due to other absorption mechanisms
dq/dt	= rate of change of the photon flux
$(dq/dt)_I$	= the induced interband transition rate corresponding to photon emission
$(dq/dt)_{FC}$	= the free-carrier absorption photon loss rate
$(dq/dt)_{EL}$	= rate of loss of photons from the ends
$(dq/dt)_O$	= the photon loss rate due to other absorption mechanisms

In Figure 5 these two situations are depicted.

It is more convenient to use absorption coefficients rather than rate terms. The photon absorption coefficients are related to the rates by

$$K = \frac{-n_o}{cq} \quad dq/dt \quad .$$

The condition for lasing in terms of the absorption coefficients is simply that the induced emission coefficient must be greater

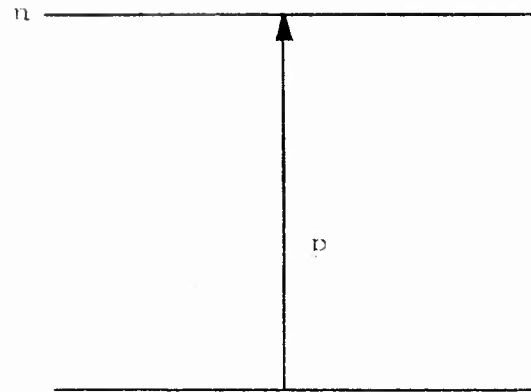


Figure 5a. Simple two level system

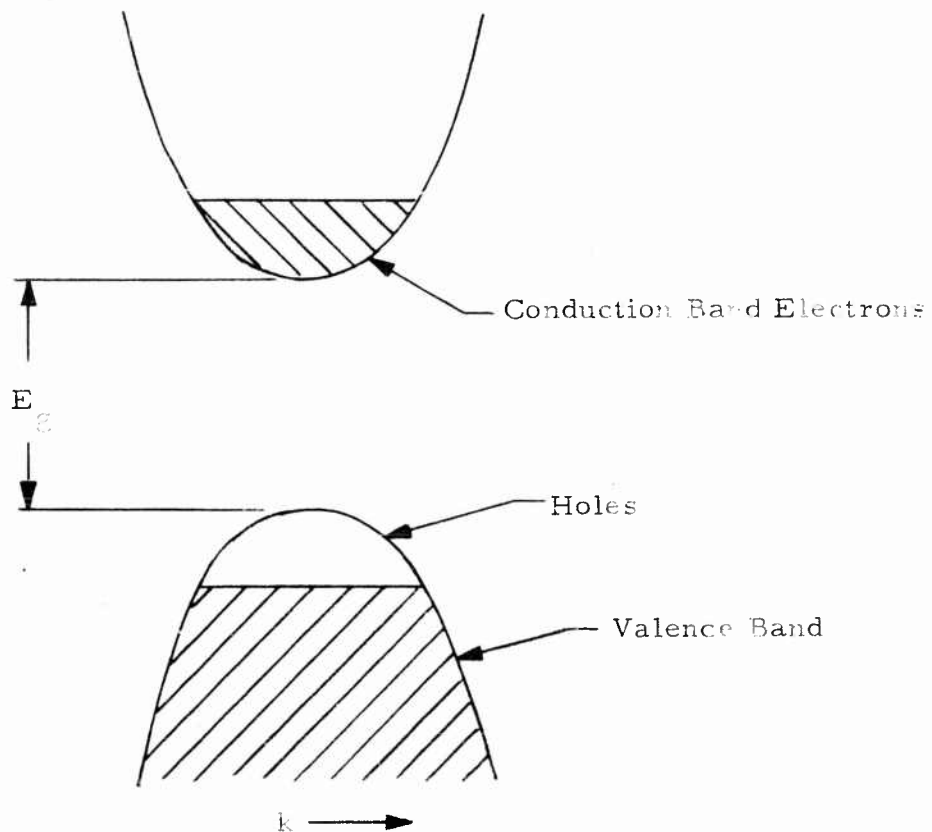


Figure 5b. Semiconductor case

Figure 5 Energy level diagram for laser action

than the sum of the absorption losses

$$|K_I| > \left| \sum K_{\text{losses}} \right|$$

The end loss term $\left(\frac{dq}{dt} \right)_{EL}$ corresponds to a decrease of photon population due to transmission losses at the reflecting surfaces. This term is given by

$$(dq/dt)_{EL} \simeq (1-R)qc/n_o$$

or

$$K_{EL} = (1-R)/\ell$$

where R is the reflectivity of the end surfaces and ℓ is the distance between them. Since R can be made close to one, e.g. 0.99, a long sample can be used, for instance 2 cm, so that the term $K_{EL} \sim 5 \times 10^{-3} \text{ cm}^{-1}$. This value is very small compared to other losses and hence can be neglected.

The term $(dq/dt)_{FC}$ represents the free-carrier losses. Although free-carrier losses are not generally considered a strong loss mechanism Dumke⁽¹³⁾ points out that this is not so, for this case, and is likely to be the most important photon loss mechanism in direct gap materials and treats the problem in the following manner.

The effects of end losses can be made small by improving reflectivity and using longer samples. However, the free-carrier absorption coefficient cannot be altered without also affecting the photon emission characteristics of the materials. In addition Dumke states that very long ($\sim 10 \text{ cm}$) photon mean free paths are required for laser action.

3.2 Magnitudes of Rate Coefficients

Absorption by free carriers consists of indirect transitions to a state in the same band which is approximately a photon energy away from the band bottom. It is of approximately the same magnitude for direct and indirect band-gap materials. Phonon scattering is usually required in order to conserve overall momentum in the transition. Impurities are relatively ineffective in supplying the necessary momentum, since the amplitudes of the Fourier components of the impurity potential corresponding to large momentum changes are very small. For very high doping, however, it is observed that impurity scattering does enhance the free-carrier absorption.

Free-carrier absorption decreases with temperature as the lattice vibrations become less excited, but because relatively high wave number modes are involved, there is little temperature dependence of free-carrier absorption at cryogenic temperatures (below 100° K.)

Excitons are expected to have cross sections for free-carrier absorption given by the sum of the cross sections of the electron and hole as long as the photon energy is much larger than the exciton binding energy. This is supported by observations that the cross section of electrons is the same whether they are in donor states or ionized^(*).

The absorption constant for the free carriers will be given simply by

$$K_{FC} = n \sigma_n + p \sigma_p$$

where σ_n and σ_p are the cross sections of free electrons and holes for photon absorption at the appropriate wavelength, temperature, and crystal purity, and n and p are the total number of free (or nearly free)

(*) Spitzer and Fan, Phy Rev 108, 268 (1957)

electrons and holes per unit volume, including those in excitons and shallow impurity states.

K_{FC} is the free-carrier absorption coefficient, using empirical values, which corresponds to the number of holes and electrons in the substance under consideration. K_{FC} must be obtained for the correct conditions of impurity scattering, temperatures and wavelength in the sample. The absorption coefficient due to other factors, K_o , is assumed to be negligible. Dumke also makes this assumption.

K_I is the absorption coefficient for an interband transition and is negative when a population inversion exists; $-K_I$ then becomes a photon amplification constant.

If $-K_I$ is greater than $K_{EL} + K_{FC}$ where other losses are negligible then the photon population will increase with time or with distance traveled and stimulated emission will result.

Consider a sample of GaAs with an electron and hole density of 10^{16} cm^{-3} which lie degenerately close to the band edges. This could occur if the thermalization times are much shorter than the recombination times. The states in the conduction band will be filled to an energy of 0.0023 eV from the conduction band edge and the heavy holes to an energy of 0.0004 eV from the valence band edge. Both bands have about the same volume in k space filled with carriers, since almost no holes go into the light hole band. Photon amplification due to induced direct transitions will be a maximum for $E = E_g + 0.0027 \text{ eV}$.

The value A' in the absorption coefficient was estimated by Dumke to be approximately $6000 \text{ cm}^{-1} \text{ eV}^{-1/2}$. Taking into account only transitions between the heavy hole and conduction bands, the photon amplification constant then becomes

$$-K_I = A' (h\nu - E_g)^{\frac{1}{2}} = 300 \text{ cm}^{-1}$$

The free-carrier absorption constant can be calculated if we assume the absorption cross section of holes to be equal to the known cross section for electrons. Dumke obtains $K_{FC} = 0.1 \text{ cm}^{-1}$.

Since the photon amplification constant is so large, e.g. 300 cm^{-1} , it would be possible to tolerate several orders of magnitude increase of K_{FC} in GaAs and still obtain amplification.

3.3 Density Variation of Rate Coefficients

As discussed in a following section, the free carriers created by the passage of a nuclear particle very rapidly fill the conduction band in the vicinity of the band edge and in a degenerate manner (Figure 5).

The inverted electron density can now be related to the filled energy level in the conduction band as follows: using a simple model of a scalar effective mass and constant spherical energy surfaces in k space centered at $k = 0$.

$$E = E_c + \frac{\hbar^2 k^2}{2m_{\text{eff}}}$$

The density of states $N(E)$ is

$$N(E) = 4 \pi (2m_{\text{eff}} \hbar^2)^{3/2} (E - E_c)^{1/2}$$

and the total number of states filled, up to an energy E , will be given by

$$N_T = \int_{E_c}^E N(E) dE$$

$$N_T = \frac{8\pi}{3} (2m_{\text{eff}} \hbar^2)^{3/2} (E - E_c)^{3/2}.$$

For GaAs which has an effective electron mass of 0.08, the results are given in Figure 6.

For an inverted density of $\eta_e = 10^{16}$ elec/cm³,
 $\Delta E = 2.7 \times 10^{-3}$ ev, using Dumke's value.

The valence band will be emptied to a lower depth due to the higher hole effective mass $m_h = 0.5 m$ hence for $\Delta E = 3.3 \times 10^{-4}$ ev.

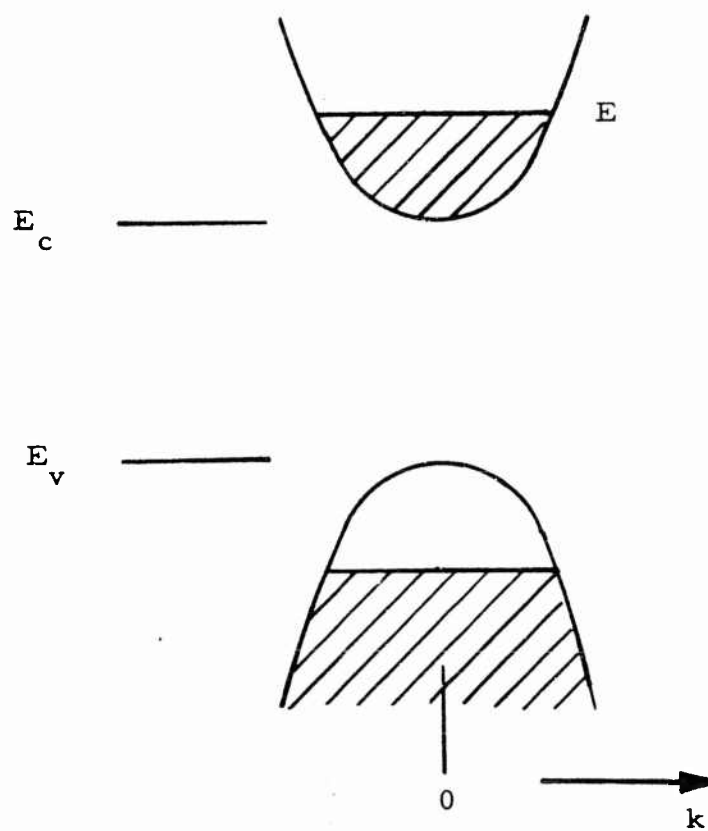


Figure 5 . Free-Carrier Generation by Nuclear Radiation

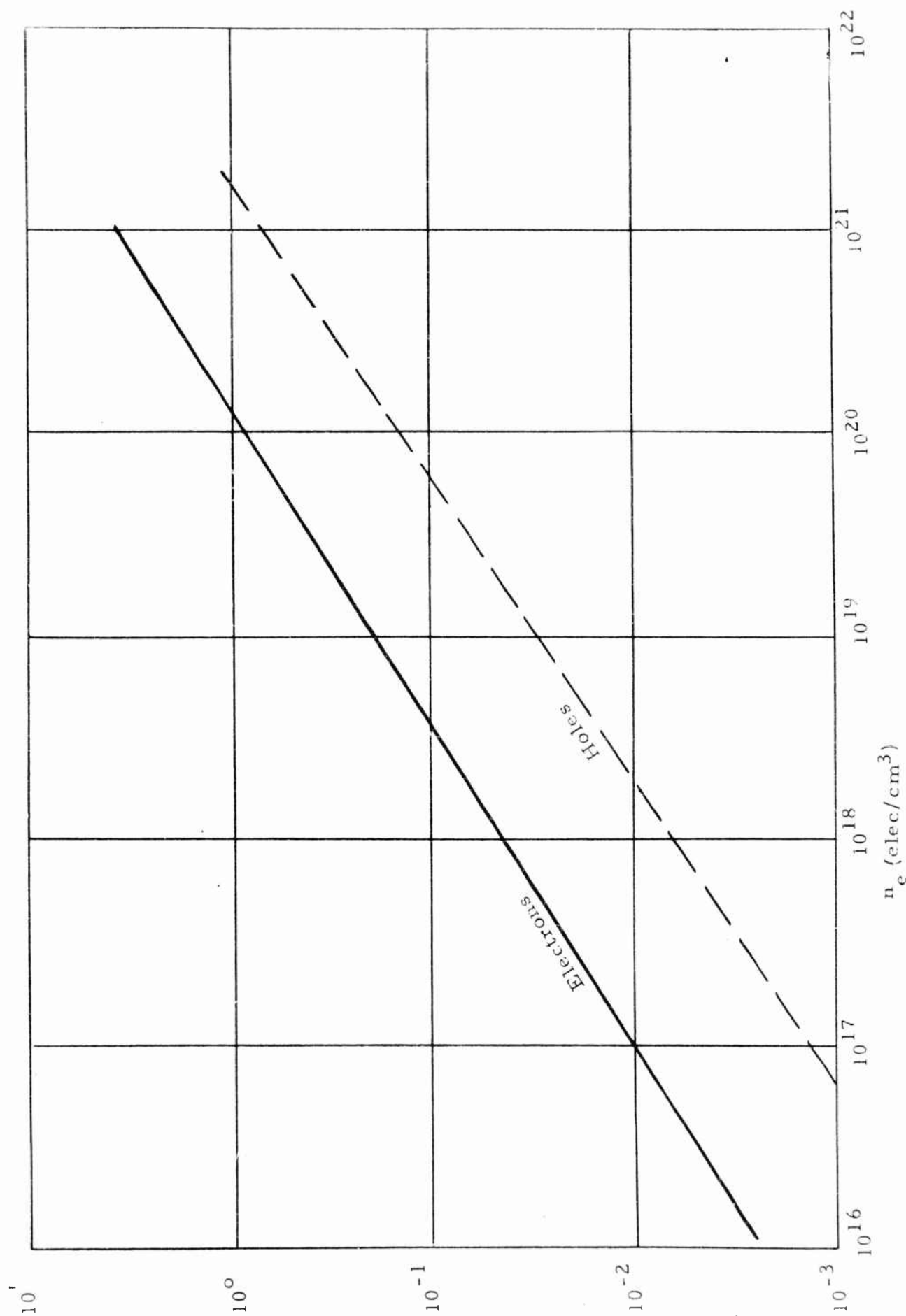


Figure 6. Total number of electrons in conduction band n_e vs energy level ($\Delta E = E - E_c$)

The negative absorption coefficient for GaAs can be estimated as a function of $\Delta E = (h\nu - E_g)$. This function is seen in Figure 7. For the higher inversion levels the negative or higher photon absorption coefficient becomes very large. For example at $\eta_c = 10^{16}$, $\Delta E = 3 \times 10^{-3}$ ev and $-K_I = 3 \times 10^2 \text{ cm}^{-1}$ and at $\eta_c = 10^{18}$, $\Delta E = 6 \times 10^{-2}$ ev and $-K_I = 1.4 \times 10^3 \text{ cm}^{-1}$.

At room temperature or below with a free-carrier concentration of 10^{16} p/cm^3 or above, free-carrier absorption appears to be small compared to induced inversion.

The free-carrier absorption constant using Dumke's equation is shown in Figure 8. The time required to reach the concentration of $10^{16} \text{ elec/cm}^3$ for several current densities is given in Table I (all loss mechanisms are ignored).

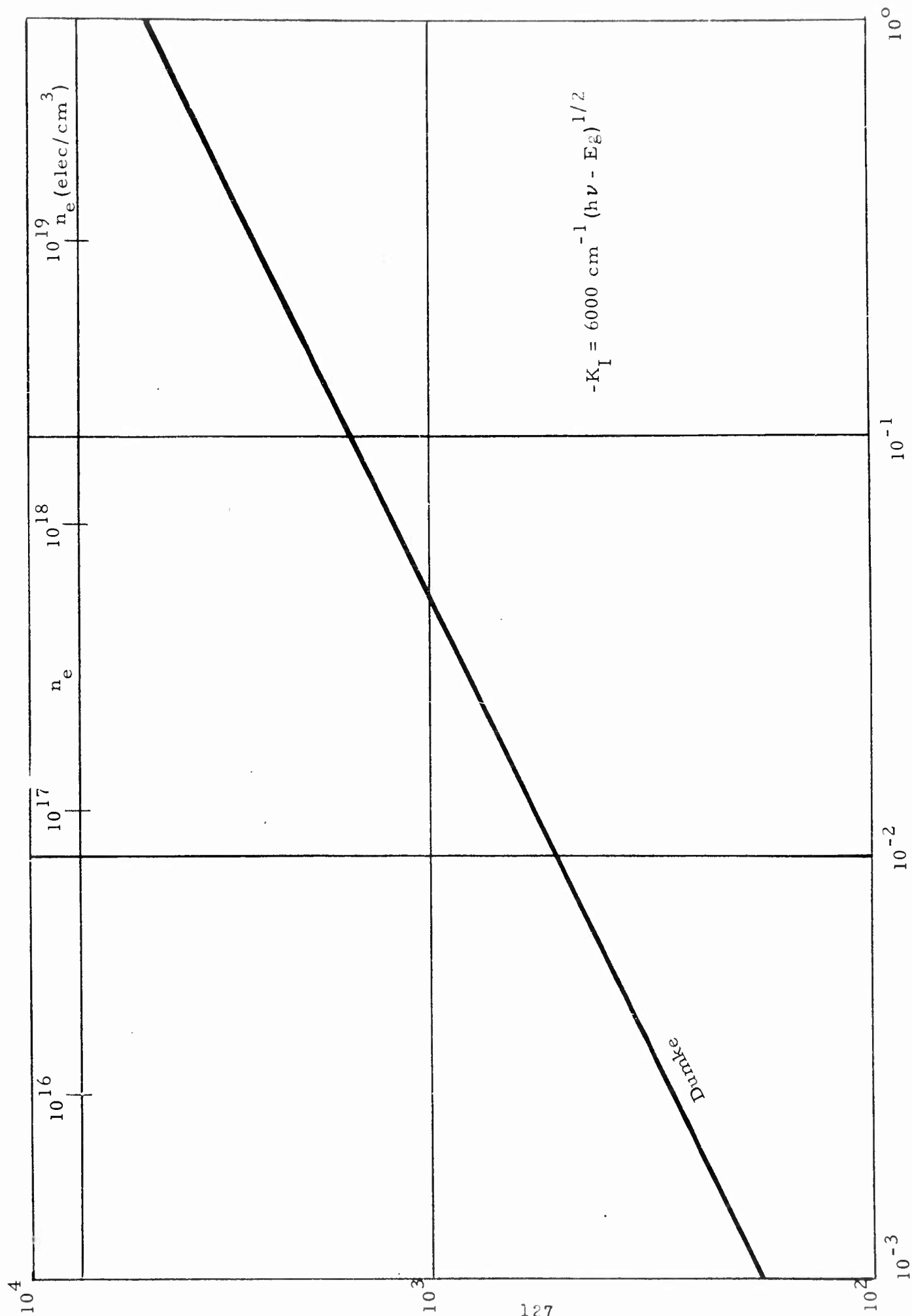


Figure 7. Estimated Negative Absorption Coefficient (GaAs) as Function of $\Delta E = (h\nu - E_g)$

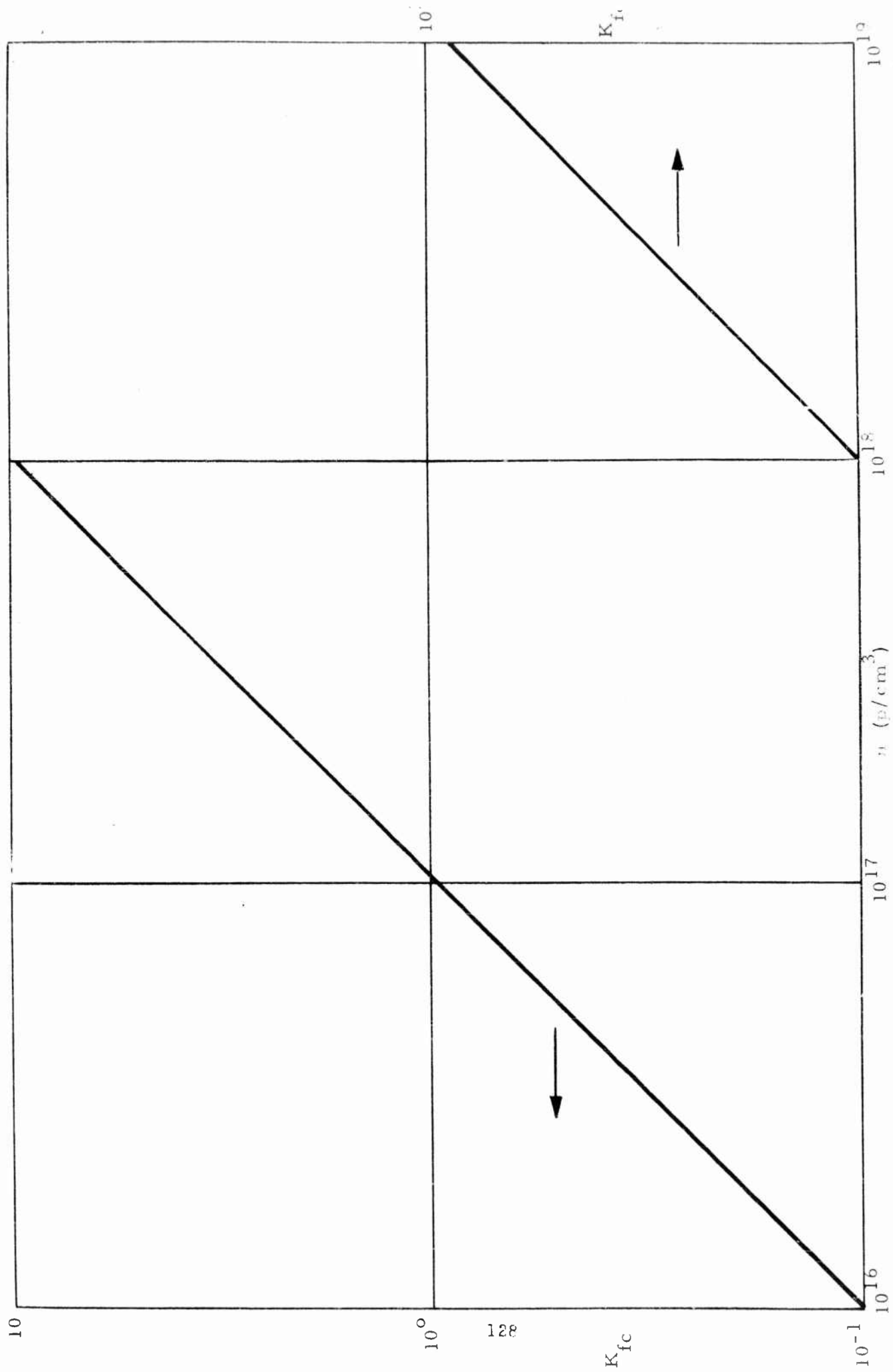


Figure 8. Free Carrier Absorption Coefficient

TABLE I A
TIME REQUIRED TO REACH SEVERAL INVERSION LEVELS

Beam Current	Rate of Generation	Time to Reach $n \sim 10^{16} \frac{\text{elec}}{\text{cm}^3}$
$I (\mu \frac{\text{amp}}{\text{cm}^2})$	$dn / dt \frac{P}{\text{cm}^3 \text{ sec}}$	Neglecting Losses
10^{-3}	5.6×10^{17}	1.8×10^{-2}
10^{-1}	5.6×10^{19}	1.8×10^{-4}
10^1	5.6×10^{21}	1.8×10^{-6}

TABLE I B

GENERATION OF FREE CARRIERS BY FISSION FRAGMENTS

Assuming GaAs U matrix in a reactor where
the neutron mean free path is $\lambda \sim 25 \text{ cm}$

Neutron Flux $\text{nts/cm}^2 \text{ sec}$	Free Carrier Generation Rate No/sec cm^3	Time t (sec) required to reach free carrier density of $m = 10^{16} \text{ elec/cm}^3$
10^{13}	10^{19}	10^{-3}
10^{14}	10^{20}	10^{-4}
10^{15}	10^{21}	10^{-5}
10^{16}	10^{22}	10^{-6}
10^{17}	10^{23}	10^{-7}

3.4 Mode Structure

Adjacent axial modes will be separated by a wave number of $\Delta(1/\lambda) = \frac{1}{2Ln_o}$ where L is the length and n_o the

index of refraction. For a sample 0.5 cm long with an index $n_o = 3.5$, $\Delta(1/\lambda) = 0.284 \text{ cm}^{-1}$ which corresponds to an energy separation of $\Delta E = 3.6 \times 10^{-5} \text{ ev.}$

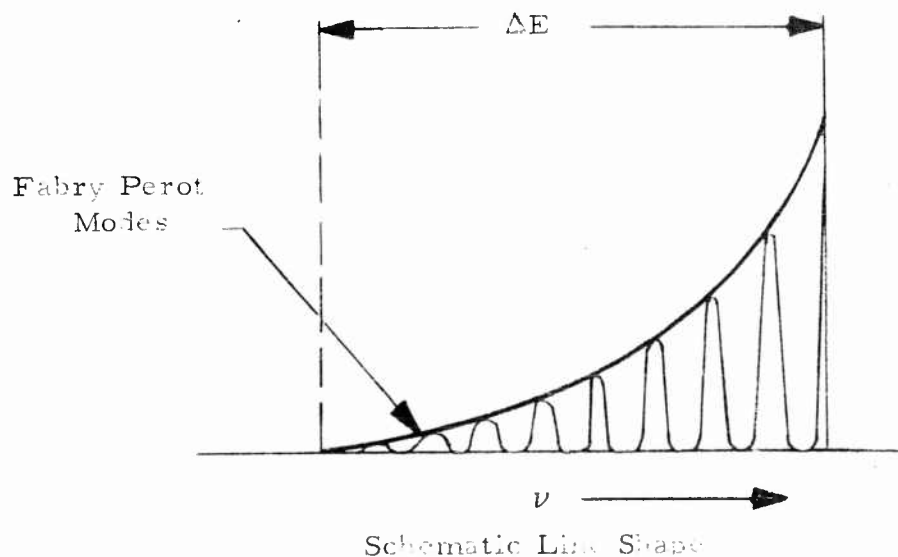
Off axis modes will have a considerably smaller separation. An estimate can be obtained using the expression

$$\frac{\Delta\nu}{\nu} = \frac{\chi_{01}^2}{8\pi n_o^2} \left(\frac{2\lambda}{d} \right)^2$$

where d is the sample diameter and $\chi_{01} = 2.405$.

This equation yields an estimate of about 200 kc for a diameter $d \sim 0.5 \text{ cm.}$

In the limit where the negative absorption coefficient is given by $K = A' (h\nu - E_g)^{\frac{1}{2}}$ the radiation emitted should be composed of many modes. The shape expected for the emitted line should be most intense at the highest emitted frequencies. A schematic sketch is shown below. Using the more exact value of K (section 2.7) the higher frequencies will be emphasized but there will be a decrease at the highest frequencies.



3.5 Line Width

A simple relation can be derived for the line width when the absorption coefficient varies as $(h\nu - E_g)^{\frac{1}{2}}$. Actually the more exact gain function should be used (section 2.7) which will modify this simple result somewhat.

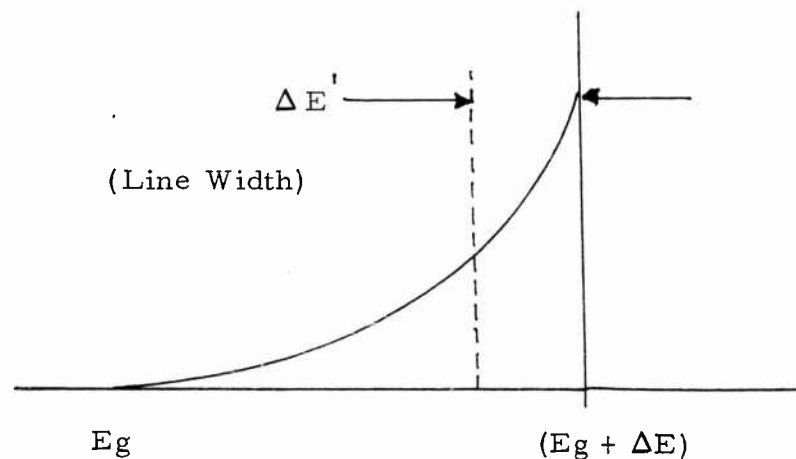
The line width we define as that characteristic width which contains one half of the emitted light. Now the emitted intensity is given by

$$I(\nu) = I_0 \exp \alpha \times (h\nu - E_g)^{\frac{1}{2}} \quad (\text{where } x \text{ is distance traveled})$$

The total light emitted will be given by

$$I_T = \int_{E_g/h\nu}^{(E_g + \Delta E)/h\nu} I(\nu) d\nu$$

now let $\xi = (h\nu - E_g)^{\frac{1}{2}}$



$$\begin{aligned} \text{Then } I_T &= \int_0^{\Delta E} I_0/2 \exp(\alpha \times \xi) d\xi \\ &= \frac{2 I_0}{\alpha \times} (\alpha \times \xi_0 - 1) \exp(\alpha \times \xi_0) \end{aligned}$$

For the half width

$$\frac{I_T}{2} = \frac{2 I_0}{\alpha \times} (\alpha \times \xi - 1) \exp(\alpha \times \xi)$$

where ξ has to be determined. Taking the ratio of $I_T/2$ to I_T we obtain

$$\frac{(\alpha \times \xi - 1) \exp(\alpha \times \xi)}{(\alpha \times \xi_0 - 1) \exp(\alpha \times \xi_0)} = 1/2$$

For our case $\alpha \times \xi \gg 1$

$$\text{so that: } \xi \exp(\alpha \times \xi) = \frac{\xi_0}{2} \exp(\alpha \times \xi_0).$$

This expression can be rewritten as

$$\ln \xi + \alpha \times \xi = \alpha \times \xi_0 + \ln \xi_0/2.$$

$$\text{Letting } \xi = \xi_0 - \Delta \xi$$

$$\Delta \xi = \frac{1}{\alpha \times} \left[-\ln \xi_0/2 + \ln (\xi_0 - \Delta \xi) \right]$$

and recalling $\xi_0 \gg \Delta \xi$

then

$$\boxed{\Delta \xi = \frac{\ln 2}{\alpha \times}}$$

For one case of interest: $n = 10^{16} \text{ p/cm}^3$

$$x = 1/2 \text{ cm}$$

$$\alpha = k \simeq 300^{-1} \text{ cm}$$

$$E_g = 1.5 \text{ ev}$$

$$\frac{\Delta \nu}{\nu} = 4.6 \times 10^{-3}$$

3.6 Approach to Threshold-Effect at Carrier Lifetimes

The excess carrier density in a semiconductor in which excess carriers are being generated (by any means) at a uniform rate, r , obeys the equation

$$\frac{dN_{ex}}{dt} = r - \frac{N_{ex}}{\tau}$$

where τ is an average lifetime at an excess carrier before recombination. If τ were constant (i. e. independent of N_{ex}), then the excess carrier density would approach the asymptotic value $r\tau$. Now τ is in fact dependent on N_{ex} and becomes quite short when N_{ex} exceeds N_{ex}^* , the threshold for laser action, since stimulated emission leads to a rapid depopulation of the conduction band. The dynamics of such a process are quite complicated and need not concern us here, the main question being what generation rates, r , are required for N_{ex} to be able to reach the laser threshold. A conservative estimate can be made if we take τ equal to

$$\tau_{min} \equiv \min (\tau (N_{ex})) \quad 0 \leq N_{ex} \leq N_{ex}^*$$

in which case the minimum generation rate, r_{min} , required for the threshold value of N_{ex} to be reached is

$$r_{min} = \frac{N_{ex}^*}{\tau_{min}}$$

In estimating τ_{min} , distinction must be made between majority and minority carrier lifetimes. Furthermore, we must

distinguish between the lifetimes for electron-hole recombination and for trapping at electrons and/or holes. To clarify this, consider the case of heavily doped p-type GaAs, in which the laser transition is the recombination of a conduction band electron with a hole bound to an acceptor atom. In such materials, the minority carrier (i. e. conduction band electron) lifetime with respect to trapping can be quite short, of the order of 10^{-13} to 10^{-10} sec^{*}, whereas the recombination lifetime is considerably longer (10^{-7} - 10^{-5} seconds). Both of these values depend markedly on doping and preparation, the general rule being the lower the resistance of the material - the shorter the minority carrier lifetime. In the present example, then, the τ_{\min} which enters the previous equation would be the minority carrier recombination lifetime, since the scattering of electrons by traps, while influencing their mobility, does not remove them as candidates for radiative recombination. Further study of this point is required. In particular, the fact that lower doping levels lead to longer lifetimes may lead to a tradeoff in the choice of impurity concentration, since both N_{ex}^* and τ_{\min} increase as the doping concentration decreases. In any event, for the purposes of this report, we shall assume $\tau_{\min} \sim 10^{-6}$ sec, with the understanding that some design optimization may be required to achieve this.

* C. Hilsum and A. C. Rose-Innes, Semiconducting III - V Compounds, p. 190, Pergamon Press, London (1961)

4. NUCLEAR PUMPING

4.1 Physical Processes

Having considered the characteristics of a semiconductor laser, we now turn to the problem of achieving the requisite density of excess carriers by means of nuclear pumping.

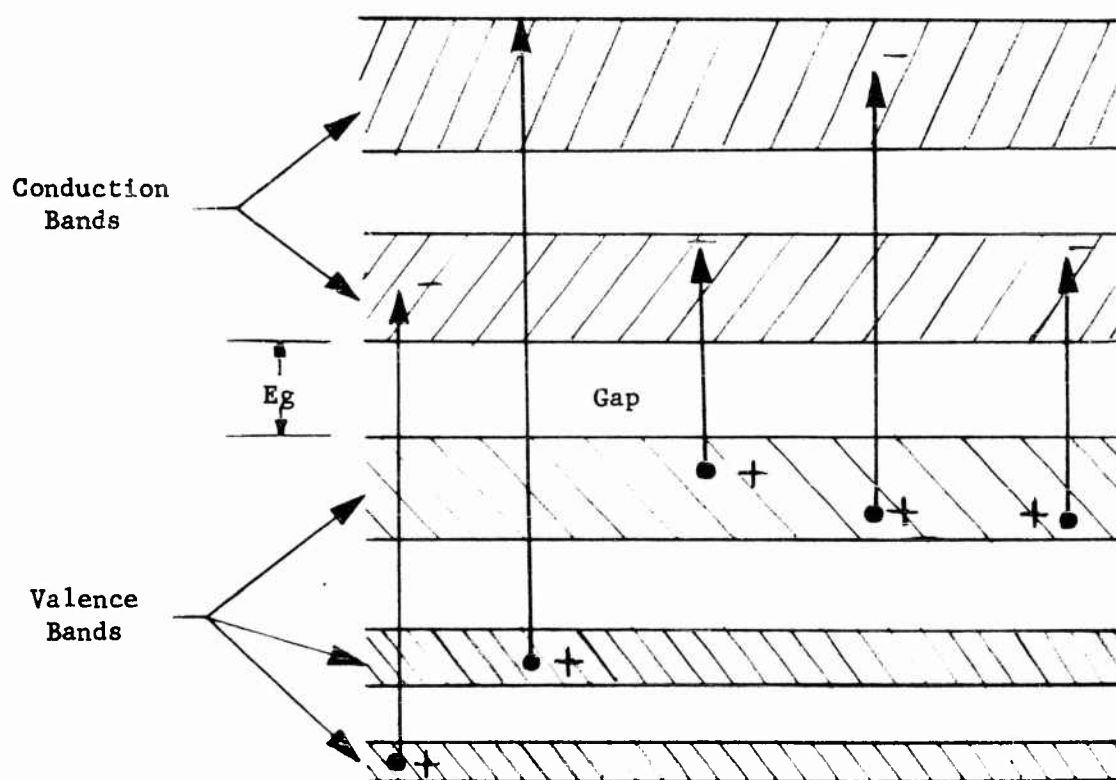
Consider the effect of bombarding a semiconductor with light nuclear particles (i. e. protons, alphas or deuterons) whose energy lies in the range 1 - 100 Mev.

In a semiconductor, the energy given up by the incident particle goes into a variety of electronic transitions as shown in Figure 9.

In addition to transitions from the valence to the conduction band, electrons from deeper lying bands are lifted to higher unoccupied bands. Thus, electrons appear in normally unoccupied bands and holes are created in normally full bands. This condition persists for only about 10^{-11} - 10^{-12} seconds, after which the situation relaxes to that illustrated in Figure 10. The interaction among the electrons, the holes and the phonons causes the electrons to fall to the bottom of the lowest unoccupied full band (the valence band). As a result of the predominant energetic Auger de-excitation process, as well as phonon interactions, many more electrons and holes are created. About as much energy ultimately goes into lattice vibrations as does into the formation of electron-hole pairs.

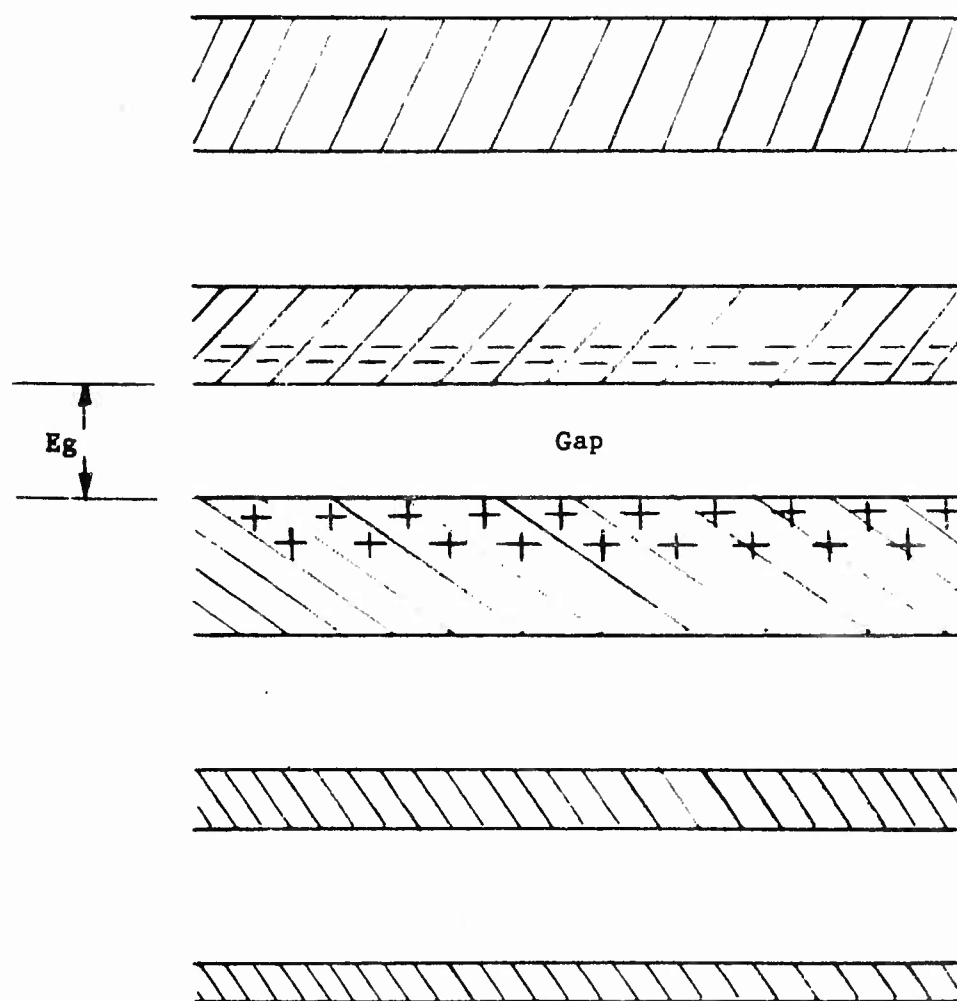
For a wide variety of particles and energies, it is found experimentally that the number of electron-hole pairs which are ultimately formed depends only on the energy lost in the solid by the incoming particle, and in a reasonably linear fashion^(*). In silicon,

(*) W. L. Brown, I.R.E. Trans. Nuc. Sci. NS-8 3 (1960)



Excitation of electrons in a semiconductor due to passage of an energetic charged particle.

Figure 9



Residual hole-electron excitation after a time $\approx 10^{-11} - 10^{-12}$ sec.

Figure 10

for example, McKay et al ^{*} found that a pair is produced for every 3.5 ev of energy loss. Comparing this with the band gap of 1.1 ev in silicon, we see that $2.4/3.5 \approx 2/3$ of the energy deposited in the solid is ultimately dissipated in the creation of phonons. Shockley ^{**} has proposed a theory from which he calculates the pair yield per unit energy loss using constants determined from data on the quantum yield for photons in the visible and near ultraviolet and the prebreakdown multiplication in silicon junctions ^{***}. He obtains a value in good agreement with the measured 3.5 ev. If we make the plausible assumption that similar effects occur in other semiconductors we have

$$N_c \sim \frac{\Delta E}{3 E_g}$$

where N_c is the number of excess carriers produced by an incident particle which loses the energy ΔE in a semiconductor of gap energy E_g . If the sample thickness is large compared to the range of the incident particle, ΔE becomes the incident energy. In this case, with energies of 1 to 100 Mev, about 3×10^5 free carriers/Mev are created per incident particle per Mev lost in the semiconductor. In the accompanying Figure 11 range energy relations for protons and alphas in GaAs are given.

^{*} McKay and K. B. McAfee, *Phy. Rev.* 91 1079 (1953).

^{**} W. Shockley, *International Conf. on Semiconductor, Physics*, (1960).

^{***} A. G. Chyroweth and K. G. McKay, *Phys. Rev.* 108 29 (1957).

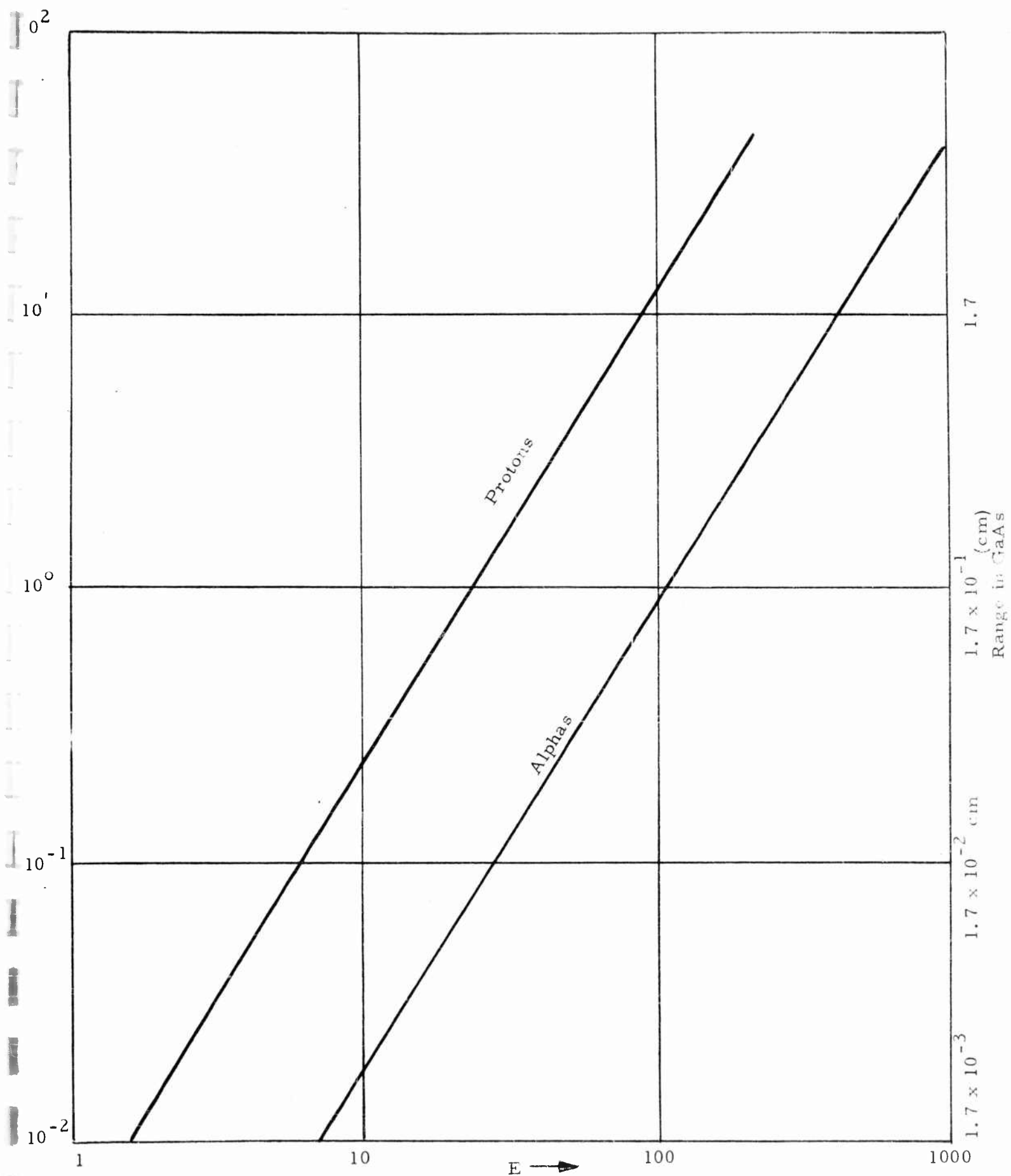


Figure 11. Range energy curve of protons and alphas in Gallium Arsenide

Consider the volume in which these excess carriers are created. The situation, say, for an α particle incident on a semiconductor is shown in Figure 12.

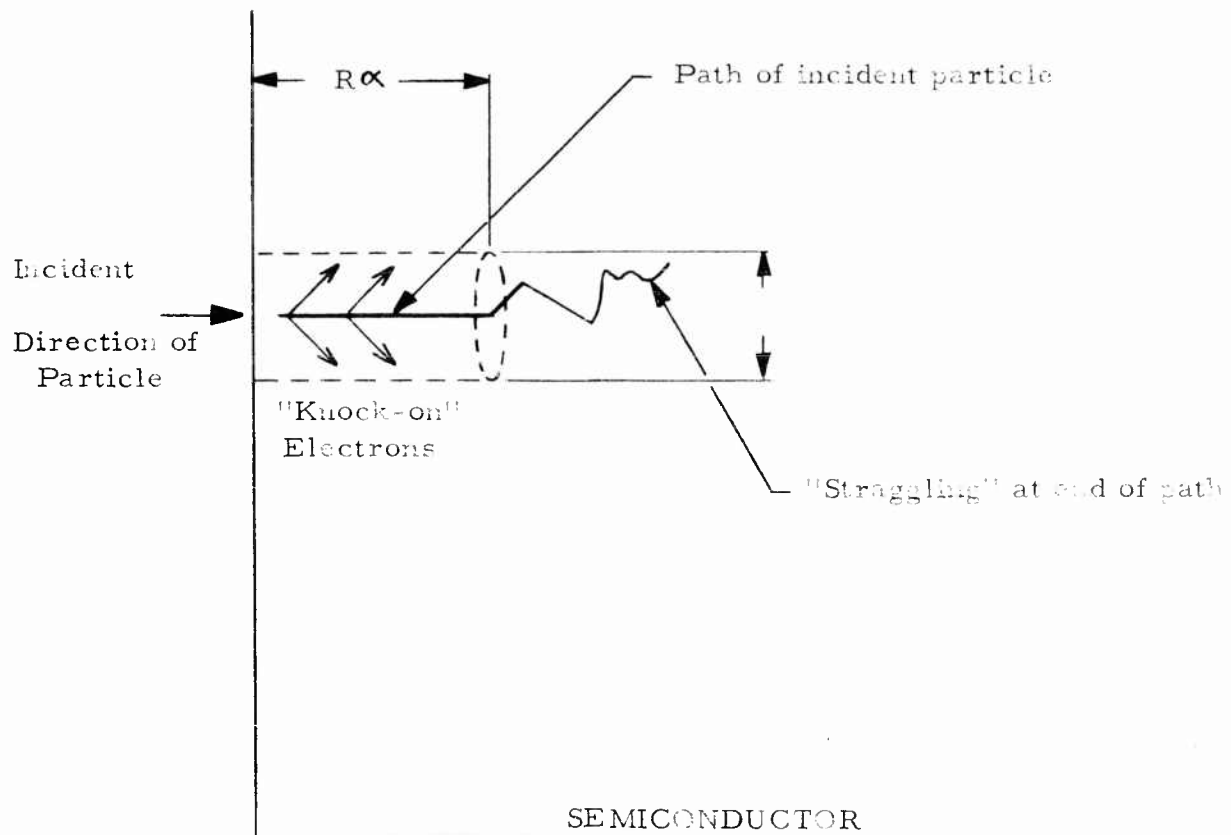
The excess carriers are produced in a (relatively narrow) cylinder whose length is the range of the incident particle and whose diameter is of the order of the range of the "knock-on" electrons produced in the slowing down process. The maximum energy which can be transferred from a (non-relativistic) heavy particle of mass M , energy E , to an electron is given by

$$E_{\text{secondary, max}} \approx \frac{4m_e E}{M}$$

For 4 Mev alphas or 1 Mev proton, this maximum is only about 2 Kev and most encounters transfer much less energy than this. The range in solids of such low energy secondary electrons is quite short, being $\sim 10^{-5}$ to 10^{-4} cm. The range of the incident particle, on the other hand, is considerably larger. An alpha particle of 6 Mev, for example, will have a range in GaAs semiconductor of about 1.7×10^{-3} cm and an 80 Mev α will have a range of 1.2×10^{-1} cm. A proton of one fourth the energy has the same range of an α with this energy. For example, a 6 Mev alpha, will produce about 10^{16} p/cm³ to 10^{18} p/cm³. Free-carrier densities of this magnitude are generally (*) what are needed for laser action.

We are thus led to the conclusion that incident nuclear particles will produce a substantial population inversion in a

(*) W. P. Dumke, "Stimulated Emission of Radiation from GaAs p-n Junctions", Applied Physics Letters Vol 1, pp 62-64, November 1962.



Volume in which carriers are produced by incident α particle

Figure 12

narrow cylindrical volume centered about the particle track. Free carriers have long lifetimes and hence they could diffuse several millimeters before recombining unless stimulated emission occurs. If a bombardment commences at $t = 0$, the excess carrier density will build up more or less spatially uniformly in a slab whose thickness is the particle range, until the average carrier density reaches the minimum threshold required for laser action, in which case a sudden depopulation would occur. This naturally assumes that the incident flux is sufficiently large to overcome other losses.

4.2 Rate of Free Carrier Generation

The number of electrons per unit length, η , raised to the conduction band along the path of a nuclear particle will be given by:

$$d\eta = \frac{dE}{\mathcal{E} dx}$$

and the total number generated will be given by

$$\eta = \int_0^E \frac{dE/dx}{\mathcal{E}}$$

where dE/dx is the rate of loss of energy per unit length by the nuclear particle and \mathcal{E} is the average energy required to form an electron-hole pair. The \mathcal{E} factor is discussed in the next section and is, generally, largely independent of the energy of the nuclear particle. Hence,

$$\eta = \frac{E}{\mathcal{E} x}$$

where we neglect the variation of dE/dx with x .

The electrons and holes are formed in the vicinity of the track in a cylindrical region of cross-sectional area a . Typical values of a are between 10^{-4} and 10^{-5} cm^2 . The volume density of electrons or holes formed by a single nuclear particle along the track will be

$$\eta_c = \frac{1E}{\epsilon_{xa}}$$

If the beam has $1/a$ particles per square centimeter distributed uniformly, η electrons or holes will be formed per unit volume and distributed uniformly throughout the range of the nuclear particle.

The volume density will increase in proportion to the beam current. For example, an 80 Mev particle has a range of 1.24×10^{-1} cm in GaAs. In GaAs ($\epsilon \sim 3$ ev)

$$\eta = \frac{8 \times 10^7}{3 (1.2 \times 10^{-1})a}$$

The electron or hole density η due to a single track η_n will be between 2.7×10^{16} and 2.7×10^{18} p/cm³ depending on the value of, a , used. But the average density of free carriers generated of nuclear particles will be given by

$$\eta = \frac{\Phi E}{\epsilon xA}$$

where A is the cross-sectional area of the beam and Φ the number of particles in the beam per unit area.

In Figure 5 the rate of generation of free carriers, plotted as a function of beam current for α particles with an energy of 80 Mev is given.

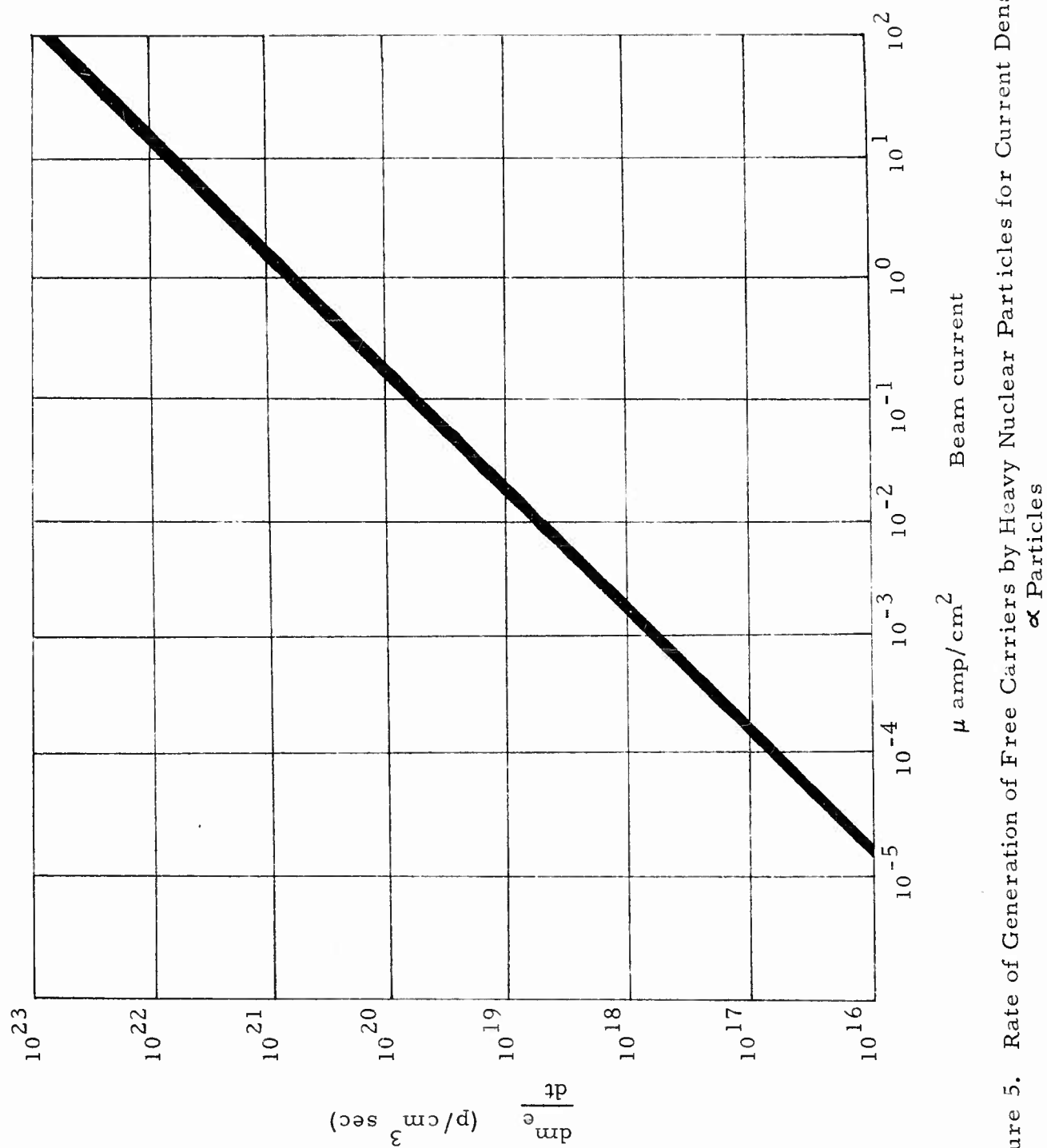


Figure 5. Rate of Generation of Free Carriers by Heavy Nuclear Particles for Current Density of \propto Particles

4.3 Fission Pumping

We can estimate the inversions levels which could be obtained in a semiconductor pumped with fission fragments produced in a nuclear reactor. We neglect any radiation damage effects which will, of course, be more serious in the case of fission fragments, as well as effects caused by the introduction of material in a semiconductor lattice. The slow neutron fission cross section is about 800 b. Consider a semiconductor, say GaAs, which is composed of 10% U^{238} by weight. This corresponds to about 5×10^{19} U atoms/cm³.

In this case the neutron mean free path for fissioning is

$$\lambda = \frac{1}{\eta \sigma} \approx 25 \text{ cm.}$$

The rate of formation of inverted degenerate electrons would be approximately:

$$\eta_e = F \Delta E / \lambda \bar{\epsilon}$$

F is the neutron flux

ΔE is the energy released in fission

λ is the neutron fission mean free path

$\bar{\epsilon}$ is the average energy required to form an electron hole pair

For $F = 10^{16}$ nts/cm² sec, $E \sim 200$ Mev, $\lambda = 25$ cm, $\bar{\epsilon} = 3$ ev,

$$\eta_e = 3 \times 10^{22} \text{ elec/cm}^3/\text{sec.}$$

The laser threshold would be reached in one micro-second if the free-carrier density required is 3×10^{16} elec/cm³.

Also, the neutron flux in present reactors can be obtained over a large area of about several square meters and into a sizable volume in contrast to the beam cross section in cyclotrons which is limited to a few square centimeters. Hence much higher energy can be placed in a sample.

Instead of using fission fragments it may be possible to disperse boron (10) throughout a semiconductor and use the $B^{10} (n, \alpha)$ reaction where the α particle would create free carriers.

5. RADIATION DAMAGE IN SEMICONDUCTORS

Radiation damage originates from the interaction of nuclear radiation with matter. The interaction displaces atoms from their equilibrium positions and puts them in nonequilibrium positions. Local regions of high transient temperatures can be created. Impurity atoms can be introduced by radioactive capture and decay or by trapping of fission fragments. Also chemical bonds can be broken and free radicals can be formed.

These processes have been called respectively: vacancies, interstitials, thermal spikes, impurity atoms, and ionization effects.

The first four processes are most important in solids whereas the last occurs in liquids and gases.

The nuclear particles that cause most of the radiation damage in solids in a reactor are fast neutrons and fission fragments, chiefly because the energy of each is tremendous in relation to the energy required to create a single defect. The uncharged nature of the neutron means that it can interact only by direct collision. However, once a collision has taken place the knocked-on atom in turn rapidly creates subsequent displaced atoms. The incident neutron travels many thousands of atomic spacings in the solid before making a collision. Thus, damage from fast neutrons is widely spaced through a reactor.

Fission fragments which are heavy and initially possess a high charge dissipate all of their energy in a few microns in solids. The spatial distribution of the radiation damage produced by fast neutrons and fission fragments is thus very different.

In the case of electrons traversing matter the radiation damage is much simpler; in fact, the energy required to create a vacancy in a solid can be determined and is complicated by the presence of other defects. Semiconductors are materials which are very sensitive to radiation. This is shown by the drastic change in electrical conductivity and by a change in the character of the conduction. The conduction mechanism may change from electron to hole conduction and vice versa with short exposures. The nature of the change depends on the original state of the material.

Relatively little information is available on the radiation damage in GaAs.

(J. P. L. Literature Search, No. 442 (July 1962) on solid state radiation detectors has only two relevant references to GaAs.) However, large changes have been observed in transport properties such as electrical conductivity for integrated neutron fluxes above about 10^{15} nts/cm² (Willardson Journal Appl. Phys. 30). The conductivity of an n type specimen decreases to a value lower than the minimum for the p type specimen with the conductivity as a function of bombardment being essentially well behaved, i.e. the theoretical minimum is attained. (Aukerman AD-204250) October 1958.

Also bombardments of injection GaAs lasers in reactors have shown significant degradation of performance for integrated fluxes above 10^{15} nts/cm².

However, annealing may remove much of the radiation damage and restore performance close to initial levels (Aukerman AD234 641) April 1960.

Finally, some very radiation resistant semiconductors exist such as silicon carbide. This compound has also been recently lased.

6.

LIQUID SEMICONDUCTORS

Since radiation damage should be greatly reduced in liquids the possibility that appropriate liquid semiconductors may exist appears a promising area of investigation.

In Table II some possible materials are listed which may possess semiconductor properties in the liquid state.

TABLE II

SEMICONDUCTOR LIQUIDS

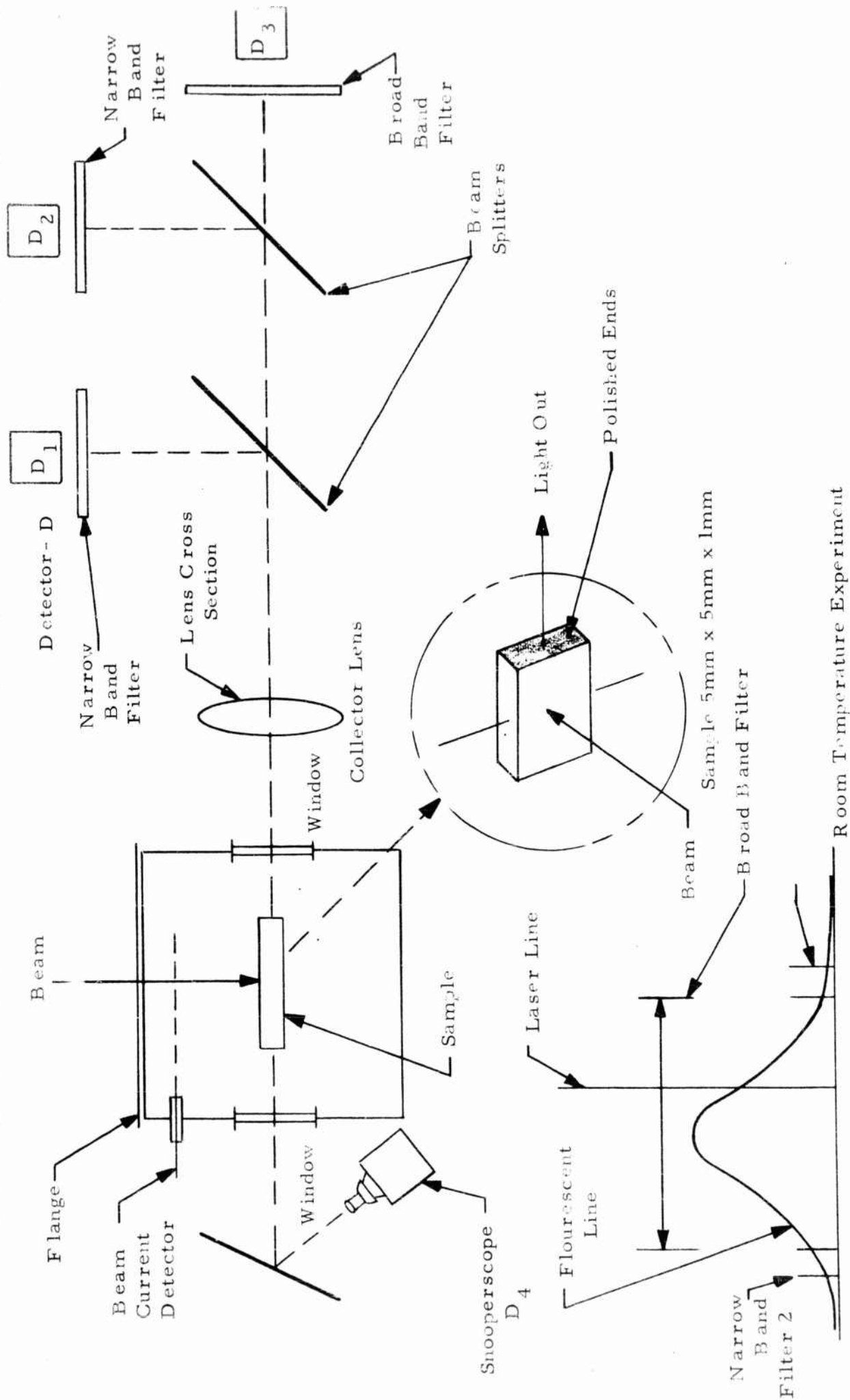
Compound	Melting Point °C	Boiling Point °C
GaAs	150	-
NbBr ₅	150	362
UClF ₃	400	-
GeBr ₅	26	186
NbI ₅	125	400
PI ₃	61	-
AlI ₃	191	360
GaBr ₄	121.5	279
BI ₃	43	210
SiBr ₄	5	153
AsBr ₃	33	221
PBr ₃	-40	173

7. DEMONSTRATION EXPERIMENT

We have designed an experiment to demonstrate the nuclear pumping of semiconductors employing the previously discussed items. The experiment is designed to employ a cyclotron such as the 88 inch high flux cyclotron at the University of California at Berkeley which appears ideally suited to this experiment.

The experiment would be performed as follows: the beam from the cyclotron would be directly on a GaAs sample in the shape of a parallelepiped with dimensions of about 5 mm x 5 mm x 1 mm. Intrinsic, n-doped and p-doped samples would be employed. The ends of the sample would be polished, and sides roughened, and electrical leads would be mounted on the roughened top and bottom. The beam would be incident on one side and the other side may be in contact with metal at liquid nitrogen temperatures. The sample would be mounted in vacuum and windows would be appropriately placed to extract the radiation from the ends. A collector lens would be employed to ease the alignment problem. Light passing through this lens would be split by appropriately placed beam splitters then passed through filters to detectors. The experimental setup is shown in Figure 15. In front of detector D_1 , would be placed a narrow band filter designed to pass fluorescent light on the low side of the fluorescent peak. In front of D_2 would be placed a narrow band filter designed to pass fluorescent light on the high side of the fluorescent peak but in front of D_3 would be placed a broad band filter designed to pass most of the fluorescent radiation.

The three detectors would register a signal when fluorescent light is emitted but when the threshold for laser action is reached only the broad band detector will register a signal demonstrating laser radiation. Since the narrow band filters are designed so



To Demonstrate Laser Action as Function of Time From When Beam is Turned On

- D 1. Monitor light in broad band filter
- D 2. Monitor light in high frequency narrow band filter
- D 3. Monitor light in low frequency narrow band filter
- D 4. Snooper scope to see line narrowing

Figure 15

as not to pass the laser radiation out of the other window, light would be directed to a screen which is monitored by a snooperscope and directional narrowing would be detected.

Possible samples to be used are shown in Table III below.

Electric leads would be placed on the sample to monitor some of the electrical properties during irradiation.

The samples would be irradiated for variable times at a given beam current. Then the beam current would be changed and the process repeated.

It may be desirable to also test samples at liquid nitrogen temperatures and such a setup has been outlined (Figure 16). In this case one of the potential problems is to avoid vapor condensation on the windows.

A convenient detector to use appears to be the DuMont 6911 photomultiplier with metal shields.

TABLE III
POSSIBLE SAMPLES

<u>Sample</u>	<u>Type</u>	<u>Size</u>	<u>No. Required</u>
GaAs	Intrinsic	5mm x 5 mm x 1 mm	3
GaAs (n type)	Te N_D 10^{18} p/cm ³	"	3
GaAs (p type)	Zn NA 10^{19} p/cm ³	"	3

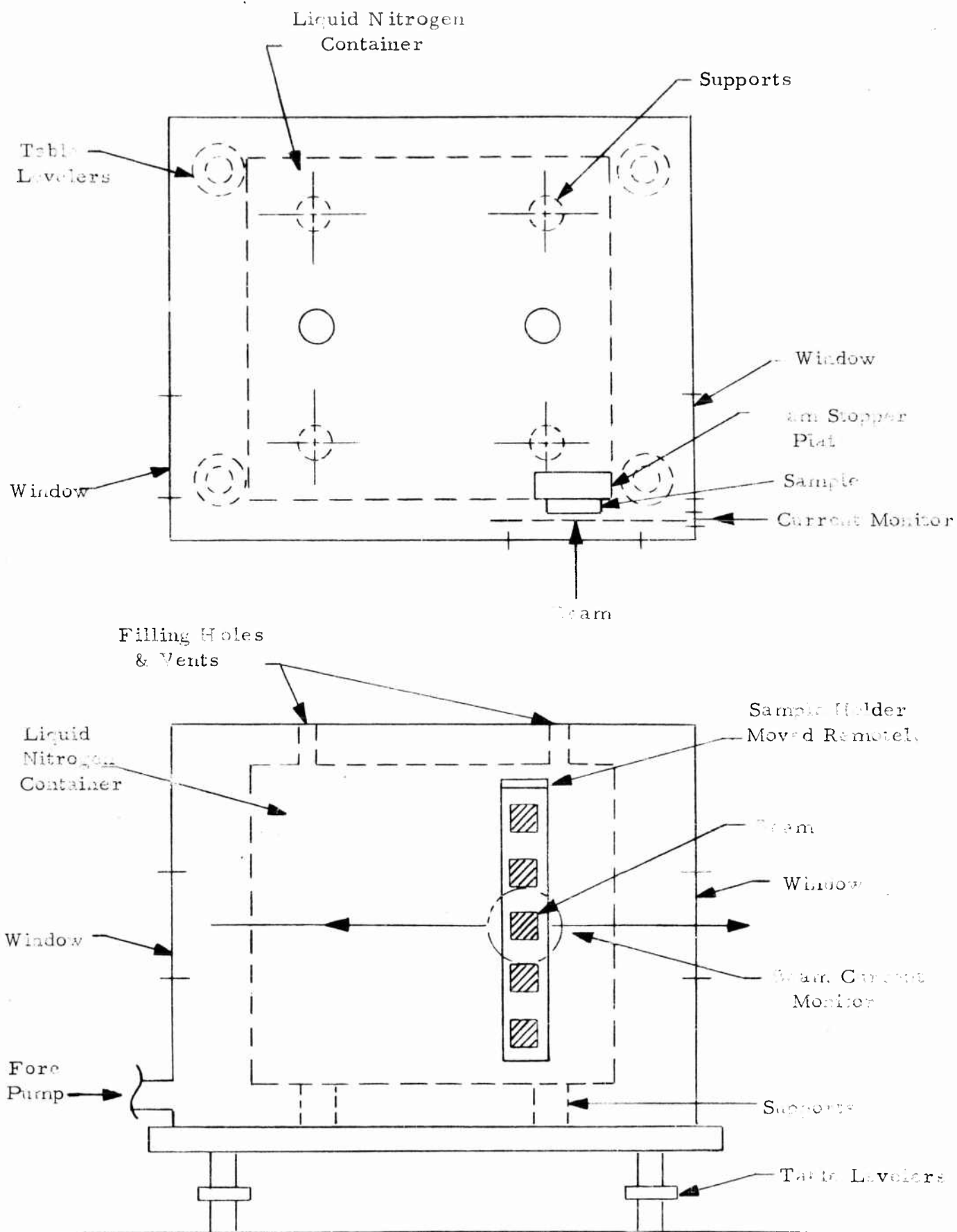


Figure 16
Liquid Nitrogen Setup
153

8. CONCLUSIONS

1. From the foregoing analysis, it appears that it may be possible to generate laser radiation by the nuclear pumping of direct gap semiconductors.

2. The primary advantages over GaAs injection lasers appear to be: (a) a larger active volume, (b) lower free carrier inversion levels are required in order to achieve lasing, (c) high rate of free carrier generation may be possible.

3. Since semiconductors are sensitive to radiation damage, this may pose a limitation on long-life operation. The use of special semiconductors such as semiconducting liquids or radiation resistant semiconductors such as SiC may reduce radiation damage susceptibility.

4. Semiconductors composed of enriched Uranium and Boron exist. Such materials appear attractive from the viewpoint of neutron actuator in a reactor. It is not known if such materials are lasable.

REFERENCES

1. R.N. Hall, G.E. Fenner, J.D. Kingsley, T.J. Soltys and R.O. Carlson, Phys. Rev. Letters 9, 366 (1962).
2. M. Natha, W. P. Dumke, G. Burns, F.H. Dill, Jr., and G. Lasher, Appl. Phys. Letters 1, 62 (1962).
3. T. Quist, R.H. Rediker, R.J. Keyes, W.E. Krag, B. Lax, A. L. McWhorter and H.J. Zeigler, Appl. Phys. Letters 1, 91 (1962).
4. D.F. Nelson, M. Gershenzon, A. Ashkin, L.A. D'Asavo, and J. C. Sarace, Appl. Phys. Letters 2, 182 (1963).
5. M.I. Nathan and G. Burns, Appl. Phys. Letters 1, 89, (1962).
6. M. Bernard and G. Durauffourg, Physica Stat. Sol. 1, 699 (1961).
7. S. Mayburg, Solid-State Electron, 2, 195 (1961).
S. Mayburg and J. Black, J. Appl. Phys. (To be published).
8. S. Mayburg, J. Appl. Phys. 34, 1791 (1963).
9. W.P. Dumke, Phys. Rev. 127, 1559 (1962).
10. J. Blakemore, Semiconductor Statistics, (Pergamon Press, New York, 1962) p. 118.
11. S. Mayburg, J. A. P., 34, 1791 (1963)
12. J. Combrisson, A. Honig and C. H. Townes, Compt. Rev. 242, 2451 (1956).
13. W. P. Dumke, Phy. Rev. 127, 1959.

APPENDIX II

DIRECT AND INDIRECT GAP MATERIALS

There are two general categories of semiconductors. One which exhibits the type of gap structure shown in Figure 1a is called a direct gap material whereas the other type exhibits a gap structure depicted in Figure 1b and is called an indirect gap material. Materials such as GaAs and InSb have a direct gap structure; Ge and Si are indirect gap materials.

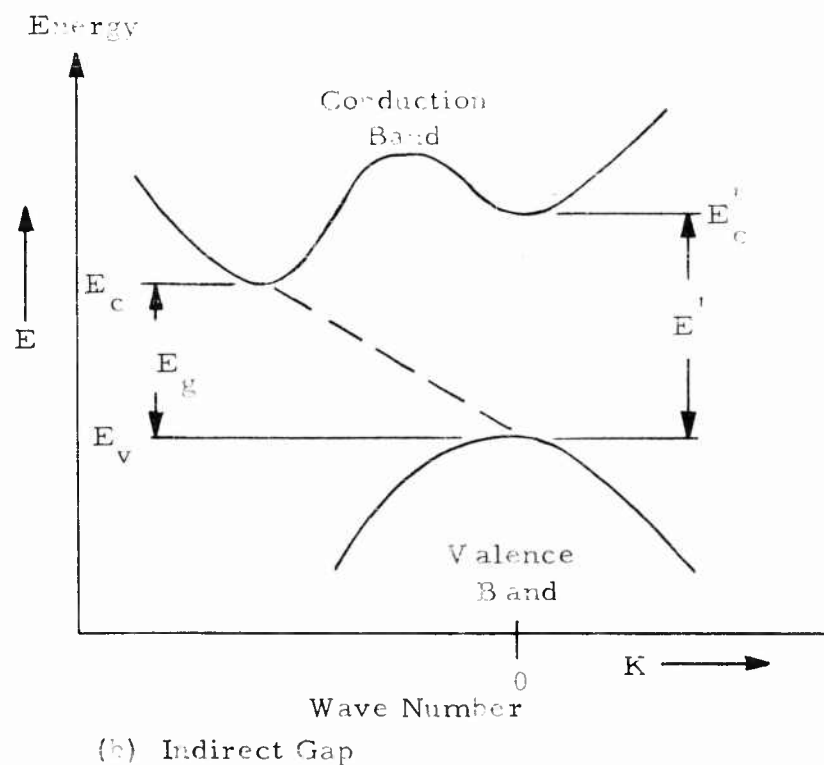
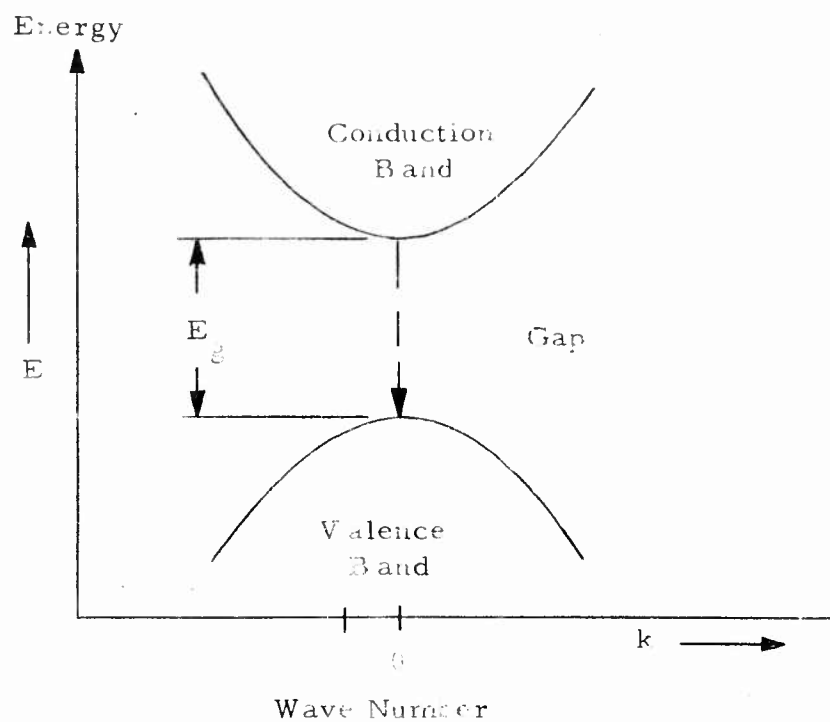
In direct gap materials only vertical transitions are allowed. In essence an electron can only make a transition from a state in one band to a state in the other bands which possess the same wave number. This is a result of the quantum mechanical selection rule, which states that the change in momentum (proportional to wave number) of the initial and final states equals the momentum carried away by the radiated quantum, $k_f - k_i = q$. For wavelengths of the order of 1μ , q is very small hence only vertical transitions are allowed.

Whether or not a transition at $k = 0$ is allowed depends on the parity of the initial and final wave functions⁽¹⁾.

For the direct transitions, absorptions would be intense for all $h\nu > E_g$, where E_g is the gap energy, and cease at $E_g = h\nu$.

For a semiconductor with an indirect gap, the minimum in the conduction band occurs in a different region of k space than the maximum of the valence band (Figure 1b). This type of structure is typical of germanium and silicon. In this case intense absorption will cease at the wavelength corresponding to the minimum vertical gap, i.e. $h\nu = E'$. Also nonvertical transitions can occur to some degree with momentum generally being conserved by interactions with phonons, so that absorption continues but to a reduced degree due to some relaxation of the selection rules down to $h\nu = E_g$.

⁽¹⁾ H. Brooks (1955), Advances in Electronics and Electron Physics, Vol. 7, Academic Press



Energy Diagrams Illustrating
the two Types of Semi-
conductor Materials.

C. RECOMMENDATIONS1. Related to Part A of this report

From the study of physical theory of liquid lasers, several specific areas for further investigation are recommended:

1.1 Measurements of the absorption coefficient of AsCl_3 in the visible and infrared.

1.2 Measurement of the refractive loss suffered by a photon beam due to the uniform heating of AsCl_3 .

1.3 Measurement of the line width and lifetime of the rare-earth luminescent emission and absorption in $\text{AsCl}_3 (\text{RCl}_3)$ where R represents a rare earth.

1.4 Measurement of the solubility of rare earth chlorides in AsCl_3 .

1.5 Measurement of the thermal conductivity, specific heat, and dielectric constant of AsCl_3 .

1.6 Perform more exact theoretical calculations within the framework of the theory as presented in Part A. Primarily, a more sophisticated and detailed calculation of the scattering losses in liquids should be performed.

2. Related to Part B of this report

From the study presented in Part B, the following recommendation can be made for further work in this area:

2.1 More detailed analysis of the dynamics of laser action should be performed including end losses and the finite extent of the laser media.

2.2 A more sophisticated analysis of the mode structure and line width should be performed.

2.3 Relevant radiation damage studies on promising semiconductors such as GaAs and GaP should be made.

2.4 A demonstration experiment to generate laser radiation to test the theory developed in this section should be performed.

2.5 Investigation of suitable enriched uranium or boron ten (B^{10}) semiconductors which possess the requisite characteristics for laser action by nuclear pumping should be undertaken.

2.6 An investigation of annealing effects and also of certain liquid semiconductors should be undertaken to see if these materials can be made to lase.

ACKNOWLEDGEMENT

We wish to acknowledge here the enthusiasm, interest and wholehearted cooperation given by Dr. Elliot Weinberg who was the technical monitor on this program. We wish to acknowledge helpful discussions during the initial phases of this work with Dr. Jack Soules. Several very useful discussions were held with Dr. Edward Teller. These discussions have been of great assistance in formulating plans for further work.

Finally, we wish to acknowledge the cooperation and assistance given to us by Dr. Bernard Harvey in the planning of the proposed demonstration experiment at the Berkeley cyclotron.

DISTRIBUTION LISTNo. Copies

Defense Documentation Center Cameron Station Building Alexandria 14, Virginia	20
Batelle Memorial Institute Attn: BMI - Defender 505 King Avenue Columbus 1, Ohio	1
Mr. C. A. Black General Electric Company Advanced Technology Laboratory Schenectady, New York	1
Mr. S. Byron Aeronutronic Division of Ford Motor Co. Ford Road Newport Beach, California	1
Mr. J. P. Chernoch General Electric Laboratory Schenectady, New York	1
Mr. R. S. Congleton Hughes Aircraft Corp. Aerospace Group Research & Development Division Culver City, California	1
Basil Curnutte, Jr. Kansas State University Manhattan, Kansas	1
Mr. G. H. Dieke Johns Hopkins University Baltimore 18, Maryland	1

MHD research, inc.

Mr. J. W. Eerkens Terra Nova MHD Research, Inc. Post Office Box 1815 Newport Beach, California	1
Mr. John Emmett Physics Department Stanford University Palo Alto, California	1
Mr. J. Gerhauser North American Aviation, Inc. Los Angeles Division International Airport Los Angeles 9, California	1
Dr. Harry Heard Radiation at Stanford 3180 Hanover St. Palo Alto, California	1
Mr. James Hobart Laser Systems Center of Lear Seigler, Inc. 2320 Washtenaw Avenue Ann Arbor, Michigan	1
Mr. C. H. Keller Pek Labs, Inc. 925 Evelyn Avenue Sunnyvale, California	1
Mr. S. P. Keller International Business Machines T. J. Watson Research Center Yorktown Heights, New York	1
Mr. C. G. Kirkpatrick Autonetics Division of North American Aviation Anaheim, California	1

Mr. A. Lempicki General Telephone & Electronics Labs Bayside 60, New York	1
Mr. T. H. Maiman Korad Corporation 2520 Colorado Avenue Santa Monica, California	1
Mr. Joseph I. Masters Technical Operations Research Burlington, Massachusetts	1
Mr. T. C. McAvoy Corning Glass Works Corning, New York	1
Mr. W. McKusick Eastman Kodak Company Apparatus and Optical Division 400 Plymouth Avenue, N. Rochester 4, New York	1
Mr. J. F. Miller Battelle Memorial Institute 505 King Avenue Columbus 1, Ohio	1
Mr. O. H. Nestor Linde Company 1500 Polco Street Indianapolis 24, Indiana	1
Mr. J. W. Nielson Airtron, A Division of Litton Industries 200 East Hanover Avenue Morris Plains, New Jersey	1
Mr. Gerald Oster Chemistry Department Polytechnic Institute of Brooklyn 333 Jay Street Brooklyn 1, New York	1

MHD research, inc.

Mr. C. B. Sclar Battelle Memorial Institute 505 King Avenue Columbus 1, Ohio	1
Secretary, Special Group on Optical Masers Oddrce Advisory Group on Electron Devices 346 Broadway - 8th Floor New York 13, New York	3
Mr. R. G. Seed Northeastern University Boston, Massachusetts	1
Mr. David Stockman Electronics Laboratory General Electric Company Syracuse, New York	1
Mr. J. W. Turner Westinghouse Electric Corporation Electronics Division P. O. Box 1897 Baltimore 3, Maryland	1
Mr. H. A. Weakliem Radio Corporation of America David Sarnoff Research Center Princeton, New Jersey	1
Mr. C. G. Young American Optical Company Southbridge, Massachusetts	1
Mr. W. P. Siegmund American Optical Company Southbridge, Massachusetts	1
ASD/ASRCE-31/ Wright-Patterson AFB, Ohio	1

Dr. Rubin Bronstein Radio Corporation of America David Sarnoff Research Center Princeton, New Jersey	1
Dr. W. Holloway Sperry Rand Research Center Sudbury, Massachusetts	1
Dr. Jerald R. Izatt New Mexico State University University Park, New Mexico	1
Professor A. K. Kamal Purdue University School of Electrical Engineering Lafayette, Indiana	1
Mr. Thomas C. Marshall Columbia University Dept. of Electrical Engineering New York 27, New York	1
Mr. Charles G. Naiman Mithras, Inc. Cambridge 39, Massachusetts	1
Dr. J. H. Schulman Solid State Division U. S. Naval Research Laboratory Washington 25, D. C.	1
Dr. Jack A. Soules Physics Department New Mexico State University University Park, New Mexico	1
Dr. Arden Sher Varian Associates 611 Hansen Way Palo Alto, California	1

MHD research, inc.

Physical Sciences Division
Army Research Office
Office, Chief, Research and Development
Washington 25, D. C.
Attn: Dr. Robert A. Watson 1

Chief Scientist
U. S. Army Electronics Command
Fort Monmouth, New Jersey
Attn: Dr. Hans K. Ziegler 1

Director, Institute for Explatory Research
Army Signal Research & Development Laboratory
Fort Monmouth, New Jersey
Attn: Dr. E. M. Reilley 1

Asst. Director of Surveillance
Army Signal Research & Development Laboratory
Fort Monmouth, New Jersey
Attn: Dr. Harrison J. Merrill 1

Director, Technical Ballistics Laboratory
Ballistics Research Laboratory
Aberdeen Proving Ground
Aberdeen, Maryland
Attn: Dr. Edwin Minor 1

Director of Research & Development
Army Ordnance Missile Command
Huntsville, Alabama
Attn: Mr. William D. McKnight 1

Office, Chief of Naval Operations /OP-07T-1/
Dept. of the Navy
Washington 25, D. C.
Attn: Mr. Ben Rosenberg 1

Bureau of Naval Weapons /RR-2/
Dept. of the Navy
Washington 25, D. C.
Attn: Dr. C. H. Harry 1

Bureau of Ships /Code 305/ Department of the Navy Washington 25, D. C. Attn: Dr. G. C. Sponsler	1
Office of Naval Research /Code 402C/ Department of the Navy Washington 25, D. C. Attn: Dr. Sidney Reed	1
Office of Naval Research /Code 421/ Department of the Navy Washington 25, D. C. Attn: Mr. Frank B. Isakson	3
Office of Naval Research /Code 406T/ Department of the Navy Washington 25, D. C. Attn: Mr. J. W. Smith	1
Naval Research Laboratory /Code 6440/ Department of the Navy Washington 25, D. C. Attn: Dr. C. C. Klick	1
Naval Research Laboratory /Code 7360/ Department of the Navy Washington 25, D. C. Attn: Dr. L. F. Drummeter	1
Headquarters USAF /AFRDR-NU-3/ Department of the Air Force Washington, D. C. Attn: Lt. Col. E. N. Myers	1
Research & Technology Division Bolling AFB Washington, D. C. Attn: Mr. Robert Feik	1

MHD research, inc.

Office, Aerospace Research /MROSP/
Washington 25, D. C.
Attn: Lt. Col. Ivan Atkinson

1

Technical Area Manager /760B/
Surveillance Electronic Systems Division
L. G. Hanscom AFB
Massachusetts
Attn: Major H. I. Jones, Jr.

1

Technical Area Manager /760A/
Advanced Weapons Aeronautical Systems Div.
Wright-Patterson AFB
Ohio
Attn: Mr. Don Newman

1

Project Engineer /5237/
Aerospace Radiation Weapons
Aeronautical Systems Division
Wright-Patterson AFB
Ohio
Attn: Mr. Don Lewis

1

Air Force Special Weapons Center /SWRPA/
Kirtland AFB
New Mexico
Attn: Capt. Marvin Atkins

1

Project Engineer /5561/ Comet
Rome Air Development Center
Griffiss AFB
New York
Attn: Mr. Phillip Sandler

1

Department of Electrical Engineering
New York University
University Heights
New York, New York
Attn: Mr. Thomas Henion

1

H

BMDR
Room 2 B 263
The Pentagon
Washington 25, D. C.
Attn: Lt. Col. W. B. Lindsay

8

Joint Advance Study Group
Joint Chiefs of Staff
Room 2 C 825
The Pentagon
Washington 25, D. C.
Attn: Col. C. A. Barninger

1